SIMULATION OF FOREST GROWTH, APPLIED TO DOUGLAS FIR STANDS IN THE NETHERLANDS

40951

G.M.J.Mohren

SIMULATION OF FOREST GROWTH, APPLIED TO DOUGLAS FIR STANDS IN THE NETHERLANDS

Proefschrift
ter verkrijging van de graad van
doctor in de landbouwwetenschappen,
op gezag van de rector magnificus,
dr. C.C. Oosterlee,
in het openbaar te verdedigen
op dinsdag 3 maart 1987
des namiddags te vier uur in de aula
van de Landbouwuniversiteit te Wageningen

Stellingen

1. De afname van de stamhoutbijgroei op hogere leeftijd in gelijkjarige bos-
    opstanden is een gevolg van een combinatie van verminderende lichtonder-
    schepping door het kronendak en verminderende toedeling van assimilaten
    aan de stam; deze afname wordt niet veroorzaakt door een toename van de
    onderhoudsademhaling als gevolg van de accumulatie van biomassa.

    (dit proefschrift)

2. De verminderde vitaliteit van Douglas in Nederland, zoals deze tot uiting
    komt in de inventarisaties van het Staatsbosbeheer in 1985 en 1986, is
    een gevolg van uitdrogingsverschijnselen en de daarmee gepaard gaande
    naaldverliezen gedurende de winterperiode in beide jaren.

    (Staatsbosbeheer, Afdeling Bosontwikkeling: Verslag van het landelijk vitaliteits-
    onderzoek, nrs. 3 en 4. Utrecht, 1985, 1986)

3. De selectie van Douglas-herkomsten behoeft hernieuwde aandacht omdat in
    de gematigde streken bij een stijgende temperatuur als gevolg van het
    toenemend koolzuurgehalte van de atmosfeer, de fysiologische aktiviteit
    van naaldbomen in de winter zal toenemen, waardoor het risico van uitdro-
    gingsverschijnselen tijdens die periode groter wordt.

4. Op droge zandgronden met gelijk vochtleverend vermogen is de groei van
    Douglas in het Zuiden van Nederland geringer dan in het Noorden omdat
    door de hogere verdamping er in het Zuiden een groter vochttekort optreedt.

    (dit proefschrift)

5. Ondanks een in principe onbeperkte levensduur, groeien bomen niet tot in
    de hemel omdat bij een boomhoogte tussen 150 en 200 meter de zuigspanning
    in de bladeren of naalden ten gevolge van de zwaartekracht verhindert dat
    de huidmondjes opengaan.

    (M.H. Zimmermann: Xylem structure and the ascent of sap. Berlin, Springer Verlag, 1983)

6. Verhoging van de houtproduktie in Nederland zal vooralsnog moeten plaats-
    vinden in bestaande bossen; dit beperkt de boomsoortenkeuze in veel ge-
    vallen tot naaldbomen en vereist bemesting op grote schaal.

7. De emotionele reakties in het Wagenings Hogeschoolblad op voorstellen tot
    bemesting van bossen in Nederland, tonen aan dat onderzoek en onderwijs
    op het gebied van voedingsstoffenhuishouding van bossen sterk is verwaar-
    loosd.

    (Wagenings Hogeschoolblad nr. 25, 28-08-'86)

8. De stelling dat bosbouwkundig onderzoek bemoeilijkt wordt door de lange
    levensduur van bomen komt voort uit een onjuiste probleemstelling en zegt
    meer over de methode van onderzoek dan over het object daarvan.

9. Het in bosreservaten verzamelen van zoveel mogelijk gegevens ten behoeve
    van allerlei, niet omschreven bosbouwkundig onderzoek, is geldverspilling
    en leidt tot frustratie bij proefveldendiensten en tot overbelaste archi-
    varissen.

10. Het benadrukken van het multiple-use principe in de Nederlandse bosbouw
    wekt de schijn dat alle doelstellingen tegelijkertijd kunnen worden
    gewaarborgd en leidt tot konflikten tussen belangengroeperingen bij de
    uiteindelijke keuze van de beheersmaatregelen.

11. Bij voortgaande privatisering van het staatsbosbeheer is het meer dan
    voorheen noodzakelijk om naast het te produceren hout ook de recreatie-
    en natuurwaarde te betalen.

12. Gezien het belang van proefschriften bij het evalueren van de onderzoeks-
    prestaties van een vakgroep ligt het meer voor de hand dat de promotor de
    promovendus bedankt dan andersom.

VOORWOORD

Dit proefschrift bevat de resultaten van een onderzoek waarvoor de kiem werd gelegd in 1979 en 1980, tijdens een doctoraal leeronderzoek Theoretische Teeltkunde aan de Landbouwuniversiteit. Op initiatief van prof.dr.ir. R.A.A. Oldeman en dr.ir. C.J.T. Spitters leidde dit tot een promotie-onderzoek dat uiteindelijk resulteerde in dit proefschrift. Ik ben beide initatiefnemers dankbaar voor het in mij gestelde vertrouwen. Prof.dr.ir. C.T. de Wit was als promotor een uitstekende begeleider, die mijn bosbouwkundige benadering wist te verbreden tot een meer fundamentele kijk op gewasgroei. Zonder zijn kritische begeleiding en steeds weer motiverend commentaar was dit proefschrift niet mogelijk geweest. Prof.dr.ir. R.A.A. Oldeman liet mij de vrije hand bij de invulling van mijn onderzoek. Dankzij de vaak fundamentele verschillen van inzicht won mijn onderzoek aan duidelijkheid, het door hem tegelijkertijd in mij gestelde vertrouwen was een grote steun bij de voortgang. Beide promotoren hebben het manuscript van kritische kanttekeningen voorzien, waarvoor mijn hartelijke dank.

Bij de uitvoering van het onderzoek zijn velen behulpzaam geweest, de bereidwilligheid om mij te helpen was steeds een stimulans. Voor het veldwerk werd medewerking verleend door het personeel van de vakgroep Bosteelt en Bosoecologie van de Landbouwuniversiteit. De vakgroep Boshuishoudkunde en het Rijksinstituut voor onderzoek in de Bos- en Landschapsbouw 'De Dorschkamp' leverden de belangrijkste meetgegevens voor de toetsing van het model. Een deel van de chemische analyses werd door Mw. Vink van de vakgroep Bodemkunde en Plantevoeding van de Landbouwuniversiteit uitgevoerd onder EG-contract BOS-067, in het kader van het project 'Growth, yield and wood quality of Douglas fir'. De heren Waenink en Krabbenborg van de Stiboka waren zeer behulpzaam bij het veldbodemkundig werk, en wisten in enkele middagen tijd met hun enthousiasme mijn belangstelling voor de Bodemkunde aan te wakkeren. Het Centrum voor Agrobiologisch Onderzoek (CABO) verleende op velerlei gebied ondersteuning: bij het verzamelen en analyseren van monsters, bij de literatuurvoorziening, en door het verschaffen van rekenfaciliteiten in de laatste fase van het onderzoek. Mw. J. Burrough-Boenisch verzorgde vakkundig de Engelse korrektie van het manuscript. Aan de redaktionele afwerking werd in belangrijke mate bijgedragen door Mw. H.H. van Laar en Mw. C.G. Uithol-van Gulijk (vakgroep Theoretische Teeltkunde). Dhr. J. Engelsman van het CABO verzorgde de tekeningen. Het Landbouw Export Bureau droeg bij in de drukkosten van dit proefschrift.

De beide paranymfen ir. A.F.M. Olsthoorn en drs. P.J.M. Schoenmakers hebben het manuscript consciëntieus en kritisch doorgewerkt, en hielden mij op de been wanneer dat nodig was. Delen van het manuscript zijn tevens van commentaar voorzien door dr.ir. J. Goudriaan (Theoretische Teeltkunde), dr.ir. H. van Keulen (CABO) en dr.ir. C.J.T. Spitters (SVP).

Bij de totstandkoming van dit proefschrift was de stimulerende werksfeer bij de vakgroep Theoretische Teeltkunde van de Landbouwuniversiteit van groot belang, en ik dank alle medewerkers van de vakgroep voor de plezierige samenwerking en de genoten gastvrijheid gedurende de afgelopen jaren.

CONTENTS

1   GENERAL INTRODUCTION

1.1   Aim of the study

Forest growth and the accompanying changes in stand structure determine
the sustained yield of a forest stand. This holds for a multitude of types of
forest uses, from production of raw material as stemwood, to the production
of landscape elements and provision of the environment for leisure in an
industrialized society.

In order to assess potential forest use under particular conditions, the
interactions between forest growth and its environment must be studied. The
aim of the research reported here was to develop a simulation model that
could be used to study forest growth from knowledge of the underlying physio-
logical, physical, and chemical processes, and the influence of weather and
soils.

The environment for growth can be thought of as consisting of a number of
separate physical and chemical growth factors such as weather conditions, and
the availability of water and nutrients in the soil. The influence of the
main growth factors can be analysed by considering processes of growth and
development on a lower integration level than total stand growth. Mutual
interference from the underlying processes and their relationship with
environmental conditions can subsequently be integrated to give growth rates
for the stand. Combining this detailed information into a simulation model
for the stand, and comparing model outcome with field data, reveals growth
potential and allows potential forest use to be assessed in relation to plant
physiology and growing conditions. This approach can be used to assess new,
hitherto unknown situations such as the influence of a change in environmen-
tal conditions, if the accompanying influence at the process level is known.
Because of this, the approach is valuable for application in situations where
empirical data on total stand growth and yield are scarce, or where growing
conditions are evolving rapidly e.g. in young stands on recently afforested
sites. Also, an approach in which total stand growth is studied from under-
lying physiological processes allows the main factors that limit plant growth

in particular conditions to be determined, and may indicate the possibilities for increasing growth by management interventions.

1.2   Primary production in forests

Primary production in plant canopies is defined as the accumulation of dry matter resulting from assimilation of carbon dioxide by green plants, in which solar radiation is used as the basic source of energy to drive the biochemical processes (Newbould, 1967). The assimilation takes place mainly in the leaves and the carbon dioxide passes through the stomata in the leaf surface, thereby allowing water vapour to diffuse out of the leaf interior into the surrounding air. This loss of water from the plant to the atmosphere has to be compensated for by root uptake of water from the soil in order to prevent desiccation. The amount of carbon that is assimilated by the plant by means of photosynthesis is temporarily stored as sugar or starch, and is transformed into structural dry matter (mainly lignins, celluloses, fats, organic acids, proteins) by enzymatic reactions.

Not all assimilation products are used in the increase of dry matter: some of the assimilates formed in the photosynthetic process are used to maintain the living plant structure and provide the energy e.g. for loading transport vessels and maintaining ion gradients across membranes. The amount of assimilates required for this maintenance depends on metabolic activity, and on the total amount of living biomass present. It can be estimated from temperature, metabolic activity, and biomass amount and composition.

As well as carbon, hydrogen and oxygen, plants contain other chemical elements, such as nitrogen, phosphorus, sulphur, potassium, calcium and magnesium which have to be taken up from the soil. If the supply of any of these nutrients falls below the minimum requirement, growth is retarded or disturbed. The same holds for water availability in the soil: if root uptake is not sufficient to balance transpiration, the plant loses water; this in turn results in a gradual closure of stomata, with decreased uptake of carbon dioxide and hence a slowing down of growth.

Vascular plants are highly organized biological organisms, and dry weight increment follows prescribed morphological and architectural development patterns. This distribution of dry weight increment over the plant interferes

with primary production, because biomass components such as foliage, stems
and roots have different roles in primary production. In addition to this,
the separate biomass components differ in biochemical composition. The
distribution patterns are therefore very important for the development of the
canopy, and in determining growth yield.

From this point of view, the ecophysiological aspects of primary produc-
tion in plant canopies can be grouped into:

- absorption of photosynthetically active radiation by the foliage;
- uptake of carbon dioxide by assimilation through the stomata;
- loss of water vapour to the atmosphere through the open stomata, compensa-
  ted for by root uptake of soil moisture, and subsequent transport to the
  foliage;
- maintenance of the living biological structure, thereby consuming assimi-
  lation products;
- distribution of the assimilates available for growth over the plant
  organs, and conversion of assimilation products into structural dry
  matter, together with incorporation of nutrients in the organic matter;
- nutrient uptake by the roots.

If complete life-cycles either for biomass components, or for complete
plants or stands are considered, ageing and senescence, if relevant, have to
be added to the list above. In the list of growth aspects given above, only
vegetative growth has been considered. If the plant invests significant
amounts of assimilates in flowering and fruiting, this must also be taken
into account.

This general physiological approach to forest growth was already described
some sixty years ago in the classic work of Boysen Jensen (1932) who gave a
qualitative analysis of plant growth, with examples from beech forests in
Denmark. His line of thought was followed by a group of Danish workers,
notably Møller, Müller and Nielsen (Møller, 1945; Møller et al., 1954a,
1954b; Müller and Nielsen, 1965) and led to strong emphasis on physiological
aspects of forest growth in the works of Polster (1950, 1961) and Mitcherlich
(1970, 1975) in Germany. During the International Biological Program (IBP,
which ran from 1964 to 1974), the approach as such gained wide acceptance
(see e.g. various contributions in Setlik et al., 1970). During the IBP

decade, the first attempts to quantify and model of physiological aspects of crop growth were also made (e.g. de Wit, 1965). With regard to forest growth and yield, attempts were made to model distinct aspects of primary production, but overall quantification and modelling of forest stand growth were not pursued on a large scale, and the analysis of the physiological aspects of total forest growth remained restricted to qualitative approaches (Kira and Shidei, 1967). In general, forest growth and yield was treated in a descriptive, empirical way by measuring large numbers of permanent field plots, and constructing standard growth curves and yield standards in the form of yield tables or descriptive growth and yield models. If based on large enough numbers of representative stands, yield tables and their successors have proven to be very useful in practical forest management. Furthermore the use of extensive time series of permanent field plot data led to highly sophisticated statistical models enabling different types of forest management to be studied (see e.g. proceedings of the IUFRO Growth- and Yield groups: Fries, 1974; Fries, Burkhart and Max, 1978; Forstliche Bundesforschungsanstalt Wien, 1983).

However, the conventional descriptive approach to forest growth and yield had to rely on systems for classifying site and yield based on characteristics of the stands themselves, because the influence of the individual growth factors on yield was either not measured in the field, or the correlation of the separate growth factors with total yield appeared to be too weak to be used to estimate growth sufficiently accurately. As height growth appeared to correlate well with total stand growth, total stand height has very often been used to classify site potential. Nowadays site index is commonly expressed in absolute terms as some reference height, e.g. at a base-age of 50 years, or as an asymptotic value to be approached in old stands (Avery and Burkhart, 1983). In order to estimate site potential or the site index of a particular species for a given site, the height of a stand with known age has to be compared with tabulated data on stand growth.

Although often of great value for practical forest management, yield tables and descriptive statistical models of forest yield are unsuitable for investigating particular aspects of tree growth, and neither can they be used in situations outside the range of data on which they are based. As soon as management interventions that change growing conditions become important (e.g. in the case of forest fertilization) the use of descriptive yield

models becomes restricted. In order to overcome this, attempts have been made to incorporate biological aspects of forest growth in statistical models and yield tables, or to base the choice for any particular descriptive model on a general notion of biological phenomena (e.g. Pienaar and Turnbull, 1973; Reed, 1980). Due to lack of sufficient detailed knowledge of the relation between the individual growth factors and total stand growth, this approach has not been very successful so far.

During the IBP, much research effort was directed towards improving understanding of the biosphere and the ecology of the main vegetation types. Therefore, structure and function of forests (being one of the major forms of land use), were studied extensively and compared to that of other vegetations. This led to an increase in understanding of forest production ecology and ecosystem dynamics in general. However, no attempts were made to model individual stands. Instead, attempts were made to put forward a general theory of forest dynamics (e.g. Patterson, 1956; Kira and Shidei, 1967; Duvigneaud, 1971; Lieth, 1973; Reichle, 1981; Edmonds, 1982; Satoo and Madgwick, 1982; Shugart, 1984; Waring and Schlesinger, 1985).

Since the mid-1970's however, several comprehensive models of forest growth at the stand level have been or are being developed (Shugart et al., 1974; Lohammar et al., 1980; Ågren et al., 1980; Linder, 1981; Hari and Kellomäki, 1981; Hari et al., 1985; Sievänen, 1983; Rook et al., 1985). Most of this research focuses on fundamental production ecology rather than on investigation of forest growth and yield at the level of forestry practice. There is an obvious need to incorporate more biological background information and knowledge in descriptive models of forest growth. Furthermore, given large amounts of data assembled by conventional descriptive research on growth and yield as well as by more fundamental ecosystem analysis and research on plant physiology, it is now possible to bridge the gap between fundamental production ecology and practical forest growth and yield by means of ecophysiological modelling. The research reported in this thesis aimed to achieve this, following the approach outlined and applied in a pilot model by Mohren et al. (1984). In the following Chapters, a deterministic model will be described, based on physiological aspects of forest growth, such as photosynthesis, respiration, and increment of biomass dry weight. This model is compatible with the conventional approach of growth and yield: it allows the use of the data from existing permanent field plots, formerly used in

descriptive studies of forest growth and yield to be used in combination with detailed information on physiological processes obtained in laboratory experiments.

1.3   Modelling forest growth

Ecosystem modelling can be viewed as studying a complex ecosystem by model calculations to mimic experiments. In this way, specific parts of an ecosystem can be studied without experimenting with the system itself. It is often impossible to do the latter, because of ecosystem complexity, or as a result of the time-scales of the processes involved. In such situations however, separate processes on a lower level can often be sampled or measured fairly accurately. If the processes essential for total stand growth can be assessed in this way, assembling this information into a model can provide a way to study the behaviour and peculiarities of the real world system itself. Forest ecosystems can be viewed as complex, long-living biological structures in which many processes interact to determine stand structure and stand dynamics. Taking into account the large periods of time involved in stand development, modelling is a particularly powerful research tool in forestry and forest ecosystem analysis.

The quantification and integration of each individual process involved in forest growth is not a realistic aim for research, as the sheer complexity of plant growth prevents all the life processes concerned being incorporated in a single model. This is not a serious drawback, however, as not all aspects of plant growth have to be taken into account with the same detail when the emphasis is on total stand growth.

A convenient procedure is to start with the simplest possible model, which incorporates only the basic growth processes, such as the carbon dioxide assimilation and respiration, and the relation of these processes with environmental conditions. Subsequently, more detail can be introduced in the calculations by incorporating aspects such as the influence of soil characteristics on these processes. Following this line of thought, a set of typical production situations can be distinguished, based on the number and type of growth factors that are taken into account in the model (de Wit and Penning de Vries, 1982).

At first, only the optimal production situation is considered, with water and nutrients in ample supply, and with no pests and diseases. In that case, primary production is determined by the amount of photosynthetically active radiation absorbed by the foliage. If daytime ambient temperature is known, total canopy assimilation can be estimated, based on the photosynthetic-light response curve of the foliage.

Next, the influence of water shortage is taken into account through simulation of the stock of soil moisture. The latter is calculated as a running balance, depleted by root uptake, evaporation from the soil surface, and downward percolation, and replenished by precipitation. After hydrological influences on growth have been incorporated in the model, nitrogen and phosphorus are taken into account in the third production situation. In this model, only nitrogen and phosphorus are considered, as they have been shown to limit forest growth in many situations in coniferous plantations on the dry sandy soils of northwestern Europe (Gussone, 1974). Production situations in which nutrients other than nitrogen and phosphorus limit growth are not considered.

Both water and nutrients have a relatively constant influence on productivity, and these influences are to a large degree determined by the site. Disturbances that reduce productivity, such as pests, diseases and weeds, and also large-scale disturbances such as windthrow or frost have more irregular modes of action and have not been incorporated in this model; neither has air pollution.

This simulation approach is not limited to a particular species or type of forest, as it relies on general plant physiology. The basic growth processes in a particular case, however, have to be described in terms of parameters relevant for the particular species, or combination of species in the stand. In this study, the main emphasis is on the relation between site conditions and growth; stand structure is of secondary importance. In the model, structural aspects of a forest stand are dealt with only as far as is necessary for quantifying the relation between environmental factors and stand growth, e.g. canopy structure and light interception, and for quantifying competition in the estimation of individual tree growth from total stand growth.

In a dynamic simulation model which simulates systems behaviour over time,
a distinction can be made between rate and state variables. In the case of a
dynamic simulation of a forest ecosystem for periods of several decades,
living biomass components such as foliage, branches, stems and roots, can be
represented as state variables, with component increment rates as the rate
variables that, amongst others, determine biomass dynamics. In addition to
these primary state and rate variables, additional properties of the system
can be represented by intermediate variables. Environmental conditions can be
introduced as driving variables which are externally supplied to the model.
Internal relations, e.g. the distribution of total dry weight increment over
the plant organs, can either be simulated using submodels, or can be descri-
bed with simple equations that relate output directly to a set of input
variables, without going into details concerning the actual processes invol-
ved. The use of submodels is necessary if the dependence of the relations
concerned on several other factors has to be taken into account in some
detail (provided sufficient data are available to do so). In the elementary
descriptive treatment of an internal relation, a certain property is assumed
to be uniquely dependent on certain other well-known (or calculated) varia-
bles. This relationship can then be described by a forcing function, which is
used as input for the model.

There are four steps that can be distinguished in building a simulation
model. First, the research objectives have to be formulated, and the system
to be investigated defined. Both are mutually dependent, because research
objectives for system analysis should be realistic in that an appropriate
system to study should be definable. An ecosystem can be viewed as consisting
of interrelated elements that are influenced by the environment. For the
purpose of the analysis here, the system is best defined in such a way that
it in itself does not influence the environment to a significant degree
within the period concerned in the study.

Second, the model as a simplified representation of the system, should be
described in general terms. This second step is called model conceptualiza-
tion. During this step, the modelling approach is chosen, as is the degree of
detail (or generality) of the model. Model conceptualization also encompasses
the choice of the data to be used for estimation of input parameters and
model evaluation, and the hierarchical levels to be incorporated.

Third, the conceptual model is tested and evaluated. This is done by translating it into a computer program and subsequently comparing calculations with field measurements. From this comparison, conclusions can be drawn about the validity of the underlying assumptions. If these prove to be wrong, model conceptualization is reiterated, and a revised version of the model is tested.

After it is concluded that the model serves its purpose and does indeed mimic those aspects of the real world system that are of interest for the purpose of the research, the model can be used as a research instrument in the fourth and last step, to simulate experiments and thus to investigate possible future developments.

The construction of a model as described above, usually goes through several development stages whereby the model evolves from a crude pilot version to a large comprehensive model incorporating large amounts of details, and finally to some kind of summary model directed towards practical use. During this process of model development, the concept that lies at the basis of the model gradually changes as the relative importance of individual parts of the model becomes clear. As a result of this, the model can focus on key issues. This implies also that during model development it becomes possible to pinpoint areas where research is most needed, and to set priorities for future research.

1.4   The simulation model

As mentioned in Section 1.1, the objectives of this research consist of studying and quantifying the influence of environmental conditions and stand structure on the growth and yield of forest stands. To evaluate the simulation approach, the model is applied in a case-study of even-aged stands of Douglas fir. This species was chosen because of the relative abundance of data available on the physiology of Douglas fir and because of the availability of permanent field plots against which the model could be tested. Furthermore, Douglas fir is of increasing importance in Dutch forestry, where first generation Scots pine stands on former heathlands are being replaced by Douglas fir, if site conditions are favourable. In the model, the simulated period has to be long enough to encompass the large differences in stand structure that occur as a result of development, and therefore has to be as

long as the average rotation. For Douglas fir in the Netherlands, rotation length is 80 to 100 years long. This implies that the model should allow simulation runs covering a period of up to 100 years.

The data used to determine the physiological parameters of the model were either based on literature data on physiological processes, on laboratory measurements of characteristic physiological aspects, or estimated on the basis of general knowledge of the processes concerned. Parameters that characterize site conditions have to be sampled in the field. The best data to use for evaluation of a model consist of separate data sets for testing and evaluation of individual parts of the model, e.g. on the hydrology of the stand or on light interception. In addition, overall model behaviour should be checked against field data. For the latter purpose, the measurement series from permanent field plots that have been used in descriptive studies of growth and yield, are of great value. This study uses three permanent field plots and one temporary plot for the main evaluation of model outcome. The field plot measurements have been made available by the Department of Forest Management of the Wageningen Agricultural University (field plot with the code SP4, located in the "Speulder- en Sprielder" forest near the township of Kootwijk, and measured from 1947 to 1984), and by the Research Institute for Forestry and Landscape Planning "De Dorschkamp" at Wageningen (the field plots with the code D12, near the city of Apeldoorn, measured from 1923 until 1984, and with the code D25, located near the township of Putten, and measured from 1948 until 1984). The temporary plot was located near Wageningen. Measurements in the temporary plot consisted only of soil moisture measurements in 1983 and 1984. For an overview of the locations of the field plots, see Figure 1.1.
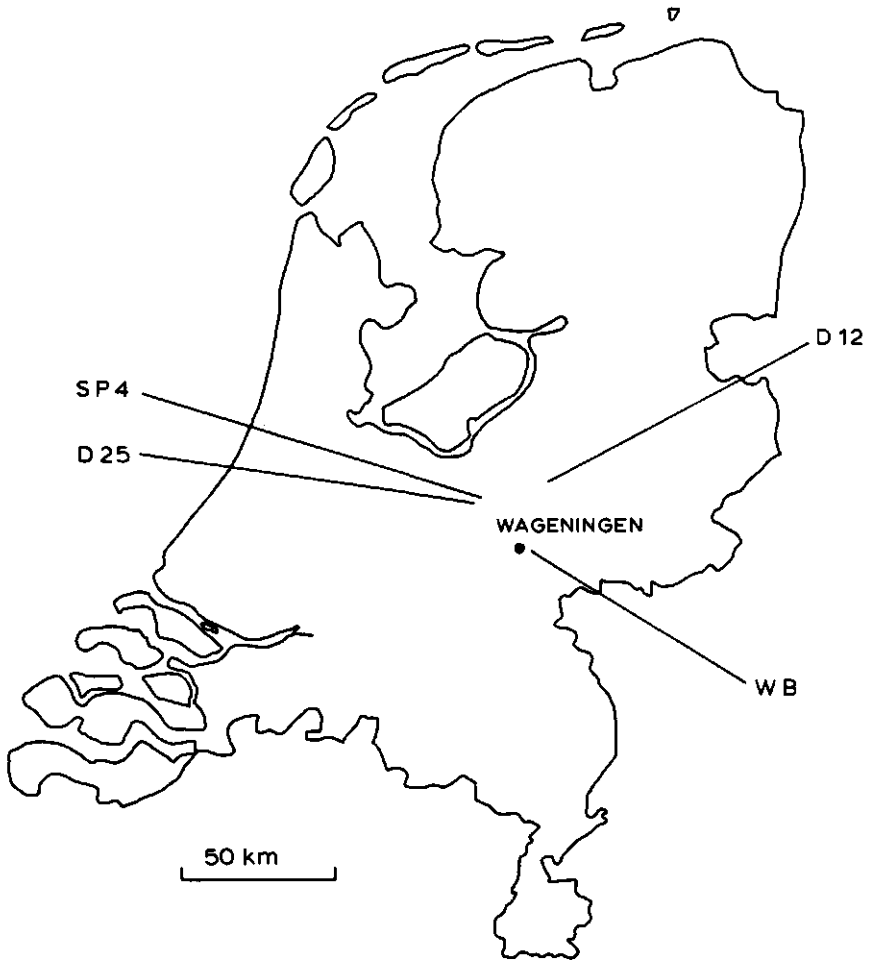
Figure 1.1
Location of the four field plots of Douglas fir, that were used to
evaluate the model.

The model produced by this research is programmed in CSMP (IBM, 1975). The present version of the model is based on an earlier pilot version (Mohren et al., 1984): given the number of different influences on growth that have been incorporated in the present model, it should be regarded a comprehensive model. For practical applications, it will be necessary to derive a summary model from the large model used here. As mentioned above, the model aims at simulating stand development over several decades in order to reveal forest dynamics, but at the same time has to take into account annual growth cycles as well, in order to allow the influence of certain factors, such as water availability, on growth to be estimated. This requires time steps of one day for the simulation program. A general relational diagram of the primary production part of the model is presented in Figure 1.2. The simulation program is available from the author upon request.
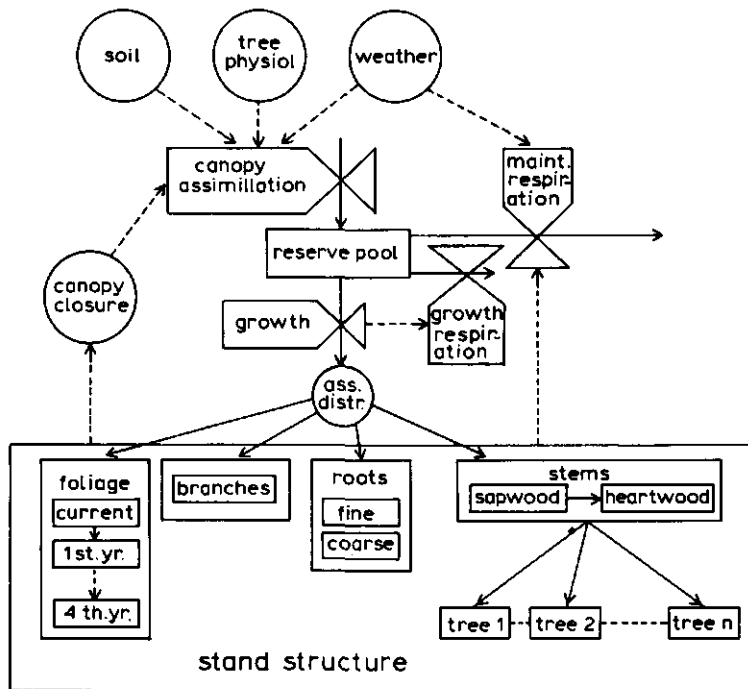
Figure 1.2
General relational diagram of the simulation model. Solid lines: material flows; dotted lines: relationships between rate variables and state variables, and between driving, intermediate, and rate variables.

2   SITE PROPERTIES AND CANOPY STRUCTURE

2.1   Introduction

In Section 1.2 it was mentioned that state, rate and driving variables are distinguished in a dynamic model. The state of the system at any moment, as far as considered relevant for the study, is quantified by a set of state variables, and a mechanistic modelling approach, as has been used in this research, relies on the assumption that the rates of change in the state of the system can be calculated entirely from the state variables in combination with the driving variables. The latter are supplied externally, and incorporate among others data on the climatological conditions of the site. Driving variables thus describe the exchange between a system and its environment, that is forced upon the system by the environment; therefore they are sometimes called forcing functions.

The relations between state and driving variables, and the accompanying rate variables incorporate the current knowledge of physical, chemical and biological processes that are considered to be relevant for the purpose of the study.

This Chapter describes the system and its environment in terms of state and driving variables. Chapters 3, 4 and 5 describe how the rate variables were calculated from state and driving variables. The rate variables lead to changes in the state of the system over time, and, in this case, describe forest dynamics.

First, the representation of site properties (weather and soils) in the model is described (Section 2.2). Section 2.3 describes the representation of the forest itself in terms of state variables for biomass and stand structure.

2.2   Site properties

2.2.1   Climate

To simulate growth over an earlier period of several decades, as in the case of the permanent field plots used in this study, the climatological information used as input to the model has to be derived from available meteorological records. Using meteorological data from standard weather stations also allows the model to be applied and tested under a wide range of different conditions. In the model, ambient weather (i.e. the immediate atmospheric environment of the stand) is calculated from the following driving variables: daily maximum and minimum temperatures (^{o}C), daily total global radiation (J cm^{-2}), daily average vapour pressure of the air (mbar), daily average wind speed (m s^{-1}), and daily precipitation (mm). Data on temperature, humidity, wind speed and global radiation were taken from meteorological observations at the local weather station in Wageningen. All the field plots were located within 50 km of Wageningen, and showed no major differences with regards to altitude or exposure. Radiation, temperature, vapour pressure, and wind speed data from the Wageningen weather station were used for the simulations covering the period 1974-1984. Temperature, vapour pressure and wind speed data for the simulation periods before 1974 were taken from meteorological records of the central Dutch meteorological station at De Bilt, which is 35 km west of Wageningen. Precipitation data were taken from rain gauge stations nearest to the individual plots, usually within a distance of 5 to 10 km (KNMI, 1935-1984). Whenever data were missing in the recordings of a particular station, average values of adjacent stations were used instead. If no data were available at all, e.g. because measurement devices had yet to be developed, averages from the first series of measure-ment that were available, were used. This is e.g. the case with the radiation data used for the 1920's, were equipment to measure global radiation was developed in Wageningen at the end of the twenties (Reesinck and de Vries, 1942; Prins and Reesinck, 1946; de Vries, 1955).

These weather variables act as forcing functions and are independent of the vegetation. Temperature, vapour pressure and global incoming radiation are assumed to be the same at the weather station (measured 2 m over short vegetation) and above a forest canopy (Pearce et al., 1980). In the model, a distinction is made between day-time and night-time conditions. Daylength and

weather conditions during the day are calculated using the expressions in
Table 2.1. The wind speed data used, were derived from measurements taken at
a height of 10 m over short vegetation. Using logarithmic wind profiles for
both short vegetation and forests, wind speed above the forest at some
arbitrary reference height (chosen here at 5 metres above the tops of the
dominant trees) can be calculated by assuming that wind speed is equal over
both vegetations at great height (e.g. at 100 m, Rutter et al., 1975). Wind
speed at great height was calculated from the wind profile over short vegeta-
tion using values for the zero-plane displacement (d) of 0.1 m and for the
roughness length (z_o) of 0.015 m.

The radiation regime is characterized by 3 components: visible short wave
radiation (400-700 nm), near-infrared short wave radiation (700-3000 nm) and
long-wave or thermal radiation (more than 3000 nm). In this study, ultravio-
let radiation has been ignored as it is a negligible component of the total
radiation budget (about 3 % at sealevel). In order to calculate light pene-
tration and canopy photosynthesis, a distinction must be made between direct
radiation from the sun and hemispherical diffuse radiation, caused by solar
radiation scattering in the atmosphere. Following Spitters et al. (1986),
global radiation (S_g) was separated into two fractions, one direct (f_{dir}) and
the other diffuse (f_{dif}), based on a measure of atmospheric transmission that
can be expressed as S_g/S_o. The radiation outside the earth's atmosphere (S_o)
was calculated from the time of the year (t, Julian date) and the radiation
at the outside of the atmosphere derived from the solar constant (1370 W m^{-2})
using expression 4 in Table 2.1. Using expressions 5a through 5d from Table
2.1 enabled the fraction that diffuse radiation (f_{dif}) formed in total global
radiation to be calculated.

All diffuse radiation was assumed to originate from a uniform overcast sky
with all parts of the hemisphere emitting an equal radiant flux density. All
radiation is important as a source of energy for transpiration and has to be
taken into account in energy balance calculations. For photosynthesis, only
the Photosynthetically Active Radiation (PAR) must be considered. The amount
of PAR is roughly equal to incoming visible radiation (400-700 nm, referred
to as 'light') and is about 50 % of the global radiation (Szeicz, 1974). The
term 'light' in connection with photosynthesis, is used here synonymously
with PAR. Outgoing long-wave radiation, needed to calculate the energy
balance of the vegetation, depends on the surface temperature and the water

Table 2.1

Equations for calculating of weather conditions from tabular input of global radiation (S_g in J $cm^{-2} d^{-1}$), daily maximum and minimum temperatures (T_{max} and T_{min} in °C), daily average vapour pressure (e_a in mbar), and daily average wind speed and its relative diurnal amplitude (v_a in m s^{-1} and A_v). Julian date is represented by t, λ is latitude of the site. Equations from Goudriaan (1977), Spitters et al. (1986), and van Keulen and van Heemst (1986). Values for A_v (varying from 0.25 in January to 0.67 in July) are taken from Wieringa and Rijkoort (1983).

Declination:

$$\delta = - 23.45 \times \cos(360 \times (t+10)/365) \quad\quad\quad\quad \text{(degr)} \quad\quad (1)$$

daylength:

$$D1 = 12 + 24 \times \arcsin(\tan \lambda \times \tan \delta)/180 \quad\quad\quad\quad \text{(h)} \quad\quad (2)$$

mean sine of solar height:

$$\sin \beta = \sin \lambda \times \sin \delta + (24/\pi) \times \cos \lambda \times \cos \delta \times$$
$$(1 - (\tan \lambda \times \tan \delta/(\cos \lambda \times \cos \delta))^2)/D1 \quad\quad\quad \text{(h)} \quad\quad (3)$$

maximum daily solar radiation:

$$S_o = D1 \times 0.36 \times \sin \beta \times 1370 \times (1 - 0.033 \times \cos(360 \times t/365)) \quad\quad (J\ cm^{-2} d^{-1}) \quad\quad (4)$$

fraction diffuse:

$$f_{dif} = 1 \quad\quad\quad\quad\quad\quad\quad \text{for} \quad\quad S_g/S_o \leq 0.07; \quad\quad (5a)$$
$$f_{dif} = 1 - 2.3 \times (S_g/S_o - 0.07)^2 \quad\quad \text{for } 0.07 \leq S_g/S_o \leq 0.35; \quad\quad (5b)$$
$$f_{dif} = 1.33 - 1.46 \times S_g/S_o \quad\quad\quad \text{for } 0.35 \leq S_g/S_o \leq 0.75; \quad\quad (5c)$$
$$f_{dif} = 0.23 \quad\quad\quad\quad\quad\quad \text{for } 0.75 \leq S_g/S_o. \quad\quad (5d)$$

outgoing long-wave radiation:

$$S_{lw} = - 8.64 \times \sigma \times (T_a + 239)^4 \times (0.56 - 0.092 \times \sqrt{e_a}) \quad\quad (J\ cm^{-2} d^{-1}) \quad\quad (6)$$
with σ equal to the Boltzmann constant ($5.688 \times 10^{-8}\ W\ m^{-2} K^{-4}$);

average daily temperatures:

$$T_a = (T_{max} + T_{min})/2 \quad\quad\quad\quad\quad\quad \text{(°C)} \quad\quad (7)$$

temperature during the daytime:

$$T_{a,d} = T_a + 0.25 \times (T_{max} - T_{min}) \quad\quad\quad\quad \text{(°C)} \quad\quad (8)$$

saturated vapour pressure:

$$e_{s,d} = 6.11 \times \exp (17.4 \times T_{a,d}/(T_{a,d} + 239)) \quad\quad\quad \text{(mbar)} \quad\quad (9)$$

relative daytime humidity:

$$RH_d = 100 \times e_a/e_s \quad\quad\quad\quad\quad\quad\quad \text{(\%)} \quad\quad (10)$$

vapour pressure deficit:

$$d_a = e_s - e_a \quad\quad\quad\quad\quad\quad\quad\quad \text{(mbar)} \quad\quad (11)$$

wind speed during the daytime:

$$v_d = (1 + 0.5 \times A_v) \times v_a \quad\quad\quad\quad\quad\quad (m\ s^{-1}) \quad\quad (12)$$

content of the atmosphere. It can be estimated from surface temperature and vapour pressure using the Brunt formula (Brunt, 1932, Equation 5 in Table 2.1, see also van Keulen and van Heemst, 1986), in combination with the degree of cloudiness. In the model the latter is approximated using f_{dif}, assuming clear sky conditions when $f_{dif} = 0.23$, and complete cloudiness when $f_{dif} = 1$. For completely clear skies the Brunt formula can be applied as such. For completely overcast situations ($f_{dif} = 1$), it was assumed that long-wave radiation is 10 % of the amount calculated with the Brunt equation for completely clear conditions.

Daily averages of global radiation, minimum and maximum temperature, vapour pressure of the air, and wind speed, were used as input in the way described above for the daily simulations for the years 1983 and 1984 only. For the simulations covering longer periods, monthly averages were used to generate daily values. For simulations using monthly means, the rainfall data were extended by the number of days with rain within the measurement period (KNMI, 1935-1984), and daily rainfall was generated from the monthly totals using a gamma distribution function with parameter estimates from Geng et al. (1985). In addition, normal distributions for global radiation and daily mean temperature were generated around the mean value that was supplied as forcing function. Standard deviations around the mean were taken from daily weather data in 1983 and 1984, and were applied to the whole period (1935-1984).

The microweather of a crop is defined as the immediate environment of the leaves or needles inside a canopy (Goudriaan, 1977). These conditions are determined by the input weather data (the conditions at some reference height above the canopy) on the one hand, and by the feedback from plants or soil on their micro-environment on the other. Plants influence their immediate environment e.g. by intercepting radiation, thereby shading lower parts of the canopy, or by gradually reducing wind speed within the canopy. Canopy surface roughness (expressed as a roughness length z_o; Monteith, 1973) determines the transport of momentum and thus the shape of the wind profile.

Temperature, humidity, wind and radiation change with depth inside the canopy, and their profiles can be simulated with detailed multi-layer models (Goudriaan, 1977; Chen, 1984). If the canopy is considerably rough, as with a tall forest stand, there is efficient air mixing and the gradients of temper-ature and humidity are small (Goudriaan, 1979). In that case, the model can

be simplified as far as transport of latent and sensible heat is concerned, to a 'big leaf' mono-layer model, by assuming temperature and vapour pressure inside the canopy to be the same as at the reference height above the canopy.

Using the approach from Goudriaan (1977, see Table 2.2), decreasing wind speed within the canopy can be estimated from wind speed at the top of the canopy (Equations 6 and 7 in Table 2.2), assuming an exponential extinction of wind speed inside the canopy. With Equation 7 in Table 2.2, wind speed below the canopy is calculated as u_c x exp ($- K_u/z_o$).

Table 2.2

Equations for calculating canopy roughness and aerodynamic exchange characteristics. Equations from Goudriaan (1977). u_r: Wind speed at reference height z_r; k: von Karman constant (about 0.41); w: average width of roughness elements, here taken as the average width of needle clusters (living branch with needles, about 0.5 m); Cl_d: Cluster density; CLAI: Cluster Area Index (ha ha^{-1}); L_c: Length of the living crown; z_c: Mean canopy height; c_d: drag coefficient for the roughness elements (= 0.2 for Douglas fir, Mayhead, 1973); and i_w a proportionality factor for wind speed, taken as 0.5 (Goudriaan, 177, p. 109, 112).

Mixing length:

$$l_m = (4 \times w \ / \ \pi \times Cl_d)^{0.5}$$
$$= (4 \times w \times L_c \ / \ \pi \times CLAI)^{0.5} \quad\quad (m) \quad\quad (1)$$

extinction coefficient for wind speed:

$$K_u = (c_d \times CLAI \times z_c \ / \ 2 \times l_m \times i_w)^{0.5} \quad\quad (-) \quad\quad (2)$$

zero-plane displacement:

$$d = z_c - (l_m \times i_w \times z_c \ / \ K_u)^{0.5} \quad\quad (m) \quad\quad (3)$$

roughness length:

$$z_o = (z_c - d) \times exp(- z_c \ / \ (K_u \times (z_c - d))) \quad\quad (m) \quad\quad (4)$$

friction velocity:

$$u* = u_r \times k \times (\ ln \ ((z_r - d)/z_o))^{-1} \quad\quad (m \ s^{-1}) \quad\quad (5)$$

wind speed at the top of the canopy (at height z_c):

$$u_c = (u* \ / \ k) \times ln \ ((z_c - d)/ z_o) \quad\quad (m \ s^{-1}) \quad\quad (6)$$

wind speed inside the canopy:

$$u_z = u_c \times exp (- K_u \times (1 - z/z_c) \ / \ z_o)). \quad\quad (m \ s^{-1}) \quad\quad (7)$$

Light intensity also decreases exponentially within the canopy, with different extinction coefficients for visible and near-infrared radiation. Light extinction can be calculated from the distribution and amount of intercepting surface (needle-, branch- and stem area) and their radiation properties. For calculations of primary production, the extinction within the canopy of the photosynthetic active radiation and its distribution over the needles, is estimated using a numerical integration. The integration routine requires light conditions at the top of the canopy for input. The calculation of canopy assimilation and growth, will be discussed in more detail in Chapter 3.

2.2.2 Soil characteristics

In order to calculate the influence of shortages of water and nutrients on growth, their availability in the rooted soil profile has to be estimated. For soil water, this can be done by simulation of total soil moisture in the rooted zone, and by estimating availability from the soil moisture retention curve: the relation between volumetric moisture content and soil suction or soil water potential. This curve can be determined experimentally, or derived from standard curves. For the present study, the curves were estimated from soil bulk density, amount of organic matter, loam fraction, and the median of the grain size distribution, using regression equations given by Krabbeborg et al. (1983) for sandy soils in the Netherlands. Table 2.3 gives the physical soil data for the four field plots used, together with the calculated soil suction curves.

The moisture holding capacity of the soil is characterized by the moisture content at field capacity, and in combination with the moisture content at permanent wilting point, this gives the amount of soil moisture that is available for uptake by plants. Moisture content at field capacity and at wilting point were calculated from the soil suction curve using a negative log-value of 2.3 for soil suction at field capacity, and a value of 4.2 at permanent wilting point. The moisture retention curve changes with soil depth because soil properties also change with depth. To account for the presence of soil layers with different moisture characteristics within the rooted zone, the soil profile was divided into five layers with separate suction curves for each layer.

Table 2.3

Bulk density, organic matter content, loam fraction, and the median of the grain size distribu-
tion for the four field plots, together with calculated Table of soil water potential (expressed
as pF) and corresponding volumetric soil moisture content (relation between pF and soil moisture
according to Krabbenborg et al., 1983).

Depth: (cm)	bulk density (kg/1)	org. matter (% DM)	loam (% DM)	M50	pore volume (% vol)	soil moisture (% vol) corresponding to pF values of:						
						1.0	1.5	2.0	2.3	2.7	3.4	4.2
D25:												
0- 60	1.30	2.0	20	180	50	43	36	21	17	14	10	6
60- 90	1.40	0.5	20	180	47	38	31	16	11	9	7	4
90-120	1.52	0.3	7	180	43	36	31	9	7	5	3	2
≧ 120	1.57	0.3	2	275	41	39	26	6	4	4	3	2
D12:												
0- 85	1.28	4.0	13	150	52	43	39	25	20	15	8	5
85-120	1.50	2.0	22	150	43	38	35	25	17	13	10	6
120-150	1.59	0.5	22	150	40	37	32	17	13	10	6	4
≧ 150	1.60	0.3	15	165	40	35	31	16	9	8	5	3
SP:												
0- 60	1.24	1.0	15	160	53	46	39	16	11	8	6	4
60-100	1.40	0.5	12	160	47	39	33	14	8	6	4	3
≧ 100	1.45	0.2	12	160	46	39	32	12	8	5	4	2
WB:												
0- 50	1.25	1.0	15	160	53	46	39	16	11	8	6	4
≧ 50	1.45	0.3	5	275	47	37	20	7	6	4	3	2

The field plots used in this study all lie on sandy soils in the centre of the Netherlands, with a water table between 5 and 15 metres below the soil surface; in the model only the full capillary zone has been taken into account, assuming no influence of a water table. Capillary rise from deeper, non-rooted zones of the soil profile was also considered negligible. The plots are all on flat terrain, and therefore lateral movements of moisture could be ignored.

In combination with the volumetric soil moisture content of each soil layer, total rootable depth determines the total amount of soil water that is potentially available to the trees. Unless the soil is either permanently water saturated or dried out beyond the wilting point, this rooting depth is determined by physical soil characteristics such as pore volume and pore distribution. If pore volume decreases (whereby bulk density is increased), and the remaining pores become smaller, the roots have to exert greater force to penetrate the soil. The limiting penetration pressure is about the same for a wide range of plant species, and equals about 300 N m^{-2} (Whiteley et al., 1981). An infiltrations pressure of around 300 N m^{-2} was measured at depths between 1.0 and 1.6 metres below the surface. Based on these penetro-meter observations in combination with the bulk density profiles as measured in the field, maximum rooting depth was estimated for the field plots used. Thus, for all plots used in this study, the maximum rooting depth varies between the plots from 1.0 m to 1.6 m below the soil surface. Simulation runs did not start before stand age 20, and it was assumed that the roots had occupied the complete rootable depth at the beginning of the simulations.

With regard to nutrient availability, only phosphorus and nitrogen were considered in this study, and both only in a elementary way. Following Wolf et al. (1986), average annual phosphorus and nitrogen availability were estimated from the total amounts of phosphorus and nitrogen in the rooted soil profile. The latter can be determined from standard soil analysis. Total nitrogen in the rooted zone in the field plots used varies from 4 000 to 15 000 kg N ha^{-1}, total phosphorus in the field plots is between 1 200 and 4 500 kg P ha^{-1} (Table 2.4). Soil nutrient status is treated more in detail in Chapter 5.

Table 2.4
Nitrogen and phosphorus contents, and organic matter content
for each soil horizon in the four field plots.

Depth:	org. matter	N-tot.	P-tot.
(cm)	(% C/.58)	(%)	(mg P/100 g)
D25:			
0- 20	2.56	0.04	16.9
20- 40	1.66	0.03	15.3
40- 60	1.34	0.03	14.3
60- 80	0.84	0.02	14.1
80-100	0.57	0.01	11.8
(100-120	0.50	0.01	10.0)*
D12:			
0- 20	5.44	0.14	42.4
20- 40	5.05	0.12	34.9
40- 60	4.99	0.11	32.0
60- 80	3.80	0.09	31.2
80-100	1.93	0.05	23.4
(100-160	1.50	0.03	10.0)*
SP4:			
0- 20	2.44	0.08	11.8
20- 40	1.72	0.04	10.7
40- 60	1.88	0.03	10.1
60- 80	1.09	0.02	10.1
80-100	0.84	0.02	9.1
(100-120	0.50	0.01	7.5)*
WB:			
0- 20	3.39	0.07	11.4
20- 40	2.30	0.06	11.0
40- 60	1.83	0.04	11.6
60- 80	2.04	0.03	10.3
80-100	1.49	0.03	9.4

* Soil layers below 100 cm were not sampled; soil characteris-
tics given are derived from data on the overlying soil layer.

2.3 Stand structure

2.3.1 Biomass state variables

Total biomass was separated into different components according to the
role these components play in the growth process; this separation reflects
harvest practice by explicitly taking into account the part of the biomass
that is harvested. To be able to evaluate a model's performance by comparison
its outcome with the field situation, model outcome has to be compatible with
field measurements. In the case of forest growth, this means that stem volume
rather than stem weight should be the main state variable simulated, and that
diameter at breast height (dbh) must be simulated, because this trait is the
main variable measured in the field.

In the model, total stand biomass is composed of the biomasses of foliage,
branches, stems and roots.

Foliage: Douglas-fir needles may live for up to 8 years (Fowells, 1965), but
have an average life span of 3 to 5 years (Burger, 1935; Silver, 1962).
Needle photosynthesis is age-dependent: current-year needles start at a low
rate of maximum photosynthesis after needle flush at the beginning of the
growing season. Maximum photosynthesis rate under light saturation increases
towards the end of the season, with the highest rates of photosynthesis being
reached in 1-year-old needles (Künstle, 1972, Leverenz, 1981) followed by a
gradual decline. To account for this in the model, total needle biomass has
been divided into 5 age classes containing current, one-, two-, three-, and
four-year-old needles. The age classes were simulated using a boxcar-train
approach (Goudriaan and van Roermund, 1987), with the net leaf increment as
the input for the zero-order boxcar that consisted of current-year needles.
After 5 years, the boxcar containing the 4-year-old needles was emptied.

Needle distribution within the crown volume is represented by a leaf area
density function. In general, the distribution of foliage area versus canopy
depth shows a maximum value in the middle or lower parts of the crown, and
foliage area density decreases both upwards and downwards. The location of
the maximum depends on crown form and density of the stand. Young conical
shaped crowns have the maximum closer to the bottom of the crown, older trees
show a more symmetrical distribution (Kestemont, 1970; Kinerson and Fritschen,

1971; Massman, 1982). This range in distributions can be covered adequately
with a parabolic leaf area density function which gives the amount of leaf
area per unit crown volume. In combination with a description of the crown
form that assumes a change from conical before canopy closure to parabolic
and eventually to cylindrical in older stands, this can be used to mimic the
above-described shift in maximum leaf area in relation to crown depth that
takes place as the trees age. The reason for choosing conical and parabolic
crown forms was the morphology of Douglas fir. This is discussed in Section
2.3.2.

The distribution of foliage biomass over the age classes is not the same
in different parts of the crown. Table 2.5 gives data on needle distributions
of some sample trees. The data show a concentration of foliage biomass in
current and one year-old needles in the upper parts of the crown, and a
greater amount of older needles in the bottom part of the crown. This sug-
gests that exposure to atmospheric influences affects the rate of needle
death. The middle third of the crown usually contains the largest proportion
of the total foliage. For this reason, and also because the distribution of
the needle biomass over the age classes in the period preceding the measure-
ments in 1984 was unknown, the model simulates an average distribution for
the whole crown, during the whole period simulated.

The distribution function itself was assumed to be the same for all needle
classes. This implies new needle growth also in the lower crown regions,
either accompanied by crown expansion or by flushing of adventitious buds
along the older branches (Edelin, 1977, 1981).

Based on average distributions of total needle weight of 15 %, 50 % and
35 % over the top, middle and bottom thirds of the crown respectively
(Kofman, 1982), the average distribution of needle biomass over the age
classes could be calculated from the data in Table 2.5. Table 2.6 gives the
results, together with literature data on foliage age-class distribution.

Table 2.5
Age-class distribution of needle biomass from 9 64-year-old
trees from plot D25, 3 57-yr-old trees from plot SP4, and 5
24-yr-old trees from plot WB. The trees were felled in Februa-
ry 1984, and therefore no current-year needles were present.
AGE = 1 - 4: needle age-classes.

	AGE	D25	SP4	WB
Crown tops:	1	44.5	49.4	71.5
	2	34.6	28.6	26.2
	3	15.6	16.4	2.3
	4	5.4	5.7	0.0
Middle part:	1	41.7	43.5	49.0
	2	31.6	26.8	34.3
	3	17.9	18.3	15.9
	4	8.8	11.5	0.8
Bottom part:	1	34.1	33.7	40.2
	2	31.7	29.2	35.5
	3	20.7	20.8	17.3
	4	13.5	16.3	6.9

Table 2.6
Measured distribution of needles over the age classes for the field plots D25,
SP4 and WB, together with literature data on Douglas fir needle distribution.
Trees in D25, SP4 and WB were sampled in February 1984, and the needles formed
in the preceding growing season were assigned to the class containing one-
year-old needles. Data from Silver (1962) and Kay (1978) are given for compa-
rison.

age cl.	D25	SP4	WB	Silver (1962)	Kay (1978)
1	39.5	41.0	49.3	28.	35.
2	32.1	27.9	33.5	23.	37.
3	18.5	18.9	14.4	17.	20.
4	9.9	12.3	2.8	13.	7.
older:	-	-	-	19.	1.

Branches: In the model, total branch biomass is represented by one state
variable only. No distinction was made between twigs, bark and branch wood in
large branches, because there were no detailed data for calibrating an
elaborate branch model. For all branch biomass a constant life-span of 30
years was assumed. With regard to position in the canopy, branch biomass was
assumed to be distributed homogeneously throughout the crown volume.

Stems: Stem biomass consists of bark, living sapwood, and dead heartwood.
Bark biomass is only a small proportion of total stem biomass and was not
explicitly considered, but was incorporated in total stem biomass. Both
sapwood and heartwood were represented by separate state variables. Sapwood
was calculated as the integral of stem increment minus the amount of wood
that has been converted to heartwood. Under normal circumstances heartwood
formation is an ageing process (Ziegler, 1967; Bosshard, 1974) in which
nutrients, notably nitrogen and phosphorus, are retained by the outer growth
rings of the living sapwood, and wood moisture decreases from about 45 vol %
in the sapwood to 25 vol % in the heartwood. From Figure 2.1 it can be seen
that in the case of Douglas fir, this transition occurs after about 15 to 20
years. The heartwood formed by transition from sapwood serves only as mechani-
cal support for the tree, and does not contain any living cells; hence it
does not require assimilates for maintenance respiration. In the model, total
stem biomass is represented not as an integral of stem dry weight, but as the
sum of the bole volumes of the individual trees (total stem volume). Stem
increment, expressed as volume increment, was calculated by dividing dry
weight increment by the amount of dry weight per unit of fresh stem volume
(average basic density).

Roots: Data on total root biomass and on root turnover are scarce. Because of
the difficulties of measuring these phenomena, and the large temporal and
spatial variations involved, the range of observations reported in the
literature is wide. In the present study, root biomass was treated as consis-
ting of two components: a fine root component (without secondary thickening)
and a coarse root component, both represented by separate state variables.
Coarse-root biomass was assumed to have a turnover rate (the rate of dying in
tonnes $ha^{-1}yr^{-1}$ divided by total living biomass in kg ha^{-1}) of the same order
of magnitude as for branch biomass. The turnover of fine roots appears to be
much more rapid. Santantonio and Hermann (1985) report turnover rates between
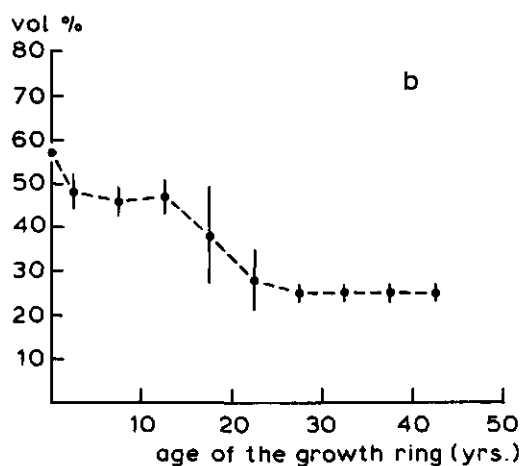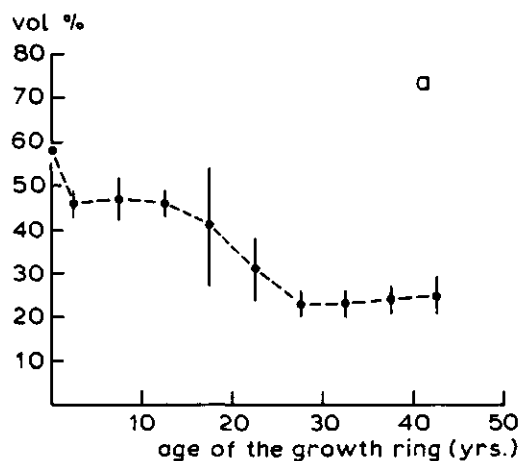1.7 and 2.5 yr^{-1}, depending on the wetness of the site, with an average value

Figure 2.1

Moisture content of Douglas fir stem wood expressed as percentage of dry weight of the stem wood, in relation to age of the growth ring. Vertical bars indicate the standard deviation around the sample mean. a: 10 trees taken from plot D25; b: 3 trees taken from plot SP4. The measurements relate to stem discs taken 2 m above the ground.

for the fine root turnover rate of 2.0 yr^{-1} on moderately wet sites. These
values, combined with the amount of assimilates available for root growth in
the present model, resulted in values for fine root biomass of around 1 000
to 2 000 kg ha^{-1}, which were considered too low for Douglas fir; therefore, a
root turnover rate of 1 yr^{-1} was used in the model instead.

To simulate the water balance of the plants, the water content of the
living tissue must be known. The average water content of the living needle,
branch, sapwood, and root biomass equals 55 %, 55 %, 45 % and 55 % of fresh
weight respectively (data obtained from sampling trees from the field plots).
With a total living biomass varying between 1 x 10^5 and 1.5 x 10^5 kg ha^{-1},
this gives the amount of water incorporated in the plant tissue to be the
same order of magnitude as a water column of 10 to 15 mm.

2.3.2   Crown and canopy structure

In the model the state variables that are distinguished at the canopy
level in addition to the biomass state variables described in Section 2.3.1
are crown form and crown dimensions, total stand height, and the number of
trees in the stand.

Crown form in coniferous trees is usually represented by cones (Edelin,
1977; Kellomäki, 1982), or combinations of cones and cylinders. As the trees
age, crown forms become blurred because of the cumulative effects of distur-
bances during crown development, damaged branches (wind damage), and adventi-
tious branching which may disrupt the regular branching pattern. Other
important factors regulating crown form are tree density, the spatial distri-
bution of the trees in the stand and the position of their crowns in the
canopy.

To take the foregoing into account, an individual-tree model incorporating
branching structure and irregular crown development, such as the one used by
Mitchell (1975), would be needed. The model used in the present study does
not take individual tree-to-tree distances into account, and simulates
average crown characteristics only. These are used to estimate horizontal
canopy closure in terms of interception of photosynthetically active radia-
tion. Tree architecture determines the interception of radiation by the
foliage within the crown. The distributions of leaf and wood surfaces within

the crown determine vertical canopy closure and the distribution over the leaves of the amount of radiation available for photosynthesis and transpiration. Tree architecture and morphology as used in Hallé et al. (1978), constitute the boundaries within which net dry weight increment of a tree is distributed over the biomass components, and also give an indication of possible crown forms. As with many temperate zone coniferous trees, Douglas fir seems to exhibit an architectural growth pattern that is intermediate between the architectural model of Massart and the model of Rauh (Edelin, 1977, 1978; Evers, 1981a, 1981b; for a description of these models see Hallé and Oldeman, 1970, and Hallé et al., 1978), and the shape of the crown can be adequately described as a cone or a cylinder. Typically, the crown form of a young Douglas fir is cone-shaped, and tends to change into a more parabolic or cylindrical shape as the tree grows. In the model this is described by descriptive crown parameter (A) which determines crown radius (R_c) as a function of distance from the top of the tree and crown radius at the base of the crown (R_b) using $R_c = (1_i/1_c)^A \times R_b$, with 1_c representing crown length (m), 1_i representing the distance from the top of the crown (m); and R_b crown radius at the base of the crown (m). A = 1 results in a conical crown form, 0 < A < 1 gives a parabolic crown shape and A = 0 results in a cylinder. To simulate changes in crown form during stand development, the parameter A equals 1 in juvenile trees and decreases from the moment that stand height growth culminates. The parameter A eventually approaches zero when maximum stand height is approached. This results in a cylindrical approximation of crown shape in older stands.

Stand height in even-aged stands is usually characterized by the dominant height of the stand (h_{dom}), which is defined as the mean of the height of the highest tree in each of the 10 m x 10 m squares after the surface area of the plot has been divided as such. The development of h_{dom} usually follows an S - shaped curve, which can be characterized by the Chapman-Richards growth function (Richards, 1959; Pienaar and Turnbull, 1973):

$$h_{dom} = S \times (1 - \exp^{- c1 \times t})^{c2} \qquad \text{(m)} \qquad (2.1)$$

with t stand age in years, and S the asymptotic value for dominant height at older ages, usually called Site Index. The coefficients c1 and c2 in expression 2.1 are the regression coefficients determining the shape of the curve. Because the model uses height growth as a forcing function, these empirical

surface and maximum rooting depth. In the model the soil compartment is trea-
ted as a one-dimensional system, and no spatial heterogeneity in the horizon-
tal plane is taken into account.

A forest stand is simulated here as a collection of individual trees. This
has to be taken into account for two reasons: First, the number of trees,
their spatial arrangement and the dimensions of the individual crowns deter-
mine the degree of horizontal canopy closure and thus the degree to which a
production level (determined by availability of water and nutrients) is
actually attained in the field. Second, marketable yield does not consist of
stem-volume per se, but of a total number of stems with different dimensions.
Total number of stems and their sizes can be represented with different
degree of sophistication. In combination with models of whole stands as used
here, a frequency distribution describing the variation in size of the trees
within the stand is often used, usually by employing some kind of diameter
distribution (see e.g. Alder, 1979; van Gerwen et al., 1987). The model
described here is limited to simulating average tree sizes only, as most
emphasis was on total stand growth and its correlations with site conditions.
Using an earlier version of the model, it was shown that incorporating tree
size distribution poses no additional problems (van Gerwen et al., 1987;
Mohren et al., 1984).

3   PRIMARY PRODUCTION

3.1   Introduction

Primary production of a plant canopy is defined as the accumulation of dry
matter by means of carbon dioxide assimilation using solar radiation. Canopy
photosynthesis can be calculated as the sum of the contributions of the
individual foliage layers. Under optimal production conditions (defined here
as optimal supply of water and nutrients, and absence of disturbances as
pests and diseases), leaf photosynthesis at air temperature is directly
related to the amount of photosynthetic active radiation absorbed by the
foliage, and given the temperature of the air, canopy photosynthesis can be
calculated from individual leaf photosynthesis once both the canopy light
climate and the position of the foliage area within the crown canopy are
known.

In order to arrive at an estimate of net dry matter production per unit
time, the maintenance requirements of the living biomass have to be taken
into account, together with the efficiency of converting the resulting
carbohydrates into structural plant matter.

Net increment of the separate biomass components can now be calculated
from the distribution of net primary production over the plant parts and the
death rate of the biomass components. The latter results in a steady loss of
leaves, branches and roots to the litter. Only live biomass should be consid-
ered when maintenance requirements are calculated. Of the stemwood, only the
sapwood contains living cells, and the transition from living sapwood to dead
heartwood parallels the loss of needles, branches and roots as litter, and
was treated in the model in essentially the same way. The net growth rates
for the biomass components (i) can then be expressed as:

$$G_{n,i} = DWC_i \times DC_i \times (P_g - R_m) - L_i \qquad (kg\ ha^{-1}yr^{-1}) \quad (3.1)$$

with $G_{n,i}$: net component dry matter increment; DWC_i: conversion efficiency
expressed as kg DM formed per kg CH_2O; DC_i: the allocation to component i, of

assimilates available for growth; P_g: Gross canopy assimilation; R_m: total maintenance requirements; and L_j: litter loss or death rate.

The approach used in this study was essentially that described half a century ago by Boysen Jensen (1932), and later used in a qualitative sense by researchers such as Polster (1950) and Kira and Shidei (1967). de Wit (1965) published a calculation model based on the same theory. The forest simulation model described in this thesis is derived from the BACROS simulation model (de Wit et al., 1978), and the SUCROS summary model again derived from the latter (van Keulen et al., 1982; van Kraalingen et al., 1987). The microclimate simulations with regard to the light climate follow Goudriaan (1977, 1979), and van Gerwen et al. (1987). Leaf photosynthesis is represented according to Goudriaan (1982), and canopy photosynthesis is calculated using the approach from Spitters (1986).

This Chapter gives the procedures used to calculate the amount of radiation intercepted by the leaves and branches, based on the distribution of leaf and branch areas within the crown as described in Section 2.3. From this, photosynthesis and net biomass component increment under optimal growing conditions can be calculated.

For the interception of rainfall by the canopy, essentially the same procedure as for light interception was used, using the equations for black leaves. This is treated in Chapter 4.

3.2   Light climate

In order to estimate the rate of photosynthesis from a photosynthesis light response curve, the flux of photosynthetically active radiation (PAR) that is absorbed by the foliage must be calculated. PAR is roughly equal to the visible part of the spectrum, and will henceforth be referred to as 'light'. The extinction of incoming radiation in a foliage canopy is approximately exponential with the amount of intercepting needle and branch surface area (represented by LAI and BAI) measured from the top:

$$I = I_o \times exp^{- (k_L \times LAI + k_B \times BAI)} \qquad (W\ m^{-2}) \qquad (3.2)$$

in which I_o and I are radiation levels (PAR) above and below the canopy respectively; k_L is the extinction coefficient for leaf surface area, and k_B is the extinction coefficient for branch surface area. For the extinction of radiation inside the crown canopy the extinction by the stem surface area can be ignored as this is some 5 % of total projected area index. This is not the case when total interception of radiation at the forest floor by a dense stand of tall trees is considered. In that case, projected bole area can decrease radiation at the forest floor by an additional 20 - 30 % (Halldin, 1985).

In calculating light distribution over the leaf layers in the canopy using Equation 3.2, three fluxes of light must be considered: 1) the flux of diffuse radiation that reaches all foliage area, 2) the unobstructed flux of direct radiation that is scattered and absorbed by the sunlit foliage area only, and 3) the additional flux of direct radiation that results from scattering of unobstructed direct radiation by the sunlit foliage area. Sunlit foliage receives the sum of the three fluxes, shaded leaves receive the flux of diffuse radiation together with the flux of scattered direct radiation.

Using this approach the amount of PAR absorbed at any level in the canopy can be calculated from the incoming radiation at the top. The conditions at the top of the canopy are characterized by the total flux of photosynthetically active radiation, together with its composition in terms of diffuse and direct radiation.

Equation 3.2 has been derived for canopies with random distribution of leaf and branch areas, but has been proven to be valid in a wide range of closed crop canopies. If the area distribution in the canopy deviates too much from the random model, the equation cannot be applied in its simple form, but has to be modified. This can be done by explicitly taking into account the gaps in the canopy through which radiation travels freely to the forest floor, and by taking into account the clustering of the intercepting surface within the crown (as is e.g. the case when leaves are clustered around branches and when branches occur in distinct whorls, see Figure 3.1).
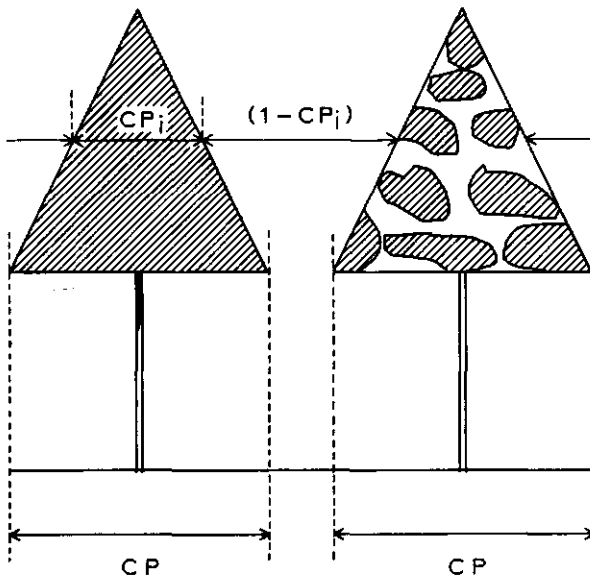
Figure 3.1
Levels of clustering of the foliage in a forest canopy. Left:
clustering of the foliage in separate tree crowns, accounted for in
the model by estimating horizontal canopy closure; Right: clustering
of foliage around branches inside the tree crown, resulting in
increased transmission of radiation through the crown canopy.

These three degrees of detail in modelling a forest canopy are described
in the following sections. Model I refers to a uniform canopy with a non-
clustered distribution of leaf and branch areas; Model II, the horizontally
discontinuous canopy, takes into account horizontal canopy closure based on
crown geometry and crown dimensions and allows for light passing through gaps
between adjacent tree crowns; Model III allows in addition to model II for
clustering of foliage area within the crowns of the trees.

3.2.1   Model I: Horizontally uniform canopy

In this simple model situation, both leaf as well as branch surface areas
are assumed to be distributed at random within the sublayers of the canopy.
Total leaf and branch area are calculated from total simulated leaf and
branch weights using a specific foliage area of 5.3 m^2kg^{-1}, and a specific

branch area of 0.3 m^2kg^{-1}. Based on the simple extinction model (Equation 3.1), total radiation extinction can now be calculated if the radiation characteristics and angular distribution of the leaves are known. In the model, a spherical leaf angle distribution was assumed. All branch surface area is assumed to be horizontal in accordance with the plagiotropic branch differentiation in the Massart architectural model (Hallé et al., 1978; Evers, 1981b). Leaf transmission (τ) and reflection (ρ) are assumed to be equal, and to be half of the scattering coefficient σ: $\tau = \rho = 0.5 \times \sigma$. The expressions to calculate the extinction coefficients for horizontal elements, spherical elements with direct radiation, and spherical elements with diffuse radiation, respectively, are:

$$k_h = (1 - \sigma)^{0.5} \tag{3.3}$$

$$k_{sph,dir} = \frac{0.5 \times (1 - \sigma)^{0.5}}{\sin \beta} \tag{3.4}$$

$$k_{sph,dif} = 0.8 \times (1 - \sigma)^{0.5} \tag{3.5}$$

The scattering coefficient depends on the wavelength of the incoming radiation: Jarvis et al. (1976) give values for coniferous species of $\sigma = 0.10$ for visible light and $\sigma = 0.7$ for near infrared radiation. The branch surface is treated as effectively black ($\sigma = 0$). The extinction coefficient for horizontal surfaces k_h, is the same for diffuse and direct radiation; $k_{sph,dir}$ and $k_{sph,dif}$ are the extinction coefficients for spherical leaf angle distributions and direct and diffuse light respectively. Equations 3.3 to 3.5 are valid only when $\tau = \rho$. Substitution of $\sigma = 0.10$ for the foliage in Equations 3.3 to 3.5, and using a value for β of 30° (the average value for β during the growing season at 52 ° northern latitude), gives values of 0.95 for $k_{dir,L}$, the coefficient for extinction of direct radiation by the foliage, and 0.76 for $k_{dif,L}$, the coefficient for extinction of diffuse radiation. For branches, Equation 3.3 gives a value of 1 for the extinction coefficient (k_B) for both direct and diffuse radiation. To calculate the unobstructed penetration of direct light into the canopy, an extinction coefficient for black leaves ($k_{dir,bl}$) must be calculated. Setting $\sigma = 0$ gives the expression $0.5/\sin \beta$ for $k_{dir,bl}$, with for example $\beta = 30°$ giving a value of 1.0.

If LAI is greater than 4 to 5, most of the reflection back to the atmosphere comes from the foliage, and the influence of the soil surface in total canopy reflection can be ignored. Usually, the amount of branch area is small compared to the leaf area (Halldin, 1985), and total canopy reflection can be approximated using (Goudriaan, 1977):

$$\rho_{c,h} = \frac{(1 - (1 - \sigma)^{0.5})}{(1 + (1 - \sigma)^{0.5})} \tag{3.6}$$

$$\rho_{sph,dir} = \frac{2}{(1 + 1.6 \times \sin \beta)} \times \rho_{c,h} \tag{3.7}$$

$$\rho_{sph,dif} = \rho_{c,h} \tag{3.8}$$

The total canopy reflection coefficient for incoming visible radiation can now be estimated as $\rho_c = (1 - f_{dif}) \times \rho_{sph,dir} + f_{dif} \times \rho_{sph,dif}$.

The amount of radiation per unit of foliage at any canopy level i can now be calculated on the basis of the derivative of Equation 3.2, for the diffuse flux, the total direct flux, and the direct component of the direct flux respectively:

$$I_{abs,dif} = (1 - \rho_{sph,dif}) \times I_{o,dif} \times k_{dif,L} \times$$
$$\exp^{-(k_{dif,L} \times LAI_i + K_B \times BAI_i)} \tag{3.9}$$

$$I_{abs,dir,tot} = (1 - \rho_{sph,dir}) \times I_{o,dir} \times k_{dir,L} \times$$
$$\exp^{-(k_{dir,L} \times LAI_i + k_B \times BAI_i)} \tag{3.10}$$

$$I_{abs,dir,dir} = (1 - \sigma) \times I_{o,dir} \times k_{dir,bl,L} \times$$
$$\exp^{-(k_{dir,bl,L} \times LAI_i + k_B \times BAI_i)} \tag{3.11}$$

with LAI_i and BAI_i the leaf and branch area indices of the part of the canopy extending above level i.

Shaded leaves receive both diffuse radiation and the scattered component of direct radiation:

$$I_{abs,sh} = I_{abs,dif} + (I_{abs,dir,tot} - I_{abs,dir,dir}) \qquad (3.12)$$

$I_{abs,dir,tot} - I_{abs,dir,dir}$ represents the diffused component of direct radiation that is absorbed by the shaded leaves.

The amount of light received by the sunlit foliage consists of the flux received by the shaded leaves plus the direct component of the direct flux. If leaf angles vary, as with a spherical leaf angle distribution, the angle of incidence of the direct flux is not constant, and the assimilation rate has to be integrated over the leaf angles. This can be done using the absorption of the direct component of the direct flux by foliage elements perpendicular to the direct beam (de Wit, 1965):

$$I_{sl,dir} = (1 - \sigma) \times I_{o,dir} / \sin \beta \qquad (3.13)$$

The assimilation rates of the sunlit and of the shaded foliage will be dealt with in Section 3.3 (Equation 3.31).

In order to estimate canopy photosynthesis from the amount of light absorbed by the foliage, as described above, the fraction of total leaf area that is sunlit (f_{sl}) must be calculated. The fraction sunlit leaf area equals the fraction of the direct beam that reaches canopy level i:

$$f_{sl,i} = \exp^{- (k_{dir,bl,L} \times LAI_i + k_B \times BAI_i)} \qquad (3.14)$$

3.2.2   Model II: Horizontally discontinuous canopy

When the canopy contains considerable gaps through which radiation passes unobstructed, then these gaps must be accounted for. This can be done most simply by considering perpendicular crown projection area; however, as a

forest canopy can have considerable depth relative to gap dimension, and most incoming radiation does not come from the sky directly above the gap, this leads to considerable underestimation of canopy closure. Therefore, horizontal canopy closure has to be estimated with regard to the angle of incidence of the incoming radiation. Thus horizontal canopy closure (C_h) is defined as the degree of canopy closure with regard to incoming solar radiation, with the individual crowns viewed as solid black bodies. In that case the radiation intercepted by a solitary crown depends on crown shape (defined by the shape parameter A, see Section 2.3.2) and crown dimensions, which were characterized by the crown radius at its base R_b and crown height l_c (see Figure 3.2a and 3.2b). If light is direct, the ratio CPC between the actual shadow area (CC), and the area of perpendicular crown projection for an isolated tree (CP = π x R_b^2, see also Figure 3.2), can be calculated as (example for a cylindrical crown, A = 0, and for a conical crown, A = 1):

$$CPC_{dir,A=0} = 1 + 2 \times \tan(90 - \beta) \times l_c / (\pi \times R_b) \qquad (3.15)$$

$$CPC_{dir,A=1} = (\pi - \theta_o + \sin \theta_o \times \tan \alpha \times \tan(90 - \beta)) / \pi \qquad (3.16)$$

with $\theta_o = \cos^{-1}(\tan \beta \times \tan(90 - \alpha))$ and with $\alpha = \tan^{-1}(l_c/R_b)$, see also Figure 3.2b.

For diffuse radiation the amount of radiation intercepted is related to the crown mantle area, and CPC_{dif} becomes:

$$CPC_{dif,A=0} = (\pi \times R_b^2 + l_c \times R_b) / (\pi \times R_b^2)$$

$$= 1 + l_c / (\pi \times R_b) \qquad (3.17)$$

and

$$CPC_{dif,A=1} = \pi \times R_b \times (l_c^2 + R_b^2)^{0.5} \times (1 + \cos \alpha) / (2 \times \pi \times R_b^2)$$

$$= (1 + 1 / \cos \alpha) / 2 \qquad (3.18)$$

The calculations can be carried out at any level (i) in the crown canopy, giving estimates of horizontal canopy closure $(C_{h,i})$ from crown radius (R_i), perpendicular crown projection area (CP_i) and crown length (l_i) extending above the particular level i.
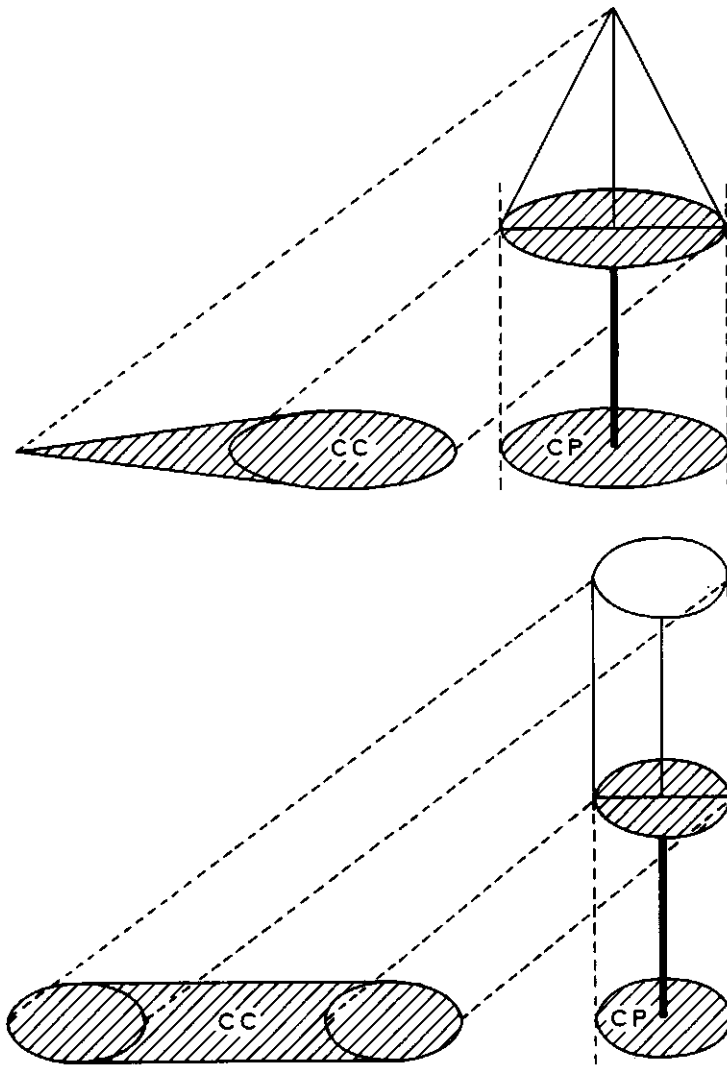
Figure 3.2a
Projection areas of a cone (above), and of a cylindrical-shaped
crown (below). CC: effective crown projection area, with regard
to incoming radiation with an angle of incidence β.
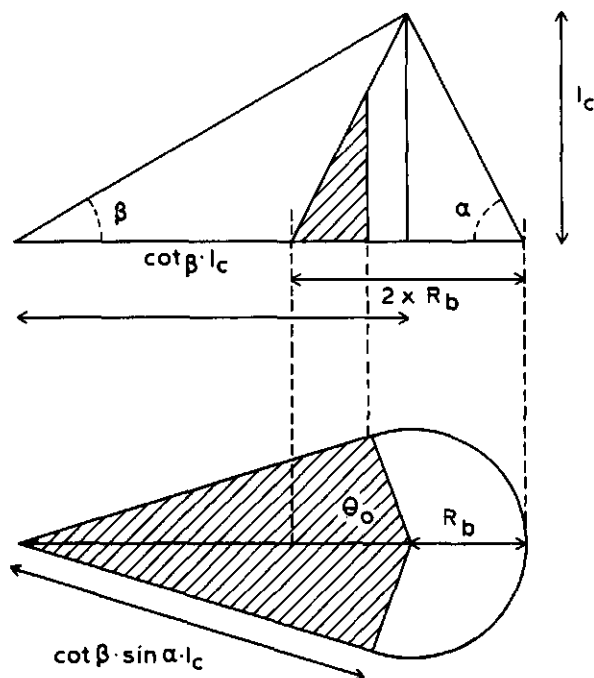
Shadow cast by a cone of height 1_c and base radius R_b for solar height β. See text for an expression of θ_o.

To estimate the degree of horizontal canopy closure (C_h) of a stand of trees with black crowns two approaches are possible: to estimate the fraction of total radiation that is intercepted by the crowns, or to estimate its complement: the fraction of radiation transmitted through the gaps. For diffuse radiation, C_h is best estimated from total gap area, number of gaps and canopy depth. This can be approximated by estimating the fraction of diffuse radiation relative to an open field situation, that passes through an average gap. For direct radiation, the calculations quickly become cumbersome, as the position of the individual tree crowns within the canopy vis-à-vis the position of the sun determines whether direct radiation is transmitted between the crowns. As these individual tree positions are not taken into account in our model, the calculations have been confined to diffuse light

only, and it is assumed that the degree of canopy closure for diffuse light holds for direct light also.

Total gap area in m^2 equals $1 - N \times \pi \times R_b^2$, with N representing the number of trees per m^2, and R_b equal to the mean crown radius at the base of the live crown. In the standardized situation with the trees in an equilateral triangle spacing, the total number of gaps (n) is best approximated by 2 x N. The surface area of an individual gap (G) equals $1/n - \pi \times R_b^2$. In the case of a squared lattice planting, it is more appropriate to set the total number of gaps (n) equal to the number of trees N, instead of to 2 x N.

If a canopy has closed completely by horizontal crown expansion, and the stand has subsequently been thinned (with the trees that have been removed evenly distributed in the stand) then the number of gaps is set equal to the number of trees removed by the thinning. In the case of thinning in an open stand with incomplete crown closure thereby creating a number of additional, large gaps, the number of gaps after thinning is set to equal the mean of the number of gaps before thinning, and the number of gaps created by the thinning operation (the number of trees that were thinned). In this way, it was accounted for in an approximate way, that there are a number of small gaps remaining from the situation before thinning, together with a number of large, new gaps.

The amount of diffuse radiation transmitted through the gap, expressed as the a fraction of the diffuse radiation that a horizontal surface with the same area would receive from an unobstructed uniformly overcast sky, is now estimated by calculating this fraction for a square gap with side s = $\sqrt{G}$, and with sloping side walls of total height l_i, where l_i equals the distance between the top of the trees and the canopy level for which canopy closure is calculated (see Figure 3.3).

For the distance R between the projected border of the gap at the top of the canopy and at the level at which canopy closure is calculated, the weighted average of the crown radius (R'), and the distance from a point halfway between two adjacent crowns to the nearest second order crown (R'', see Figure 3.4), is taken. In this case, the weighting is done proportional to the ratio of crown diameter over the average tree-to-tree distance. When this ratio equals 1, then R = R'. If the ratio approaches 0, then R becomes R''.

Figure 3.3
Calculation of the fraction of diffuse radiation that passes through
a gap in the canopy. For explanation, see text.

Thus, the fraction of diffuse radiation transmitted through the gap was
calculated according to (see also Figure 3.3):

$$f_{dif} = \frac{1}{\pi \times s^2} \int_0^s \int_0^s \left\{ (\sin \alpha_2 - \sin \alpha_1) \times (\frac{\beta_2 - \beta_1}{2} + \right.$$

$$\left. \frac{\sin 2 \times \beta_2 - \sin 2 \times \beta_1}{4}) \right\} \, dX \, dY \tag{3.19}$$

with: $\alpha_1 = \tan^{-1}(\frac{X - s - R}{1_i})$ $\alpha_2 = \tan^{-1}(\frac{X + R}{1_i})$

$$\beta_1 = \tan^{-1}\left(\frac{Y - s - R}{1_i}\right) \qquad\qquad \beta_2 = \tan^{-1}\left(\frac{Y + R}{1_i}\right)$$

writing out the integral gives:

$$f_{dif} = \frac{2}{\pi \times s^2} \times \{((s + R)^2 + 1_i^2)^{0.5} - (R^2 + 1_i^2)^{0.5}\} \times$$

$$\{(s + R) \times \tan^{-1}\left(\frac{s + R}{1_i}\right) - R \times \tan^{-1}\left(\frac{R}{1_i}\right)\} \qquad (3.20)$$

Horizontal crown closure ($C_{h,i}$, in m^2 per m^2) can now be calculated by multiplying projected gap area ($1-CP_i$, with CP_i equal to N x π x R_i^2/10 000) by f_{dif}, for any level (i) in the crown canopy. This results in a profile of canopy closure from zero at the top to a maximum value at the bottom of the canopy. Some values for f_{dif} and the resulting C_h are given in Table 3.1, for different degrees of canopy closure.
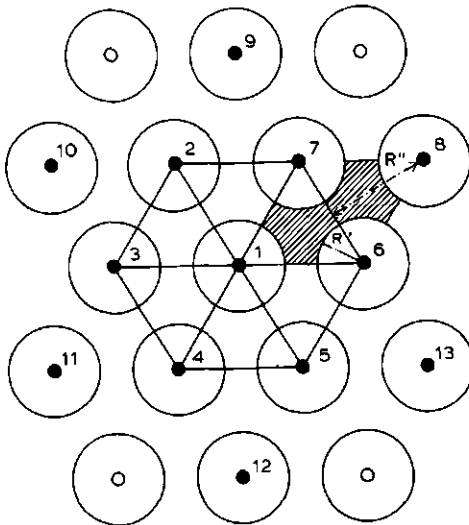

Figure 3.4
Equilateral triangle spacing of identical trees. Object tree: 1; 1st order neighbouring trees: 2, 3, 4, 5, 6 and 7; 2nd. order neighbouring trees: 8, 9, 10, 11, 12, and 13.

Table 3.1
Horizontal canopy closure with regard to diffuse radiation as calcu-
lated from Equations 3.19 and 3.20. The calculations are carried out
at three different 'slenderness' ratio's (H/R ratio's), i.e. the
ratio between crown length and crown width at the base of the crown,
with two different values for perpendicular crown projection area
(CP), and for cylindrical and for conical crowns. The number of trees
does not influence the result as the stands for the purpose here can
be completely characterized by CP and the slenderness ratio.

H/R ratio:	1	3	5
Cylindirical crowns:			
CP = 0.8:			
f_{dif}	0.18	0.02	0.01
C_h	0.96	0.99	0.99
CP = 0.4:			
f_{dif}	0.76	0.27	0.12
C_h	0.54	0.84	0.93
Conical crowns:			
CP = 0.8:			
f_{dif}	0.74	0.23	0.09
C_h	0.85	0.95	0.98
CP = 0.4:			
f_{dif}	0.91	0.50	0.26
C_h	0.45	0.70	0.84

Incomplete canopy closure is taken into account in the calculation of
canopy photosynthesis by relating foliage and branch area to the closed part
of the canopy only:

$$LAI_i = (SLA \times FW_i) / C_{h,i} \tag{3.21}$$

with SLA the specific leaf area in $m^2\ kg^{-1}$; FW_i the foliage weight in the
canopy part extending above level i in $kg\ m^{-2}$; and $C_{h,i}$ the degree of canopy
closure at level i.

3.2.3 Model III: Horizontally discontinuous canopy with clustering of foliage within the crown

In models I and II leaf and branch surface area is assumed to be distributed at random within the crown sublayers. The validity of this assumption however, depends on crown architecture and tree age. In the case of young trees with small crowns this may be a useful approximation, but in older trees leaf area is grouped around branches (Edelin, 1977) and the branches occur in distinct whorls. This clustering of intercepting surfaces results in decreased extinction of radiation because of increased mutual shading within the sublayers. In this case, upper crown sublayers intercept less radiation, and radiation levels in the lower parts of the crown increase. This can be modelled by considering the individual clusters as virtual 'leaves' with unequal transmission and reflection (Goudriaan, 1977). From the leaf area within the cluster (LAIC) and the appropriate extinction coefficient k^*, cluster reflection (ρ_{cl}) and transmission (τ_{cl}) coefficients can be calculated:

$$\rho_{cl} = \frac{\rho^* \times (1 - \exp^{-2 \times k^* \times LAIC})}{1 - (\rho^*)^2 \times \exp^{-2 \times k^* \times LAIC}} \qquad (3.22)$$

and:

$$\tau_{cl} = \frac{(1 - (\rho^*)^2) \times \exp^{-k^* \times LAIC}}{1 - (\rho^*)^2 \times \exp^{-2 \times k^* \times LAIC}} \qquad (3.23)$$

with $\rho_{sph,dir}$ and $k_{sph,dir}$ resp. $\rho_{sph,dif}$ and $k_{sph,dif}$ for ρ^* and k^*.

From cluster reflection and transmission, apparent canopy extinction and reflection coefficients can be calculated from:

$$k_c = ((1 - \tau_{cl})^2 - \rho_{cl}^2)^{0.5} \qquad (3.24)$$

$$\rho_c = (1 - \rho_{cl} - K_c) / \rho_{cl} \qquad (3.25)$$

k_c has to be used in combination with a 'cluster area index' (CLAI) instead

of with LAI. CLAI is the amount of foliage cluster area per unit of ground area, calculated from:

$$CLAI = LAI / LAIC \tag{3.26}$$

in which LAIC is the leaf area index of the individual clusters. Table 3.2 gives some values for k_c and the resulting light extinction in a canopy with LAI = 5, and with different degrees of clustering.

Branch surface area is assumed to be distributed at random within the crown canopy, with a constant branch area density throughout the canopy. Therefore, for the extinction of light by branch area, the simple extinction coefficient of model I can still be used.

Table 3.2

Extinction coefficients, the degree of light extinction and the apparent extinction coefficient for diffuse light for some values of the leaf area index within the cluster (LAIC) in combination with a value for total LAI of 6 and for β equal to 30°. The values for the random model in the same situation are $K = 0.7589$ and I/I_o in that case equals 0.0105. CLAI represents the cluster area index, I/I_o is the fraction of light remaining at the bottom of the canopy.

LAIC	0.1	0.5	1.0	2.0	4.0
CLAI	60.0	12.0	6.0	3.0	1.5
k_c	0.0731	0.3157	0.5317	0.7806	0.9516
I/I_o	0.0125	0.0226	0.0412	0.0962	0.2399
$k_{app,dif}$	0.7308	0.6314	0.5317	0.3903	0.2379

In the model, leaf area index inside the cluster (LAIC) is used to describe the degree of clustering of the foliage. The degree of clustering is related to the ratio of branch dimension (main axis + twigs + needles) to crown dimension. If the size and number of branch clusters is small relative to the volume of the crown, then clustering is more pronounced than in the situation in a small crown, where branch clusters occupy most of the crown volume. In the latter case, foliage area can be regarded as randomly distributed within the crown volume, and the basic expressions given in Section 3.2.1 can be used. The same result is achieved by using a small value (e.g. less than 0.1) for LAIC. This gives a high value for CLAI and the coefficient

of apparent extinction k_{app} approaches the value given by Equations 3.3 and 3.4. (See Table 3.2).

In the model, the degree of clustering, described as LAIC, is related to tree age, assuming an increase in LAIC from 0.1 (virtually no clustering) at germination to LAIC = 1 at age 40, and LAIC = 2 from age 60 onwards. An alternative procedure for estimating LAIC would be to derive LAIC from the dimensions of an average branch with needles, the average number of branches in a whorl, and the average crown width. Branch dimensions can be approximated as branch length (f) times branch width (g), with branch length equal to the crown radius at the bottom of the crown, and branch width equal to e.g. 1 m. Length and width refer here not to a single branch, but to a branch complex, i.e. all needle material attached to one main branch sprouting from the stem. Using an average number of 5 branches per whorl, LAIC might then be estimated from $(\pi \times R^2 - 6 \times f \times g) / (6 \times f \times g)$. Thus LAIC is small in small crowns, and increases when the crowns develop from value of 0.6 for LAIC when R_b is equal to 2.5, to LAIC = 1.6 for R_b = 3.5 and to LAIC = 1.8 for R_b = 4 (assuming a maximum value for the length of the cluster of 3 m). This has the advantage of linking the degree of clustering with overall dimensions of the crown, but requires assumptions about branch dimensions. The calculations below use the value for LAIC that is derived from tree age.

3.2.4   Canopy reflection and transmission: Comparison of the three models

To estimate net radiation budgets, overall canopy reflection and transmission have to be calculated. After calculating total transmission by using separate extinction coefficients for leaves and branches, an apparent extinction coefficient (k_{app}) can be calculated for use in summary models or based on total area index only: $k_{app} = - \ln (I / I_o) / LAI$. If C_h at the base of the live crown canopy is less than 1, soil reflection through the gaps contributes to total stand reflection. The soil surface is incorporated using a reflection coefficient of 0.04. If horizontal canopy closure is incomplete, the contribution of soil reflection is calculated as $(1-C_h) \times \rho_{soil}$. Total reflection then becomes $C_h \times \rho_{canopy} + (1 - C_h) \times \rho_{soil}$. Table 3.3 gives examples of apparent extinction coefficients for a typical canopy, using all three models. Model I is independent of C_h. In situations of complete horizontal closure (C_h = 1) model II gives the same results as model I.

Table 3.3
Overall transmission and extinction coefficients of a standard canopy, estimated with the models I, II and III. LAI=5., BAI=1., σ_{leaves} = 0.10, β = 30°, LAIC = 1. I/I_c : fraction transmitted, using F_{dif} = 0.5.

Model	I		II (C_h=0.8)		III (C_h=0.8)		III (C_h=1.0)	
	LAI	LAI+BAI	LAI	LAI+BAI	LAI	LAI+BAI	LAI	LAI+BAI
ρ_c	0.0567	0.0567	0.0534	0.0534	0.0389	0.0401	0.0429	0.0429
$k_{c,dir}$	0.7797	0.8164	0.7797	0.8164	0.6218	0.6974	0.5407	0.6173
$k_{c,dif}$	0.7155	0.7629	0.7155	0.7616	0.5883	0.6706	0.5104	0.5920
I/I_o	0.0249	0.0092	0.2099	0.2029	0.2495	0.2142	0.0735	0.0271
k_{app}	0.7388	0.7823	0.3122	0.2658	0.2776	0.2568	0.5220	0.6017

3.3   Photosynthesis and stomatal resistance

The photosynthetic performance of a leaf surface depends on the amount of photosynthetic radiation received, on temperature, on ambient carbon dioxide concentration, on leaf water status and on the photosynthetic characteristics of the leaf itself. Ignoring any direct influence of humidity or of plant water status for the moment (see Section 4.5.1. for discussion), this means that under a given temperature regime and concentration of carbon dioxide, the assimilation of carbon dioxide can be estimated from leaf characteristics plus the amount of photosynthetically active radiation that is absorbed by the leaf surface. If data on photosynthesis rates are available, then these can be used to calibrate an elementary response curve, which is then used as a forcing function in a general primary production model. In this way it is not necessary to go into detail about the actual biochemical process of photosynthesis. The response curve is characterized by the maximum assimilation rate at light saturation, its slope at low light intensities (the efficiency with which the absorbed radiation is used), and the maintenance respiration of the tissue.

During its assimilation, carbon dioxide passes through the stomata, and thus stomatal opening is an important factor controlling photosynthesis. At the same time as carbon dioxide enters the leaf, water vapour leaves the stomatal cavity by the same pathway. This implies that assimilation and

transpiration are closely linked and that both are controlled by stomatal behaviour. Through this coupling, water shortage, causing the stomata to close, exerts a strong influence on carbon dioxide exchange. When water is not limiting, stomatal opening is controlled by light, resulting in stomatal closure during the night and the opening of stomata during the day. During daytime, stomatal opening is not constant but varies with light and photosynthesis rate (Raschke, 1975; Goudriaan and van Laar, 1978; Wong et al., 1985). The relationship between carbon dioxide assimilation and stomatal resistance can be modelled using a constant ratio between the concentration of carbon dioxide in the substomatal cavity, and its concentration in the air surrounding the foliage (Goudriaan, 1982). An additional factor influencing stomatal resistance, at least in young needles, is the vapour pressure deficit of the surrounding air (Meinzer, 1982a): Dry air causes stomates to close in newly formed needles, even when bulk needle water content and xylem water potential are apparently sufficient for maximum opening. This effect imposes an upper limit to stomatal conductance, whether the conductance is determined by soil moisture availability and by plant water status, or by the assimilation of carbon dioxide. The influence of plant water status and soil moisture availability on stomatal conductance will be discussed in Chapter 4. In the program, all three estimates of stomatal conductance (determined by water vapour pressure deficit of the air, determined by plant water status, and as a result of assimilation of carbon dioxide), are compared. The lowest conductance is subsequently used in the model calculations.

If the stomatal resistance of the needles that is calculated in this way, exceeds stomatal resistance as estimated from assimilation of carbon dioxide, then the latter is adjusted accordingly. In this way, the effect of plant water status on the assimilation of carbon dioxide is accounted for in the model.

After estimating individual leaf assimilation, total stand assimilation can be calculated as the sum of the photosynthesis rates of each leaf layer in the canopy. This is done by summing the gross photosynthesis rates of the different layers ($A_{g,i}$; gross photosynthesis, equals net photosynthesis plus dark respiration), which yields an estimate for gross carbon dioxide assimilation or gross primary production (P_g) for the total canopy. Afterwards, respiration of the whole stand is taken into account by estimating autotrophic respiration needed to maintain the living biomass (R_m, see Penning de

Vries, 1974, 1975) and by estimating losses of carbon that occur as a result of growth respiration which is coupled to the conversion of assimilates into structural dry matter.

3.3.1   Photosynthesis of the needles

For a given temperature and carbon dioxide concentration, and in the absence of any influence of water shortage or low humidity, photosynthesis of an individual leaf surface can be characterized by a photosynthesis-light response curve (see Figure 3.5). Per unit of leaf surface this curve can be described by an asymptotic exponential equation:

$$A_n = A_m \times (1 - \exp^{-\varepsilon \times H / A_m}) - R_m \qquad (kg\ CO_2\ ha^{-1} h^{-1}) \qquad (3.27)$$

with A_n the net photosynthesis rate, A_m the maximum (gross) photosynthesis rate (maximum net photosynthesis at light saturation plus maintenance respiration), H the amount of PAR absorbed by the leaf surface ($W\ m^{-2}$), ε the initial light use efficiency at low irradiance, here expressed as kg carbon dioxide $ha^{-1} h^{-1} J^{-1} m^2 s$, and R_m the maintenance respiration.

In the model, gross photosynthesis of a leaf surface (A_g) is calculated as $A_m \times (1 - \exp(-\varepsilon \times H / A_m))$. The parameters A_m, ε and R_m can be estimated by fitting Equation 3.27 to series of photosynthesis measurements at different light intensities. Literature data on maximum photosynthesis rates of coniferous species range from 10 kg carbon dioxide $ha^{-1} h^{-1}$ to about 20 kg $ha^{-1} h^{-1}$ (see e.g. Krueger and Ferrell, 1965; Krueger and Ruth, 1969; Künstle, 1971 and 1972; Künstle and Mitcherlich, 1975; Salo, 1974; Schaedle, 1975; Szaniawski and Wierzbicki, 1978; Larcher, 1980; Linder, 1979, 1981; Leverenz, 1981a, 1981b). In order to estimate A_m, ε and R_m, photosynthesis-light response curves were measured on excised branches taken from Douglas fir trees in the temporary field plot WB. The equipment used to measure photosynthesis and transpiration was described by Louwerse and van Oorschot (1969). It was assumed that by taking large enough branches, which were well supplied with water and transported in closed plastic bags to prevent dessication, the measured photosynthesis rates would equal the photosynthesis rates on intact
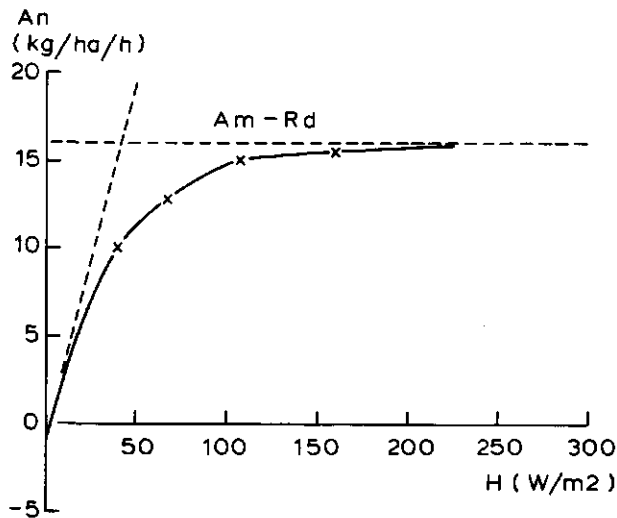
shoots in the field (Larcher, 1963). The measurements were carried out in
August 1984, using current-year and 1- and 2-year-old shoots. The branches,
between 0.5 and 1 m long, were cut off from 21-year-old trees in the middle
of the crown (at a height of 4 to 6 metres) in the morning, and reached the
laboratory within half an hour. In the laboratory, the lowest few centimetres
of the base of the branches were cut off under water, to ensure water supply
to the needles. After fitting the equipment to the shoots, with only one age
class inside the assimilation chamber, photosynthesis measurements were
started. At the time of the first measurement, less than two hours had
elapsed since the branches had been excised in the field. Following the
photosynthesis measurements, nitrogen and phosphorus content of the needles
were determined, together with the Specific Leaf Area (SLA) of the needles.

Projected needle surface area enclosed in the assimilation chamber ranged
from 80 cm^2 to 150 cm^2. Figure 3.5 shows the results of one of the measure-
ment series, using current-year needles at 13° C. Each data point in the
graph represents the mean of 4 to 6 measurements, each taken at intervals of
approximately five minutes. The standard deviations of the data points were
small, giving a coefficient of variation of 1-2 %. Tables 3.4 and 3.5 give
the results of 12 series of measurements, with shoots of different ages at
different temperatures.

The data in Tables 3.4 and 3.5 show no consistent pattern of photosynthe-
sis rate with temperature. This is in agreement with the conclusions of Salo
(1974), Künstle and Mitcherlich (1975), and Emmingham and Waring (1977) that
optimum temperature range for photosynthesis of current-year Douglas fir
needles covers a wide range of 10° to 20°C. The data obtained show lower
assimilation of carbon dioxide in older foliage. Künstle (1971) reported that
maximum carbon dioxide assimilation of Douglas fir, measured on intact shoots
in the field, occurred during July and August, with a gradually decreasing
maximum rate in 1- and 2-year-old needles. The relation of maximum photosyn-
thesis rate within the optimum temperature range (10-20°C) and foliage age
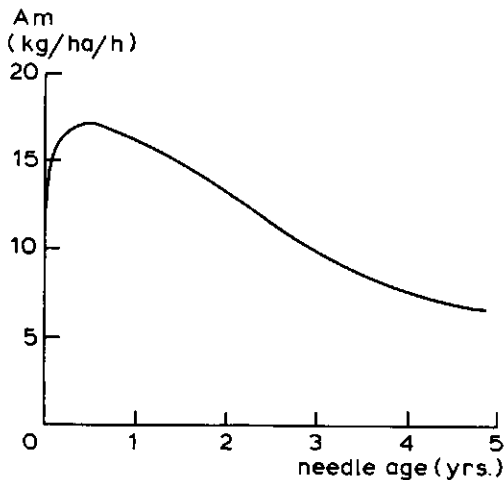used in the model, is represented in Figure 3.6.

Figure 3.6
The relation between maximum gross photosynthesis (A_m, in kg CO_2
ha^{-1} h^{-1}) and needle age (yrs), as incorporated in the model.

Table 3.4
Summary of 12 photosynthesis-light respons curves, as measured
using the equipment described by Louwerse and van Oorschot (1969).
The measurements were carried out on excised branches, sampled in
the temporary plot WB. The 1 st column refers to the number of the
experiment. Needle ages were current (C), one-year-old (1), and
two-year-old (2). The measurements were carried out at 13°C, 18°C,
and 23°C. In columns 4 and 5 maximum gross photosynthesis
(A_m, in kg ha^{-1} h^{-1}) and initial light use efficiency (ε, in
kg ha^{-1} h^{-1} J^{-1} m^2 s) are given. A_m and ε were estimated by fitting
Equation 3.27 to the measurements, see also Figure 3.5, with the
results from experiment no. 9. R^2 gives the fit of the equation to
the data in terms of variance explained by the regression model.
N % and P % represent nitrogen and phosphorus concentrations in the
needle tissues, SLA gives the specific leaf area in m^2 per kg, as
determined with a Li-cor area metre (model 3100).

	age	temp.	A_m	ε	R^2	N %	P %	N/P	SLA
1	C	18	12.46	0.27	0.9982	1.34	0.07	19	5.5
2	C	18	14.94	0.39	0.9987	1.34	0.07	19	5.5
3	C	23	14.06	0.49	0.9987	1.34	0.07	19	5.5
4	1	18	10.06	0.19	0.9956	2.04	0.07	29	4.8
5	1	18	18.49	0.36	0.9993	2.04	0.07	29	4.5
6	1	23	11.58	0.31	0.9996	2.04	0.07	29	4.9
7	1	23	9.30	0.23	0.9971	1.48	0.09	16	5.7
8	C	13	15.39	0.50	0.9998	1.40	0.10	14	5.9
9	C	13	16.76	0.44	0.9996	1.40	0.10	14	5.6
10	C	23	17.40	0.56	0.9977	1.40	0.10	14	6.4
11	2	23	11.80	0.29	0.9987	1.67	0.07	24	4.3
12	2	23	10.70	0.40	0.9985	1.67	0.07	24	5.0

Table 3.5
Mean values of A_m and ε depending on temperature (13°
C, 18°C, and 23°C) and age (current, one-year-old,
and two-year-old needles from Table 3.4).

	C	1	2	mean:
13	16.08	-	-	16.08
	0.47	-	-	0.47
18	13.70	14.28	-	13.99
	0.33	0.28	-	0.30
23	15.73	10.44	11.25	12.47
	0.36	0.27	0.34	0.33
mean:	15.17	12.36	11.25	13.58
	0.44	0.27	0.34	0.37

As for the influence of low temperatures on maximum photosynthesis rates: photosynthesis has been shown to occur at temperatures below 0°C, provided no dessication occurs (Keller, 1965; Schwarz, 1971; Ducrey, 1981; Guehl, 1982; Guehl et al., 1985). In the model it was assumed that non-optimal temperatures reduce maximum photosynthesis in all age classes, see Figure 3.7.
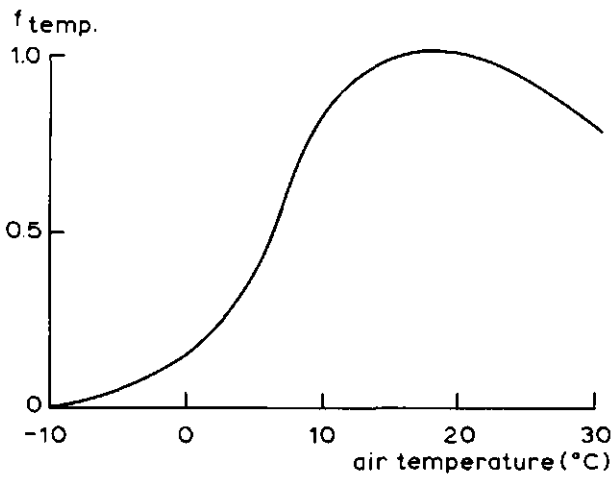

Figure 3.7
The dependence of maximum gross photosynthesis (A_m in Equation 3.27) on temperature.

Light use efficiency at low light levels can be expected to increase with decreasing temperature (Ehleringer and Björkman, 1977; Farquhar et al., 1980; Björkman, 1981), because the carbon dioxide compensation point Γ decreases with decreasing temperature. Most tree species belong to the group of plant species in which the Calvin cycle predominates as the carbon fixing mechanism, with carboxylation occurring primarily through the enzyme ribulose-1,5-biphosphate carboxylase-oxygenase (Schaedle, 1975). Following Goudriaan (1982, p. 102), the light use efficiency of these so-called C_3-plants can be calculated from:

$$\varepsilon = (1. - \Gamma / C_e) \times \varepsilon_o \qquad \text{(kg } CO_2 \text{ ha}^{-1}\text{h}^{-1}\text{J}^{-1}\text{m}^2\text{s)} \quad (3.28)$$

with Γ : the compensation point in vppm carbon dioxide; C_e the external carbon dioxide concentration in vppm and ε_o equal to 0.5 kg CO_2 ha^{-1}h^{-1}J^{-1}m^{2}s, or 14 x 10^{-9} kg CO_2 J^{-1} (as photosynthesis rates were expressed as kg ha^{-1}h^{-1}, the light use efficiency was expressed as kg ha^{-1}h^{-1}J^{-1}m^{2}s in order to be used in combination with radiation fluxes expressed as W m^{-2}). From photosynthesis rate vs. external carbon dioxide concentration response curves (measured at high light level), Γ can be found (Figure 3.8).

For current-year needles, Γ equals 27 vppm carbon dioxide at 13°C and 42 vppm carbon dioxide at 23°C. With a Q10 value for Γ of 42/27 ($\cong$ 1.6), Γ can now be calculated as a function of temperature, using $\Gamma = (Q10)^{0.1\times(T-T_b)} \times \Gamma_b$. In the model, 13° and 27 vppm are used for T_b and Γ_b, respectively. The resulting values for Γ at 5°, 15°, and 25°C were 0.45, 0.43 and 0.39 Kg CO_2 ha^{-1}h^{-1}J^{-1}m^{2}s, respectively.

The ratio of the internal carbon dioxide (C_i) and the external carbon dioxide concentration (C_e) is constant over a wide range of environmental conditions (carbon dioxide concentrations) for most C_3 plants, with a value of around 0.7 (Goudriaan, 1982, p. 102). If water supply is non-limiting, the stomata respond to photosynthesis and changes in the concentration of intercellular carbon dioxide by maintaining a constant ratio of C_i over C_e, as put forward by Raschke (1975, see also Goudriaan and van Laar, 1978), and thus stomatal conductance is coupled to net photosynthesis rate.
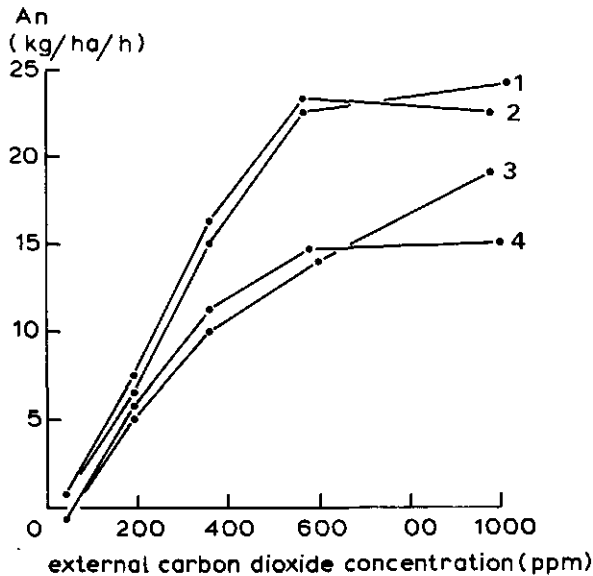
Figure 3.8

Measured net photosynthesis rates on current-year needles, under conditions of full light (appr. 300 W m^{-2} PAR), at different concentrations of external carbon dioxide. Curves 1 and 2: measurements at 13°C, curves 3 and 4 at 23°C.

With regard to the influence of nutrient content of the foliage on photosynthesis rates, it is in general acknowledged that high nitrogen concentrations correlate positively with maximum photosynthesis rates (Linder and Rook, 1984; Wong et al., 1985). If nitrogen concentrations of 1.5 to 2.0 % are regarded as optimal for Douglas fir (Blok et al., 1975; van den Burg, 1976), no clear influence of nitrogen content in our measurement series is to be expected. The relation between phosphorus content of the foliage and photosynthesis rates is less clear. Blok et al. (1975) give values of 0.15 % to 0.25 % P as optimal phosphorus concentrations, and expect reduced growth at P % less than 0.15. Phosphorus content of the foliage on which photosynthesis rates were measured was below that, around values of 0.10 % (see Table 3.4), and photosynthesis in the needles was probably below normal. The direct effects of N and P concentrations on photosynthesis rates are not explicitly taken into account in the model because sufficiently detailed measurements are lacking. The influence of N and P availability on total stand growth is discussed in Chapter 5.

3.3.2   Stomatal resistance

If both the carbon dioxide concentration inside the leaf and the external carbon dioxide assimilation are known, then the stomatal resistance to diffusion of carbon dioxide can be calculated as:

$$r_{1,c} = \frac{C_e - C_i}{A_n} - r_{b,c} \qquad (s\ m^{-1}) \qquad (3.29)$$

with $r_{1,c}$ the resistance to carbon dioxide diffusion from the air surrounding the leaf to the stomatal cavity; C_e the external carbon dioxide concentration in kg m^{-3}, C_i the internal carbon dioxide concentration in kg m^{-3}, A_n the net carbon dioxide assimilation rate in kg CO_2 $m^{-2} s^{-1}$, and $r_{b,c}$ the boundary layer resistance to the transport of carbon dioxide. In the model C_i was calculated from C_e, assuming a ratio between C_i and C_e of 0.7.

The resistance to the diffusion of carbon dioxide from the surrounding air to the leaf interior ($r_{1,c}$) consists of a stomatal resistance ($r_{s,c}$) and a boundary layer resistance ($r_{b,c}$). Stomatal resistance to water vapour can now be calculated using the ratio of stomatal resistance to the diffusion of carbon dioxide and the resistance to diffusion of water vapour ($r_{s,c}/r_{s,v}$, equal to 1.67, the ratio between molecular weights of carbon dioxide and water vapour) and the similar ratio for the boundary layer resistances ($r_{b,c}/r_{b,v}$, equal to 1.42, Monteith, 1973):

$$r_{1,v} = \frac{(C_e - C_i)}{1.67 \times A_n} - 0.85 \times r_{b,v} \qquad (s\ m^{-1}) \qquad (3.30)$$

with $r_{b,v}$ calculated as $90 \times (w/u)^{0.5}$, w being the width of the needles (0.02 m) and u_c the wind speed inside the canopy in m s^{-1}. The net assimilation rate A_n is converted from kg CO_2 $ha^{-1} h^{-1}$ to kg CO_2 m^{-2} s^{-1} by multiplication by 2.78×10^{-8}. Conversion of carbon dioxide from vppm to kg m^{-3} was done by multiplication by 1.83×10^{-6}.

For a value of A_n of 15 kg CO_2 $ha^{-1} h^{-1}$, a ratio of C_i/C_e of 0.7, C_e equal to 340 vppm, and u equal to 3 m s^{-1}, this gives a value of 262 s m^{-1} for $r_{1,c}$.

3.3.3   Canopy photosynthesis

With the equation for photosynthesis rate as a function of incident light (Equation 3.27), together with the calculated distribution of photosynthetically active radiation over the foliage as described in Section 3.2, the total canopy assimilation carbon dioxide can now be calculated. The total amount of gross photosynthesis over the day at a particular level in the canopy $(A_{g,i})$ can be calculated as the sum of sunlit leaf area in the layer times the average photosynthesis rate of the sunlit leaf area, and by the product of the shaded leaf area and its photosynthesis rate. The assimilation rate of the shaded foliage area equals:

$$A_{i,sh} = A_m \times (1 - \exp^{ - \varepsilon \times I_{sh} / A_m }) \qquad (\text{kg } CO_2 \text{ ha}^{-1}\text{h}^{-1}) \quad (3.31)$$

with I_{sh} equal to $I_{abs,dif} + (I_{abs,dif,tot} - I_{abs,dir,dir})$, see Equations 3.9 through 3.11.

For direct light in combination with a spherical leaf angle distribution, integration over the sine of incidence of direct light gives an assimilation rate of sunlit leaf area of (Spitters, 1986):

$$A_{i,sl} = A_m \times (1 - (A_m - A_{i,sh}) \times (1 - \exp^{ - \varepsilon \times I_{sl,dir}/ A_m }) /$$

$$(\varepsilon \times I_{sl,dir})) \qquad (\text{kg } CO_2 \text{ ha}^{-1}\text{h}^{-1}) \quad (3.32)$$

with $I_{sl,dir}$ equal to $(1 - \sigma) \times I_{o,dir} / \sin \beta$ (Equation 3.13). $A_{g,i}$ can be calculated from $A_{sh,i}$ and $A_{i,sl}$ when the fraction of sunlit leaf area is known. The latter is the product of the fraction sunlit cluster area and the fraction sunlit leaf area inside the cluster:

$$f_{sl,i} = \exp^{ - (k_{c,dir,bl} \times CLAI_i + k_B \times BAI_i) } \times \exp^{ - k_{dir,bl,L} \times LAIC } \quad (3.33)$$

Total canopy assimilation (P_g) is calculated using the Gaussian three-point integration method in which $A_{g,i}$ is calculated for three levels in the canopy, with the levels determined by the distribution of leaf area inside the canopy.

Average assimilation rate per unit of leaf area for the whole canopy can now
be calculated using the weighting procedure corresponding to the three
points. For further detail on the Gaussian integration method, see Goudriaan
(1986), van Kraalingen et al. (1987), and textbooks such as Johnson and Riess
(1977).

Total canopy conductance was estimated with the Gaussian approach also, by
averaging the inverse of $r_{l,v}$ (Equation 3.29) of the three Gaussian integra-
tion levels, using the appropriate weights, and multiplying the resulting
average leaf conductance by total LAI. Implicit in this procedure it is
assumed that the immediate environment of the foliage, as far as temperature,
carbon dioxide concentration, and water vapour is concerned, do not change
with depth in the canopy. This assumption holds for canopies of considerable
roughness, and thus with efficient mixing of the air, as in the case of a
tall forest stand (see also Goudriaan, 1979). The model is used to calculate
instantaneous rates of photosynthesis (using radiation fluxes). Daily totals
can be found by using the Gaussian method again, this time for integration of
the instantaneous rates over the day, see Goudriaan (1986).

3.4   Respiration

In order to calculate net dry matter increment from gross photosynthesis,
growth respiration and maintenance respiration have to be taken into account.
Maintenance respiration is needed e.g. to cover the energy requirements for
resynthesis of degraded cell structures (especially protein), and for main-
taining ion gradients across cell membranes. After taking into account the
amount of assimilates needed for maintenance processes, the remaining
products of photosynthesis have to be converted to structural dry matter.
Depending on the type of biomass formed, a conversion efficiency accounts for
changes in weight going from assimilates (soluble sugar) to structural dry
matter. The reduction in weight due to this conversion process in which
carbon, hydrogen, and oxygen atoms are split off, is called growth respira-
tion (Penning de Vries, 1974).

3.4.1   Maintenance respiration

Maintenance processes are coupled with the build-up of degrading proteins
and with maintaining differences in ion concentration, and depend on the
protein and mineral content of the active plant material (de Wit et al.,
1978; Penning de Vries and van Laar, 1982). Maintenance respiration of
assimilation products provides the energy for the maintenance processes.
Needles have a higher metabolic activity than other organs such as stems and
branches, and different maintenance respiration coefficients have to be used
in order to estimate the maintenance respiration of the total stand. When
estimating stem maintenance respiration, only the living sapwood should be
taken into consideration. The core of heartwood in older trees has a support-
ing function only, and does not contain any living cells. In the model,
maintenance respiration is calculated according to the procedure used in the
BACROS model (de Wit et al., 1978) in which average metabolic activity of the
biomass is taken into account as well as protein and mineral content. This is
based on the observation (Penning de Vries, 1975) that the more active
tissues have higher rates of respiration than less active ones. Maintenance
requirements due to average metabolic activity are set at 5 % of total canopy
assimilation (de Wit et al., 1978, p. 52). Protein content is estimated from
nitrogen concentration of the tissue, assuming 16 % N in the protein. Total
mineral content of the tissue is estimated from the total amount of potas-
sium, calcium, phosphorus and magnesium in the tissue. Maintenance respira-
tion is now estimated for each biomass component (i) from Equation 3.34 (de
Wit et al. 1978):

$$R_{m,i} = 0.04 \times PF_i + 0.08 \times MF_i \qquad (kg\ CH_2O\ kg^{-1}\ DM\ d^{-1}) \qquad (3.34)$$

with PF_i and MF_i representing the fractions of protein and minerals. The
coefficients 0.04 and 0.08 are taken from the BACROS model (de Wit et al.,
1978; updated version April 1981), and relate to a temperature of 25°C. The
effect of actual temperature on respiration is calculated with a Q_{10} value of
2, assuming that maintenance respiration doubles when the temperature rises
by 10 degrees.

For needles, with typical concentrations of nitrogen and minerals in the
tissue of 2 % and 1 % respectively, Equation 3.34 yields a maintenance rate
at 15°C of 2.9×10^{-3} kg CH_2O kg^{-1} DM d^{-1}. For sapwood, with the

concentrations of nitrogen and minerals typically around 0.06 % and 0.08 %, the calculated maintenance rate is equal to 0.107×10^{-3} kg CH_2O kg^{-1} DM d^{-1}. If these conditions apply to a growing period of 200 days, then this results in maintenance requirements of 0.58 kg CH_2O per kg needle dry weight, and 0.0214 kg CH_2O per kg sapwood. With 10 000 kg needles (LAI=5.5), and 75 000 kg sapwood, total maintenance requirements over this 200 day period would amount to 5 800 kg CH_2O for the needle biomass and 1 605 kg CH_2O for the sapwood.

These rates of maintenance are lower than values reported for agricultural crops, because of the lower protein and mineral content of needles and of woody material. Penning de Vries (1975) tried to estimate maintenance coefficients theoretically and calculated values of $15 - 25 \times 10^{-3}$ kg CH_2O kg^{-1} DM d^{-1} at 25°C for agricultural crops. Amthor (1984) gives a review of experimentally determined values for agricultural crops; he found values ranging from about 10×10^{-3} to 90×10^{-3}. Szaniawski (1981) gives values of 13×10^{-3} for shoots and 42×10^{-3} for roots of Scots pine seedlings at a temperature of 25°C. Sievänen (1983) mentions values for leaves and current-year roots of Salix cv.'aquatica' of 9×10^{-3} at 25°C. The difference between these values and those calculated above using Equation 3.34, are probably attributable to differences in protein and mineral content of the material; the seedlings and the young roots of trees have higher protein and mineral contents, and thus resembling herbaceous crops (Kramer and Kozlowski, 1979). Although the protein and mineral content of the seedlings and of young roots are high, maintenance respiration in the model is calculated for accumulated biomass in older stands. Except for dead heartwood tissue, all biomass is taken into account in the calculation of the maintenance requirements. As the nitrogen content of the living sapwood is low (see Table 3.5), the maintenance requirements of the woody material is also low. Zabuga et al. (1983) report values of 0.42×10^{-3} kg CH_2O kg^{-1} DM d^{-1} at 20°C for actively growing stemwood of Scots pine (Pinus sylvestris). As in this case some growth respiration was probably included in the measurement, this value is comparable with the 0.11×10^{-3} that was used in the model.

3.4.2   Growth respiration

To estimate the weight loss due to conversion of assimilates, conversion efficiencies for the biomass components can be calculated from the

biochemical composition of the tissue (Penning de Vries., 1975; Penning de Vries et al., 1974). For each biomass component, a dry weight conversion factor is calculated using the expression from Table 3.6.

The conversion factors are calculated from average values of biomass composition for needles, branches, stems and roots. They are introduced in the model as constants. Corresponding with the conversion efficiencies for each separate biomass component, a carbon dioxide production factor (CPF_i) can be calculated to estimate the amount of carbon dioxide evolved per amount of component biomass formed. Growth respiration in kg CH_2O consumed per kg of dry matter formed, is estimated by multiplying the dry matter increment (calculated using the expression for DWC_i) by 30/44 x CPF_i. The constant 30/44 represents the ratio between the molecular weights of CH_2O and carbon dioxide. The biomass compositions given in Table 3.6 are taken from the literature (Rydholm, 1965; Sarkanen and Ludwig, 1971; Bosshard, 1974; Fengel and Wegener, 1984). Using the carbon production factors from Table 3.6 plus total increment of the stand of 15 000 kg $ha^{-1}yr^{-1}$, consisting of 4 000 kg needles, 1 000 kg branches, 4 000 kg roots and 6 000 kg stemwood, the accompanying growth respiration is 3 771 kg CH_2O $ha^{-1}yr^{-1}$.

Table 3.6

Biochemical composition in % of dry weight of Douglas fir needles, branches, stems and roots, together with the calculated conversion efficiencies (DWC) in kg DM kg^{-1} CH_2O, the carbon production factors (CPF) in kg CO_2 kg^{-1} DM and the carbon content (CC) of the biomass in kg C kg^{-1}. Conversion efficiencies in kg DM kg^{-1} CH_2O, calculated from the tissue fractions of respectively carbohydrates (f_C), protein (f_P), fats (f_F), lignins (f_L), organic acid (f_O), and minerals (f_M). Original data from Penning de Vries and van Laar, 1982).:

$$DWC_i = 1./(f_{C,i}x1.242 + f_{P,i}x1.704 + f_{F,i}x3.106 + f_{L,i}x2.174 + f_{O,i}x0.929 + f_{M,i}x0.050)$$
$$CPF_i = f_{C,i}x0.1701 + f_{P,i}x0.4620 + f_{F,i}x1.7200 + f_{L,i}x0.6589 - f_{O,i}x0.0110 + f_{M,i}x0.0730$$
$$CC_i = f_{C,i}x0.4504 + f_{P,i}x0.5556 + f_{F,i}x0.7733 + f_{L,i}x0.6899 + f_{O,i}x0.3746 + f_{M,i}x0.0000$$

	carboh.	protein	fat	lignin	org.ac.	minerals	DWC	CPF	CC
Needles	60	10	8	15	4	3	0.6541	0.3866	0.5061
Branches	65	3	4	24	2	2	0.6562	0.3526	0.5134
Stems	66	0.5	2	30	1	0.5	0.6443	0.3469	0.5262
Roots	62	3	5	24	4	2	0.6509	0.3644	0.5151

3.5   Assimilate pool, phenology, and carbon allocation

3.5.1   Assimilate pool

Assimilates produced in photosynthesis are either consumed in maintenance
respiration, lost as growth respiration, or accumulated as reserves or
structural dry matter. Growth respiration and dry matter increment are linked
and occur in the same period when gross canopy photosynthesis is high.
Maintenance respiration takes place during the whole year, although at a much
slower rate during the cold season because of low temperatures. To tide the
trees over periods when maintenance requirements may exceed photosynthetic
production (as in the dormant season during the winter), assimilates are
stored as starch or sugar in foliage and woody material. This is represented
in the model by a reserve pool. During the dormant season, or during periods
with low temperatures and low carbon dioxide assimilation, and during periods
of drought, assimilate requirements for maintenance can be drawn from this
reserve pool. The amount of reserves is expressed in kg CH_2O ha^{-1}. Storage of
assimilates can occur in a soluble and in a non-soluble form (e.g. as
starch). The location and the kind of storage are not taken into account in
the model. Instead, the reserve level (E) is represented as a running balance
of incoming photosynthetic products (P_g), outgoing maintenance respiration
requirements, and the amount of assimilates used in tissue growth (G_g).
Additional losses may occur through litter loss, e.g in the case of litter
loss caused by wind damage instead of by ageing. Growth only occurs when the
amount of reserves (E) exceeds some base level E_b, which depends on the
amount of living biomass present, and on the minimum concentrations of sugar.
The average sugar concentrations chosen to characterize E_b in the model, are
10 % for needles, 3 % for branches, 1 % for sapwood, and 5 % for roots, based
on data given by Zimmermann and Brown (1971), and Kramer and Kozlowski
(1979). Using these concentrations, the initial amount of reserves is
calculated from initial component biomass. In a stand with 6 000 kg needles
(dry weight), 25 000 kg branches, 75 000 kg sapwood, and 35 000 kg roots per
hectare, this results in a total reserve level of 3 850 kg CH_2O ha^{-1}.

In the model, maintenance respiration requirements receive priority over
growth for available resources. When the reserve level E declines, so does
G_g, becoming zero as soon as E falls below (E_b+R_m). G_g is calculated as E -
($E_b + R_m$) when E exceeds ($E_b + R_m$). When assimilate availability does not

3.5.3   Distribution of assimilates

When the reserve level exceeds the base level E_b, and if this surplus plus current gross photosynthesis exceeds maintenance requirements, then net growth occurs. The assimilates available for dry matter increment have to be allocated to the biomass components considered in the model. In most simulation models (see Penning de Vries and van Laar, 1982) this is done using a dry matter distribution key. This key is then used as an input to the model, modified by the development stage, and by water and nutrient stress as experienced by the plant. The approach relies on the general notion that foliage, branches, stems and roots will be proportional to each other: the amount of water transpired by the foliage has to be taken up by the roots, and transported by sapwood in the trunk and branches. The larger the evaporating surface, the more uptake and transporting tissue is needed. This concept of a functional balance between the biomass components (Brouwer and de Wit, 1968) is related to the pipe-model theory (Shinozaki et al., 1964a, 1964b) and to the empirical correlations reported in recent years between foliage leaf area and sapwood cross sectional area (see e.g. Grier and Waring, 1974; Whitehead, 1978; Snell and Brown, 1978; Polge, 1982; Waring, 1983; Albrekson, 1984).

The distribution keys are characteristic for each crop and have to be determined empirically or deduced from literature data on biomass composition, possibly under different growing conditions. A more fundamental approach to the study of assimilate distribution would be to consider the genetically determined growth rythms of plant organs, or, at the level of the individual plant, the specific architectural growth pattern of the plant (see e.g. Ford, 1985). Thus, the architectural growth pattern might provide theoretical support for choosing a particular carbon allocation pattern for a certain species. For application in a more encompassing model, however, the pattern will still have to be calibrated against results obtained experimentally. As this requires extensive data on biomass distribution in trees, which are hard to obtain due to practical measurement problems, the straightforward approach is used in the model instead, by employing a descriptive distribution key. Data on the distribution of annual dry matter increment over foliage, branches, stems and roots in large trees and forest stands are scarce, and often incomplete or conflicting when the analysis is restricted to aboveground biomass only. In order to be able to use published data on

distribution of increment over aboveground parts, total root increment was calculated first using shoot:root ratios determined by the ratio between actual and potential production. In this way, the effects as of shortages of water and nutrients, on carbon allocation are taken into account. Keyes and Grier (1981) compared above- and belowground production in Douglas fir stands and estimated root growth to be 23 % of total growth on a good growing site, and 53 % on a poor site. In our model, the shoot:root ratio decreases from 4 in the case of potential production, to 2.5 when a shortage of water or nutrients resulted in actual production equal to 50 % of potential production.

Of the total root growth, 80 % was assumed to go into growth of fine roots (Santantonio and Hermann, 1985). The distribution of the aboveground increment over needles, branches and stems depends on age of the trees (Turner and Long, 1975). The distribution key used here is based on production data from Heilman and Gessel (1963), Turner (1975), Turner and Long (1975), Webb (1975), Gholz et al. (1976), and Keyes and Grier (1981), see Figure 3.9.

The scatter in the data points in Figure 3.9 points to the variation that may occur in the distribution of net assimilates, and leaves room for interpretation when a forcing function for use in a general model is derived from the data. The lines drawn in Figure 3.9 represent the distribution key that was used in the model. Starting from averages of the literature data, the change in allocation of assimilates during stand development was chosen to give the best overall fit to the field plots D12, D25 and SP4. This was done by varying the fraction allocated to the stem biomass, and comparing model outcome with stem volume measurements from the plots. The value of this procedure will be discussed together with the evaluation of the model performance in Chapter 6. The distribution shown in Figure 3.9 is used as a forcing function for all plots used in this study.

Figure 3.9
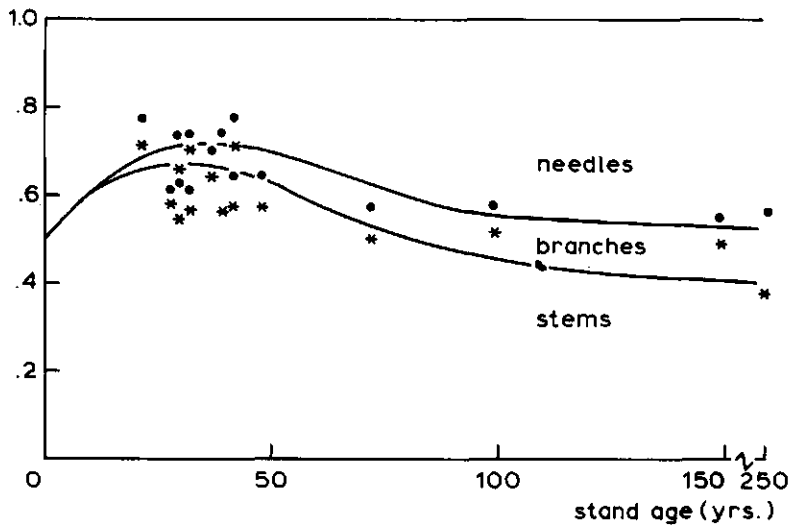Distribution of the above-ground increment over needle, branch and
stem biomass in relation to age, as simulated with the model (solid
line). Literature data on distribution of dry matter increment
(Heilman and Gessel, 1963; Turner, 1975; Turner and Long, 1975;
Webb, 1975; Gholz et al., 1976, and Keyes and Grier, 1981) are given
as the fractions allocated to stems (✱), and stems plus branches
(●).

3.6   Net increment

After the distribution of the assimilates available for growth over the
biomass components, dry matter increment for each biomass component is calcu-
lated using the conversion factors from Section 3.4.2. The increment is added
to the biomass, and subtracting the litter loss gives net increment for the
period considered. The simulation is performed with time steps of one day,
thus giving the change in biomass during the growing season. Apart from total
biomass increment, structural aspects of the stand also have to be taken into
account; e.g. position of the new needles, and the distribution of the stem
increment over the bole.

3.6.1   Dry matter increment and litter loss

Foliage. As described in Section 2.3.1 needles are represented by 5 age
classes using a simple boxcar approach: At the end of the year the needles
remaining in each class are shifted into the next one. The last class with 5
year old needles is emptied. All needle increment during the growing period
is added to the current needle class. Needle litter loss can have several
causes. Crowns may be damaged by wind or insect attack, or needles may age
and eventually die. At the bottom of the crown, complete branches may die off
at high stand densities as a result of too low light intensities and decreas-
ing photosynthetic performance.

Needle loss is estimated by multiplying total needle mass in a particular
class by a needle loss coefficient (l_i):

$$\frac{dW}{dt} = l_i \times W_i \qquad\qquad (kg\ ha^{-1}day^{-1}) \qquad (3.36)$$

with W_i the needle mass in kg ha^{-1} in needle class i, l_i the loss coefficient
in kg day^{-1}kg^{-1}, and dW/dt the resulting needle loss from class i.

Needle loss coefficients can be estimated in two ways; by measuring actual
needle loss per class and estimating the initial and final amount of needles,
and by fitting a loss coefficient such that the resulting needle distribution
over the age classes agrees with the field observations. A fixed needle loss
coefficient would result in an exponential decrease of needle biomass with

age. Such a distribution would occur when the rate of needle loss would be independent of needle age, e.g. when determined only by wind damage or insect attack. From Figure 3.10 it can be seen that this is not the case, and in the model is was assumed that the death rate of the needles is linearly related to needle age: $l_i = L_c \times t_i$, with L_c an empirically determined loss coefficient and t_i the needle age in days from budflush for the particular age class i. Combined with Equation 3.36 and after integration, this yields a description of the change in needle biomass over time:

$$W_{i,t} = W_{i,o} \times \exp^{-\,(\,0.5 \times L_c \times t^2\,)} \qquad\qquad (kg\ ha^{-1}) \qquad (3.37)$$

with $W_{i,o}$ the initial biomass after budflush is completed. When no needle loss occurs during the first year when the needles are formed, then $W_{i,o}$ represents total dry weight of the current-year needles at the end of the year. In that case L_c can be estimated from needle distributions as given in Table 2.6. Using the ratio between 3- and 1-year-old needles in the plots D25 and SP4, this results in a value for L_c of about 2.9×10^{-6}. Using the ratio between the 4- and the 1-year-old needles results in an estimate for L_c of 2.4×10^{-6} for D25, and 2.1×10^{-6} for SP4. In the model, an average value of 2.5×10^{-6} was used for all plots.

In Figure 3.10 the needle age distributions from Table 2.6 are represented in block diagrams (diagrams a, b, c, d, and e), together with the calculated distribution using $L_c = 2.5 \times 10^{-6}$. As no loss of current needles is incorporated, the amount of 1 year old needles at the beginning of the year represents the ratio between needle increment and total needle biomass, as an indication of the overall needle loss rate. Plot WB apparently has a higher needle turnover rate as compared to D25 and SP4.

Branches. Branch increment was not further specified with regard to position in the crown of the tree. Branch litter loss is calculated as a constant fraction of total branch biomass, based on the assumption of an average life span of 30 years for an individual branch.
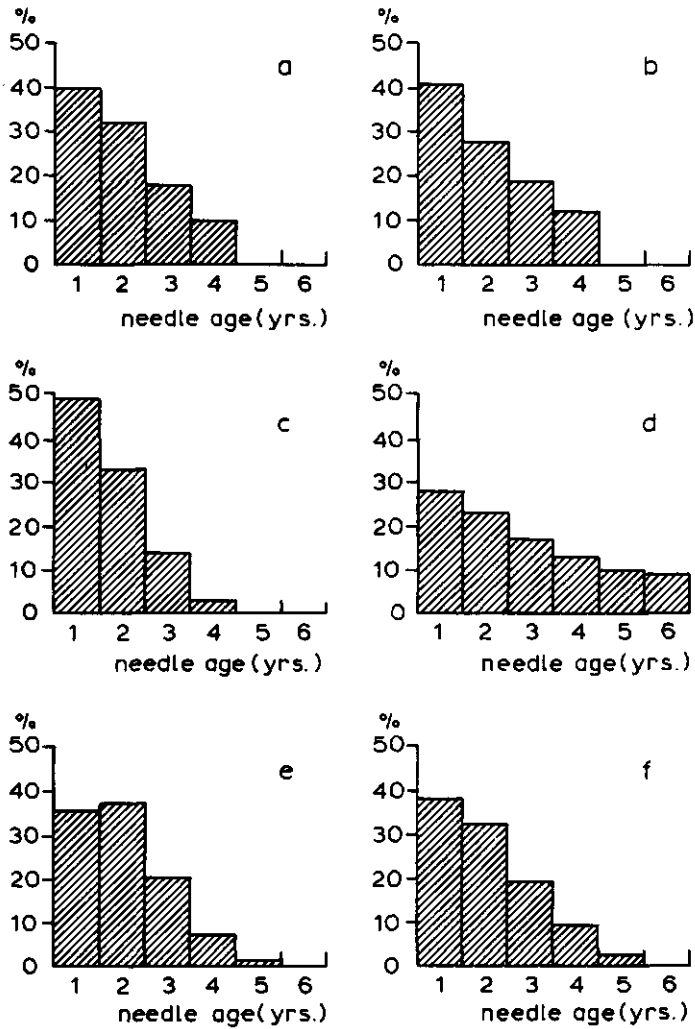
Figure 3.10
Histograms showing the distribution of needles over the age classes
for three of the field plots (a: D25, b: SP4, c: WB), and according
to Silver (1962, graph d) and Kay (1978, graph e), as well as
calculated distributions with the foliage loss coefficients equal to
1.33.

Stems. Stem biomass is represented by the sum of the volumes of the individ-
ual tree boles, with bark biomass not explicitly taken into account. Stem
volumes here and as measured in the field refer to stems with bark. Stem
increment in m^3 volume ($I_{s,vol}$) is derived from total stem dry matter incre-
ment ($I_{s,DM}$) by dividing stem dry matter increment in kg $ha^{-1}day^{-1}$ by an
average value for basic density (ρ_w, in kg DM m^{-3} fresh stemwood) of the stem
wood:

$$I_{s,vol} = I_{s,DM} / \rho_w \qquad\qquad (m^3 ha^{-1} day^{-1}) \quad (3.38)$$

Basic density follows a typical pattern during the active growing period. The
lowest values, around 250, occur directly after budflush, during the period
of shoot extension. Towards the end of the active growing period, basic
density increases, attaining 800 kg m^{-3} during late summer and fall (Smith,
1955; Bosshard, 1974), thus causing the growth ring pattern in coniferous
trees, showing light coloured springwood and dark summerwood. As the width of
the year ring decreases, the proportion of summerwood increases relative to
springwood, resulting in a higher value for basic density. Thus, a ring width
of 1 cm correlates with a basic density of 370 kg m^{-3}, which increases to 500
kg m^{-3} when ring width equals 0.1 cm (Knigge, 1958; Bosshard, 1974; Hapla and
Knigge, 1985, see Figure 3.11).

Changes in basic density during the growing season depend, among others,
on growth rate, assimilated distribution and endogenous factors (Larson,
1960, 1963, 1969). As the endogenous factors, and also the changes in assimi-
late distribution within the growing season, are not incorporated in the
model, only an average value for basic density can be used. In the model, the
value used in a particular year is derived from ring width in the previous
year.

After individual tree volume increment is added to the existing volume,
diameter at breast height (d_i) for each tree is calculated from tree volume
using the reversed form of the standard volume equation in which volume is
expressed as a function of diameter at breast height and tree height.
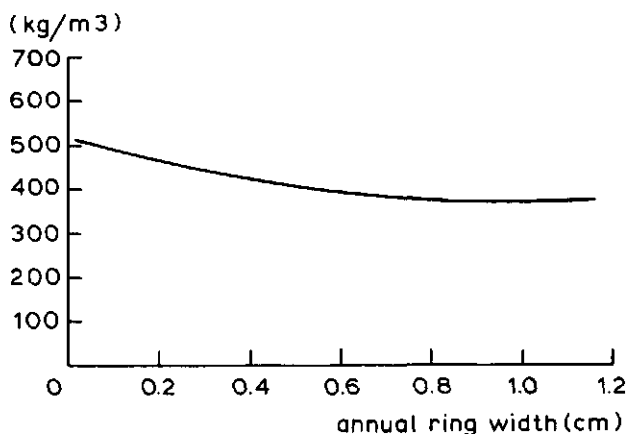
Figure 3.11
Relationship between specific gravity and annual growth-ring width
in Douglas fir, according to Hapla and Knigge (1985).

A range of equations can be used for calculating stem volume (Avery and
Burkhart, 1983). Following current practice in the Netherlands, Schumacher
and Hall's equation is used in the model (Schumacher and Hall, 1933):

$$v_i = a \times d_i^{\,b} \times h_i^{\,c} \qquad\qquad (dm^3) \qquad (3.39)$$

with the volume of the i th. tree in dm^3; d_i the diameter of the tree in cm;
h_i the height of the tree in m, and a,b and c regression coefficients from
the current yield tables (derived from bole section measurements of a large
number of trees, see Dik, 1984). For the purpose here, Equation 3.39 has the
advantage of going through the origin, thus allowing a reversed form
$(d_i = a' \times v_i^{\,b'} \times h_i^{\,c'})$ to be used for estimation of d_i from v_i and h_i. For
the Netherlands, a, b, and c in Equation 3.39 are equal to 0.0879, 1.9005,
and 0.8073 respectively. If h_i and v_i are known, d_i can now be calculated.

Roots. Comparable with branch increment, increments in fine and coarse roots
are not specified any further in the model, and losses of fine and coarse
roots are calculated as fixed fractions of total fine or total coarse root
biomass. Root turnover rates used in the model are 1 yr^{-1} for fine root
biomass, and 0.02 yr^{-1} for coarse root biomass.

3.6.2   Carbon balance

In order to check the correctness of the computer model which is based on theoretical aspects of primary production as described in this Chapter, an annual carbon balance has been incorporated in the model. This does not give any information on the validity of the model, but can be used to check for internal consistency. Carbon input in kg C was calculated by multiplying gross primary production (in kg CH_2O) by 0.4, the carbon content of the assimilates when the latter are expressed in kg CH_2O. Output consists of maintenance and growth respiration, and taking into account any change in stored reserves, the resulting amount of carbon should be equal to the total amount of carbon in dry matter increment.

3.6.3   Transition from live sapwood to dead heartwood in the bole

If no mortality or self-thinning occurs, total stem biomass does not decrease. Depending on the species, there can be bark litter, but as this is negligible in the case of Douglas fir, it is not taken into account in the model. In considering live biomass, however, account must be taken of the transition of live sapwood to dead heartwood. The latter does not add to the litter fall as it remains compartimentalized within the sapwood. As a result of this compartimentalization, nutrients immobilized in the heartwood are taken out of the nutrient cycle within the system. Heartwood does not require any maintenance respiration, and it does not participate in the water dynamics of the tree. Douglas fir shows a distinct heartwood formation with an accompanying, strong decrease in permeability of the heartwood (Krahmer and Côté, 1963). Following Ziegler (1967) and Bosshard (1974), heartwood formation was regarded as an ageing phenomenon; and it was assumed that after a fixed number of years transition from sapwood to heartwood occurs. As mentioned in Section 2.3.1, it was concluded from the decrease in moisture content, that the average lifespan of a growth ring is 15 years. The model keeps track of sapwood using a simple boxcar-train approach with 15 age-classes. Only sapwood is considered in the calculations of total water capacity of the plant, and in estimating total amount of maintenance requirements.

4   HYDROLOGY

4.1   Introduction

   Water movement in a vegetation canopy is determined by both physical and
physiological factors. Physical site factors such as precipitation and the
water-holding capacity of the soil regulate the water supply, solar radiation
provides the energy for the evaporation process, and atmospheric conditions
together with the canopy roughness determine the 'drying power' of the air.
The canopy determines net precipitation input into the soil compartment by
interception and redistribution of rainfall. When the canopy is completely
closed so that direct soil evaporation can be ignored, the vegetation also
controls the rate of water loss from the soil to the atmosphere by means of
regulation of the transpiration flux. The combination of precipitation,
evaporation of intercepted precipitation, transpiration, and direct soil
evaporation, determines the rate of soil water depletion or replenishment and
thus the flow of water through the system.

   Soil moisture, if present in limited amounts, influences primary produc-
tion. A decrease in soil moisture content in the rooted zone results in a
lower water potential in the soil, and restricts root uptake. As transpira-
tion continues, the plant loses water and bulk leaf water potential drops,
resulting in stomatal closure. This causes a reduction of transpiration to
the atmosphere but also limits the influx of carbon dioxide to the stomatal
chamber and to the carboxylation site in the leaf where photosynthesis takes
place. In this way, shortage of soil moisture may depress growth and yield.
Figure 4.1 gives a general relational diagram for the hydrological part of
the model.

   The total living biomass acts as a buffering system by way of its water
content. In case of a lack of available soil moisture, plant water content is
depleted until the resulting decrease of plant water potential near the
stomata prohibits them from opening fully and, by means of increased stomatal
resistance, transpiration balances the uptake of soil moisture at a slower
rate compared to a situation with potential transpiration.
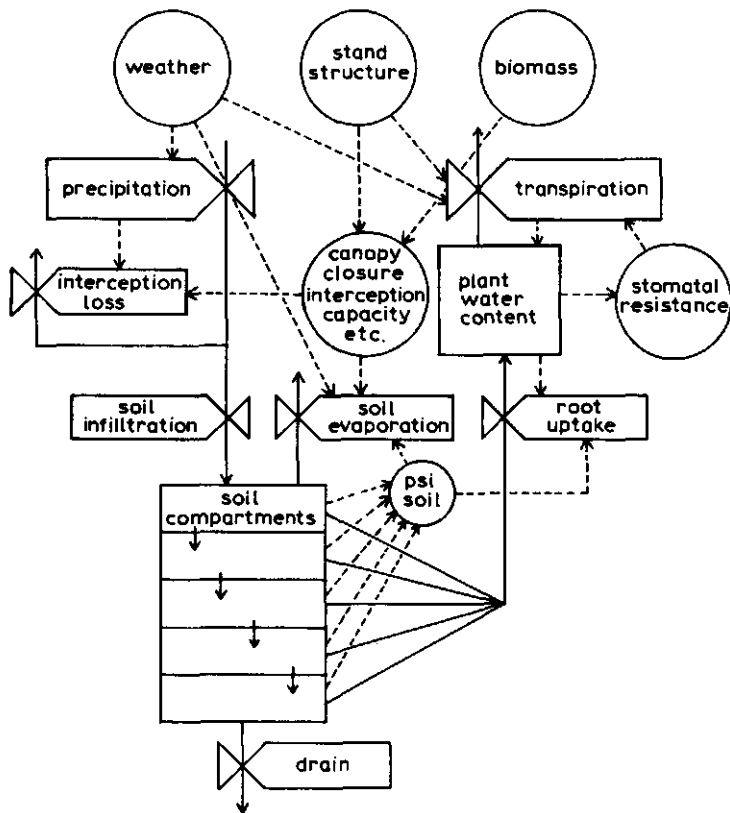
Figure 4.1
Simplified relational diagram of the hydrological part of the model.
Solid lines: material flows; dotted lines: relationships between
rate variables and state variables, and between driving, interme-
diate, and rate variables. Stand structure and total amounts of
biomass are considered as driving variables in this hydrological
part of the model, whereas they were indicated as state variables in
the general diagram presented in Section 1.4 of the introductory
chapter. Apart from plant water content, stomatal resistance is also
determined by net leaf assimilation as explained in the text. In
addition to stand structure and biomass composition, stomatal
resistance is an important intermediate variable between the primary
production part and the hydrological part of the model.

Evapotranspiration in plant canopies can be estimated with the Penman-Monteith equation using daily temperature, net radiation and humidity above the canopy as input variables. Wind speed above the canopy, together with the aerodynamic roughness of the stand, gives the turbulent exchange capacity for transport of latent heat (water vapour) and sensible heat from the canopy to the atmosphere.

In the model, the stock of available moisture in the root zone of the profile is simulated from day to day as a running balance, with the soil profile divided into five compartments. Each of the soil compartments is characterized by its water content at field capacity, the water content below which root uptake is zero (the wilting point), and a soil moisture retention curve (see Section 2.2.2). The soil profile is compartmentalized to account for vertical inhomogeneity of the soil and for uneven distribution of moisture resulting from infiltration from the forest floor into the top compartment only. The model is limited to stands with rooted soil profiles that are not supplied with water from a water table by capillary rise. If the infiltrated water plus the amount of water stored in the rooted zone exceed the maximum soil moisture that can be held in the soil matrix suction against gravitational force (which state is, by definition, equal to field capacity), the model arranges for the surplus to be drained to the underground.

With canopies of considerable roughness direct evaporation of intercepted water from the vegetation surface has to be taken into account. Because a rough vegetation has a large aerodynamic conductance, water stored on the canopy may evaporate at rates several times the rate of the water inside the leaf or needle, which has to pass through the stomata. Therefore, interception of precipitation, and evaporation of the amount of water stored on the canopy, may present an additional loss of water from the system to the atmosphere. Estimation of the amount of evaporated interception water can be based entirely on physical factors, as no physiological control is involved. The total interception capacity of the vegetation, plus rainfall amounts and size distribution of individual rainfall events determines the amount of total intercepted rainfall.

In recent years, detailed models have been developed to calculate interception of rainfall and stand evaporation. These models are often based on hourly input values for the meteorological variables (e.g. Rutter et al.,

1975; Gash, 1979; Mulder, 1983; Running, 1984). The model described in this
thesis simulates forest hydrology over a period of several consecutive years
and this limits the degree of detail in the description of the individual
processes. In accordance with the daily averages used as input variables for
the meteorological traits, the time step used here equals one day. The model
is therefore limited to a summary model for evaporation, derived from more
extensive comprehensive models. The evaporation part of the model follows the
approach developed by van Keulen (1975), Stroosnijder (1982) and Driessen
(1986). Simulation of interception is based on the work by Gash (Gash, 1977;
Gash et al., 1978), and uses the summary procedure from Makkink and van
Heemst (1975).

4.2   Evapotranspiration

    Evapotranspiration is the loss of water from the system to the atmosphere,
either as transpiration, direct soil evaporation, or evaporation of intercep-
ted water stored on the canopy. Evapotranspiration of moisture requires
energy to enable the phase transition from liquid to vapour, and the water
vapour has to be transported from the evaporating surface to the atmosphere.
In the absence of advection, the energy for evapotranspiration is provided by
incoming radiation. Absorbed radiation is partitioned between heat storage of
the canopy, loss of sensible heat to the atmosphere, transpiration and
photosynthesis. The energy requirements of photosynthesis are of the order of
magnitude of 3 to 5 % of total incoming radiation and can therefore be
ignored in the energy balance. In the model, heat storage of the vegetation
is not taken into account explicitly; it was assumed that an increase in heat
storage early in the growing season would be compensated by a decrease at the
end of the season. Thus, the available energy (as net radiation, S_n) has to
be distributed over the loss of sensible and latent heat. This can be done
using the Penman-Monteith equation (Penman, 1948; Monteith, 1965):

$$E \quad = \quad \frac{1}{\lambda} \quad \frac{\Delta \times S_n + \rho \times c_p \times (e_s - e_a) / r_a}{\Delta + \gamma \times (1 + r_c / r_a)} \qquad \text{(mm)} \qquad (4.1)$$

with E: evaporation rate, expressed in mm; λ : latent heat of vaporization of
water (2.39×10^6 J m^{-3} H$_2$O); Δ : The slope of the saturated vapour pressure
curve at air temperature calculated as $4158.6 \times e_s / (T + 239)^2$, in mbar K^{-1},
with T representing the air temperature during the day; S_n : Net radiation
absorbed by the canopy in W m^{-2}; $\rho \times c_p$: volumetric heat capacity of the air

(about 1240 J m^{-3} K^{-1}); e_s: saturated vapour pressure of the air; e_a:
actual vapour pressure of the air (mbar) γ : psychrometer constant (0.67 mbar
K^{-1}), and r_c: the bulk canopy resistance to water vapour, consisting of
stomatal resistance and the needle boundary layer resistance. r_c is calcu-
lated using Equation 3.30, with canopy assimilation P_g substituted for needle
assimilation A_n, and r_a instead of $r_{b,v}$.

In this expression, S_n, e_a and, mediated by Δ and e_s, T_{ad}, are meteorol-
ogical variables relatively independent of canopy parameters. The aerodynam-
ic resistance, r_a, is determined by wind speed and canopy roughness (charac-
terized by the zero plane displacement d and roughness length z_o):

$$r_a = \frac{(\ln (z - d) / z_o)^2}{k^2 \times u (z)} \qquad (s\ m^{-2}) \qquad (4.2)$$

As the model uses daily average values of temperature and wind speed, no
corrections for stability were made. Basically, this estimate for r_a applies
to the transport of momentum from reference height to a plane at height
z_o + d inside the canopy, the level at which the logarithmic wind profile
would predict zero wind speed. In the case of a canopy of considerable
roughness, differences between aerodynamic resistance to momentum on the one
hand, and mass and heat exchange on the other, must be taken into account.
Resistances to mass and heat exchange will be larger because these traits
cannot be transferred by pressure interactions. This can be taken into
account by adding an excess resistance (r_{ex}) to the turbulent resistance
calculated from the wind profile. In the single-layer model used here, r_{ex} is
estimated following Chen (1984, p. 83) as:

$$r_{ex} = B^{-1} / u_* \qquad (s\ m^{-1}) \qquad (4.3)$$

with B^{-1} a dimensionless parameter set equal to a value of 4, and u_* the
friction velocity calculated from the wind profile (Equations from Table 2.2)
as : $u(z) \times k / \ln ((z_r-d)/z_o)$, with z_r equal to the reference height above
the canopy. The value for B^{-1} in Equation 4.3 is taken from Chen (1984, p.
84) and applies to a rough canopy with an LAI value greater than 4.

In the case of transpiration by plants, the pathway of water vapour from
the position of the leaf inside the canopy to the atmosphere can be separated
into the diffusion of water vapour through the stomata and through the
boundary layer surrounding the leaf, and the turbulent transfer of water

parts of the soil profile. As mentioned above, redistribution of soil mois-
ture within the rooted zone is not simulated by the model (see also next
section), and therefore, following van Keulen (1975) soil moisture extraction
by evaporation is distributed over the soil profile by assuming a weighted
exponential extinction with depth for the moisture withdrawal, taking into
account differences in depth between the soil layers:

$$F_i = D_i \times \delta_i / \sum_{i=1}^{n} \delta_i \qquad (4.8)$$

with δ_i the moisture weighted extinction factor:

$$\delta_i = \exp(-F_{prop} \times Z_i) \times (M_{c,i} - M_{lim,i}) / D_i \qquad (4.9)$$

(δ_i becomes zero when $M_{lim,i}$ exceeds $M_{c,i}$)

$$E_{s,i} = F_i \times E_s \qquad \text{for} \quad F_i \times E_s \leq M_{c,i} - M_{lim,i} \qquad (4.10)$$

$$E_{s,i} = M_{c,i} - M_{lim,i} \qquad \text{for} \quad F_i \times E_s > M_{c,i} - M_{lim,i} \qquad (4.11)$$

with F_{prop} the proportionality factor, set equal to 15; Z_i the distance from
the centre of the soil compartment to the soil surface (m); D_i the thickness
of the soil compartment in m; $M_{c,i}$ total soil moisture in the compartment
(mm); $M_{lim,i}$ the limiting soil moisture below which no evaporation takes
place (equal to 1/3 of the soil moisture at wilting point).

4.3   Soil water balance

The consecutive compartments in the profile for which the water balance is
calculated are defined by their thickness (D_i) and the distance from the
centre of the compartment to the forest floor (Z_i). The rate of change of the
water content of each compartment ($\Delta M_{c,i}$) is calculated as the balance of the
rate of water inflow at the top of the compartment ($R_{in,i}$), the rate of water
uptake by the roots of the trees in the compartment (U_i), the share of the
compartment in direct soil evaporation ($E_{s,i}$) and the rate of water outflow
at the bottom of the compartment ($R_{out,i}$). The same calculations are carried
out for all compartments using the rate of water outflow from the overlying
compartment as the rate of water inflow to the underlying compartment. In

this way, the compartments are successively filled up to field capacity, from the soil surface downwards.

The outflow at the bottom of a soil compartment ($R_{out,i}$) was calculated from $R_{out,i} = R_{in,i} - U_i - E_i - (M_{max,i} - M_{c,i}) / \Delta t$, with $M_{max,i}$ the maximum amount of moisture that can be withheld against gravitational force (field capacity), $M_{c,i}$ the actual soil moisture content and Δt the period of time concerned (here equal to 1 day). When the soil moisture deficit ($M_{max,i} - M_{c,i}$) plus the withdrawal by root uptake and soil surface evaporation exceeds $R_{in,i}$, no water percolates to the next compartment, and $R_{out,i}$ is set equal to zero. The subscript i refers to the soil layer, counted from above. After calculation of the flow rates for each compartment, the moisture content of each compartment is updated using:

$$M_{c,i} (t+1) = M_{c,i} (t) + R_{in,i} (t) - R_{out,i} (t) \qquad (mm) \qquad (4.12)$$

The calculations are carried out beginning with the uppermost soil compartment with net precipitation (precipitation above the canopy minus interception losses) as the rate of infiltration. The rate of water uptake by the roots in each soil compartment depends on plant water requirements, availability of water and on the ability of the roots to take up water. Plant water requirements are determined by transpiration plus an amount of water to account for changes in water content of the plant body itself. Availability of water depends on the moisture content of the soil in the rooted zone. No root uptake is possible below the moisture content at wilting point, but root uptake is usually already limited to some degree before the permanent wilting point is reached. This is accounted for in the model by defining a critical soil moisture content in addition to wilting point and field capacity, below which root uptake is possible but at a restricted rate.

The critical soil moisture content is calculated as $M_{cr,i} = (1-p) \times (M_{max,i} - M_{min,i}) + M_{min,i}$, with the empirical reduction factor p depending on transpiration rate of the canopy (Doorenbos and Kassam, 1979). This reduction factor p was assumed to decrease linearly from 0.95 at a transpiration rate of 1 mm per day to 0.5 at a transpiration rate of 8 mm per day. Furthermore, it is assumed that the fraction of soil moisture available for uptake, decreases linearly from 1 at $M_{cr,i}$ to 0 at the permanent wilting point. Assuming a linearly decreasing uptake of soil

moisture by the roots between critical soil moisture and wilting point, the total amount of water, readily available for root uptake in each compartment ($M_{a,i}$) can now be calculated.

In a steady state condition, root uptake equals transpiration, and in its simplest form the flux of water through the plant can be written as:

$$E = \frac{\psi_s - \psi_f}{r_p} \qquad (g\ m^{-2}\ s^{-1}) \qquad (4.13)$$

with ψ_s the water potential of the soil moisture in bar; ψ_f the bulk water potential of the foliage in bar, and r_p the pathway resistance to transport of water from the soil to the evaporating surface in the substomatal cavity inside the plant. When E is expressed in $g\ m^{-2}s^{-1}$, r_p has the dimension bar $m^2\ s\ g^{-1}$ (estimation of r_p is treated in Section 4.5.2). Soil water potential (ψ_s) is calculated from the weighted average (with regard to soil moisture content), of the soil layers, and equals -0.2 bar at field capacity (pF = 2.3), and -16 bar at permanent wilting point (pF = 4.2). For a given combination of ψ_s and r_p, the value for ψ_f required to maintain a flux E, calculated with the Penman equation (Equation 4.1), can now be calculated. If ψ_f is very low, stomatal resistance increases, thereby decreasing transpiration and thus the value for E, allowing ψ_f to increase somewhat. In this way the system approaches equilibrium for a given set of environmental conditions.

The total amount of water that can be transpired from a canopy until stomata close to prevent desiccation, and without any supply of water from the roots, is of the order of magnitude of $1 - 2$ kg m^{-2} (Waring and Running, 1978). With a transpiration rate of 0.1 $g\ m^{-2}\ s^{-1}$, this means that the steady state is reached within 3 to 6 hours. Dynamic simulation of this mechanism would require time steps of 15 minutes or less. In the present model, which uses time steps of one day, it is therefore assumed that equilibrium is reached instantaneously, and for a given value of E_{pot} (calculated with Equation 4.1 and using the maximum canopy conductance from the simulated net assimilation rate), ψ_s, and r_p, the equilibrium values of ψ_f and E_{act} are calculated using an iterative procedure.

4.4   Interception of precipitation

At any rainfall event, part of the precipitation is intercepted by the
canopy and does not reach the forest floor but evaporates directly from the
canopy to the atmosphere. In that case, with a wet canopy, transpiration will
be suppressed whereas the stomata remain open, and assimilation can continue.
Thus, part of the decrease in soil infiltration resulting from interception
of precipitation (the interception loss), will be compensated for by reduced
transpiration and root uptake. However, water stored on the canopy as inter-
cepted precipitation evaporates at rates that are higher that transpiration
rates under comparable meteorological conditions, because there is no stoma-
tal resistance, i.e. the greatest part of the pathway resistance for trans-
piration is absent when intercepted water evaporates. A typical order of
magnitude would be $10 \ s \ m^{-1}$ for the aerodynamic resistance to turbulent
exchange, and 100 to 150 $s \ m^{-1}$ for the bulk canopy resistance. Another factor
that causes interception to be a real loss is the evaporation of water
intercepted by stems and branches, because these surfaces do not contribute
to transpiration and water loss to the atmosphere when the canopy is dry.
Therefore, interception has to be estimated in a model that calculates the
influence of soil moisture availability on growth, as it can be a consider-
able loss in the total water budget especially in situations with frequent,
light rains (Calder, 1976).

Detailed models of the interception process use time-steps of one hour or
less (Rutter et al., 1975; Mulder, 1983) and give a detailed description of
the wetting-up phase of the canopy, and of evaporation from the partially or
totally wet canopy during and after the rain. Using time steps of one day,
this is not feasible, and therefore a simplified approach was adopted,
following Makkink and van Heemst (1975). Essentially total interception
during any one period of time is simulated by estimating the total intercep-
tion capacity of the canopy, and subtracting this from total precipitation
during individual rainfall events. In order to do this, precipitation must be
described in some detail, including average number of showers on days with
rain, and the size distribution of the total number of rainfall events.
Implicit in the approach is the definition of an individual rainfall event in
such a way that intercepted water can evaporate completely before the next
rain occurs.

Gross precipitation (precipitation above the canopy) can be divided into throughfall, interception, canopy drip and stemflow. Stemflow is negligible in most coniferous forests (Rutter, 1975), mainly due to tree architecture and bark roughness, and is not considered here. Throughfall reaches the forest floor without interference by the canopy and depends on canopy closure. In the model a horizontal and a vertical component of canopy closure are distinguished and thus unobstructed throughfall can be estimated as:

$$T_f = (1-CP) \times P + CP \times \exp(- K_p \times LAIT) \times P \qquad (mm) \qquad (4.14)$$

with CP horizontal canopy closure (accounting for large gaps in the canopy, expressed as a fraction of the total ground surface area) for vertical fluxes; $\exp(- K_p \times LAIT)$: vertical canopy; and P precipitation above the canopy (gross precipitation). The expression $(1-\exp(- K_p \times LAIT))$ gives the fraction of the precipitation that is intercepted by the closed part of the canopy. The extinction coefficient K_p is calculated in the same way as the extinction coefficients for radiation, only for 'black' leaves ($\tau = 0$) and using an angle of incidence of 90° ($\beta = 90$). From Equations 3.3 and 3.4 in Section 3.2.1 it can be seen that the coefficient equals 0.5 for a spherical leaf angle distribution, and becomes 1 for horizonal black branches.

The total amount of water intercepted during a rainfall event depends on the storage capacity of the canopy, on canopy closure and on the total amount of rainfall. If evaporation during the rain is important, rainfall intensity and duration of the rainfall have to be taken into account as well. The total interception capacity of the canopy is typically 1 to 2 mm (see literature review by Rutter, 1968) and is estimated here as a function of projected needle and branch area LAI and BAI respectively:

$$I_c = I_{LAI} \times LAI + I_{BAI} \times BAI \qquad (mm) \qquad (4.15)$$

with I_{LAI} and I_{BAI} the interception capacities of unit leaf area and unit branch area ($I_{LAI} = 0.3$, $I_{BAI} = 0.4$, Rutter, 1975). Temporarily ignoring any effects of incomplete canopy closure ($T_f = 0.$), the interception per individual rainfall event is now estimated by comparing I_c and P. If the interception capacity I_c is equal to or less than P, then interception equals the interception capacity I_c. If I_c exceeds the total amount of precipitation, all rain is intercepted and interception equals P. Evaporation during rain is

not explicitly taken into account. As no effect on transpiration of the occurrence of a wet canopy during part of the day was taken into account, it was implicitly assumed that evaporation during rain is equal to the average daily transpiration rate.

The precipitation input data consist of daily rainfall, or of total amount of rainfall during periods of 30 days: in the latter case the number of days with rain during the same periods are also input to the model. In order to estimate interception in the way outlined above, size distribution of the individual showers must be known. This distribution can be generated from a gamma function fitted to observed distributions. This was done using the programs and parameter estimates from Geng et al. (1985). The resulting distribution applies to daily amounts of rainfall. No differentiation into the size of the individual daily rainfall events was made. The average number of rainfall events (n) per day with rain, averaged over the year, equals about 1.3 (Levert, 1954).

4.5   Canopy resistance to transpiration

Two main physiological traits influencing the transport of water through the soil-plant-atmosphere continuum emerge from Sections 4.2 and 4.3: the stomatal resistance, determining the flux of water vapour from the inside of the leaf to the leaf boundary layer and to the atmosphere, and the bulk plant resistance that determines water availability at the evaporating surface of the substomatal cavity. This pathway resistance to the transport of water inside the plant, from the soil to the site of evaporation inside the foli-age, can be regarded as being composed of two separate resistances: the root resistance for uptake of soil moisture, and the transport resistance through the xylem. Root uptake of moisture involves metabolic activity, and therefore depends on temperature of the soil as well as on uptake capacity (i.e. total fine root biomass). The xylem resistance to the ascent of water is of mere physical origin and depends on the amount and the structure of the conducting sapwood tissue, and on the pathway length (Zimmermann, 1983).

Soil moisture availability expressed as soil water potential, determines, together with the transport resistance, the water status of the foliage under a given evaporative demand. This water status of the foliage can be expressed in terms of a negative water potential or in terms of foliage water content

relative to the water content at saturation. Together with the vapour pressure deficit of the surrounding air, foliage water status determines the maximum stomatal conductance that can be obtained under light saturation.

4.5.1   Needle water status and stomatal resistance

Needle water status, expressed as bulk water content of the foliage, xylem or twig water potential, or bulk foliage water potential, exerts a strong influence on stomatal conductance. Insufficient root uptake relative to transpiration, leads to loss of water from the foliage. As a result, the water potential of the foliage decreases, and stomatal conductivity starts to decline. This feedback phenomenon can be modelled by defining a relative conductance (g'_c), which depends on foliage water potential, which is used together with the maximum conductance $(g_{c,m})$. Needle water status is represented here by 'bulk foliage water potential' ψ_f, assumed to be equal to twig water potential, which can be measured using a pressure bomb (Scholander et al., 1965). Twig water potential decreases from the bottom to the top of the crown, and outwards along the branches (Richter, 1972). Because of this, twig water potential is similar on all positions of the crown mantle; this justifies the use of a single value for all needles, as is done here (Hellkvist et al., 1974; Hinckley et al., 1978). The relationship between relative conductance (g'_c) and water potential, can be described adequately with a straight line (Running, 1976): $g'_c = 1 - \psi_f / \psi_{min}$, with ψ_{min} a threshold value for water potential where stomatal conductance becomes equal to cuticular conductance. Values for ψ_{min} in Douglas fir reported in the literature vary between −20 and −25 bar (Running, 1976; Hinckley et al., 1978; Lopushinsky and Kaufmann, 1984), a value of −20 bar was used in the model. To arrive at an actual value for stomatal conductance, g'_c has to be multiplied by the appropriate maximum conductance $g_{c,m}$ under those circumstances. Apart from the influence of assimilation rate on stomatal opening as described in Section 3.3.2, this maximum conductance is mainly determined by needle morphology; and published data for Douglas fir range from 0.33 to 0.2 cm s^{-1}, equivalent to a stomatal resistance of 300 – 500 s m^{-1} (Running, 1976; Hinckley et al., 1978; Spittlehouse, 1981). In addition, and especially in young needles, maximum stomatal conductance appears to depend on the vapour pressure deficit of the air surrounding the needles, through a local negative feedback by peristomatal transpiration (Meinzer, 1982c). As the needles mature, and the cuticule develops, this sensitivity to vapour pressure

deficit declines. Using the same experimental set-up as described for the photosynthesis measurements, an attempt was made to measure the dependence of stomatal conductance on vapour pressure deficit. Vapour pressure deficit was varied between 5 and 20 mbar under full light, and stomatal conductance was estimated from measured transpiration rates. The empirical relationship between the maximum conductance $g_{c,m}$ and the vapour pressure deficit that emerged from the measurements is given in Figure 4.2. The measurements were done in August, when the needles were fully developed, and the results showed only a modest reduction of conductance with increasing vapour pressure deficit. In the model, this relation was used for all needle classes, under the assumption that it gives an average value for $g_{c,m}$.
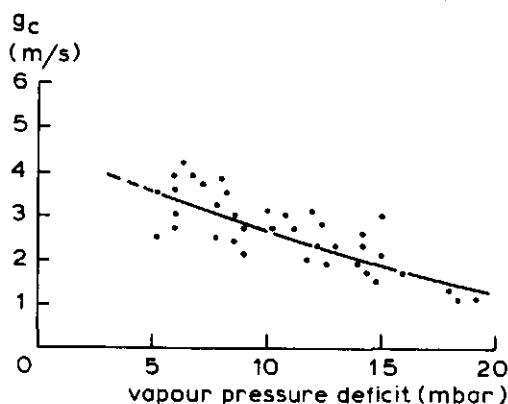
Figure 4.2
Stomatal resistance as determined by the vapour pressure deficit of the surrounding air.

4.5.2   Bulk resistance to transport of water within the plant

To predict bulk foliage water potential for a given value of ψ_s and to estimate potential transpiration rate using Equation 4.1, an estimate of the total transport resistance within the plant (r_p) is needed. The latter can be thought of as consisting of two main components: root resistance (r_r), determining the water flux from the soil to the xylem tissue in the roots,

and xylem resistance (r_x), acting in series with r_r and determining the flow of water from the roots to the evaporating surface inside the foliage. Root resistance depends on several factors such as the amount of roots in the soil, soil temperature, the rate of suberization in relation to the rate of fine root growth, the presence of mycorrhizae, and the degree of root-soil contact. Xylem resistance depends on the length of the transport pathway (the average height of the foliage above the soil surface), on transport capacity (which was expressed as sapwood cross-sectional area) and on the relative water content of the sapwood. Both root and xylem resistances can be studied in detail. With xylem resistance, the concentration, dimensions, and permeability of the conducting elements (tracheids in conifers, vessels in hardwoods) must be considered in combination with the viscosity of the water flowing through (see Zimmermann, 1983). To model this, a considerable number of processes would have to be quantified, and many parameters would have to be estimated from scarce biological data. Because of the lack of consistent data applicable to field situations, and given that the model uses a time step of one day, both root and xylem resistance were treated in a more descriptive way. Total transport resistance was estimated from measured difference in water potential between foliage and the soil solution using Equation 4.13, in situations were the transpiration flux E is also known. To illustrate this, consider a thriving stand 30 m high, and with a total basal area at breast height of 20 m^{-2} ha^{-1}, on a soil at field capacity ($\psi_s = -0.1$ bar). On a sunny day in the middle of the growing season the transpiration flux at midday is some 0.3 to 0.4 mm hr^{-1} or 0.08 - 0.11 g $m^{-2} s^{-1}$ with a bulk foliage water potential of around -10 to -15 bar under steady state conditions (data taken from reviews by Hinckley et al., 1978, and Whitehead and Jarvis, 1981). This implies that, using Equation 4.13, total plant resistance $(r_p = r_x + r_r)$, required to maintain this potential drop from the soil to the atmosphere, must be around 120 - 180 bar m^2 s g^{-1}. According to Nnyamah et al. (1978), root resistance makes up 20 % of total plant resistance, in this case 20 - 40 bar m^2 s g^{-1}, thus leaving 100 - 140 bar m^2 s g^{-1} as bulk xylem resistance. Root resistance is inversely related to total fine root weight, being small in the case of many fine roots all acting as parallel resistances, and increasing as the fine root mass decreases.

Root water uptake, a physiologically controlled process, is strongly influenced by soil temperature; in the temperature range concerned, this can be simulated using a Q10 value of 3 (Kuiper, 1964; de Wit et al., 1978).

Assuming a fine root weight (W_{fr}) of 3 000 kg DM ha^{-1} (0.3 kg m^{-2}) and an average soil temperature of 10°C in the example mentioned above, specific root resistance at 20°C can now be calculated as:

$$r_{r,sp} = r_r \times W_{fr} \times 3^{(0.1 \times T_s - 2)} \qquad \text{(bar kg s g}^{-1}\text{)} \quad (4.14)$$

In the case of r_r = 30 bar m^2 s g^{-1}, W_{fr} = 0.3 kg m^{-2} and T_s = 10 °C, this results in a value of 3 bar kg s g^{-1} for $r_{r,sp}$.

Xylem resistance is best expressed per unit length and per unit cross-sectional area of the conducting stems. Relative water content of the conducting sapwood tissue is related to conductivity, which decreases with decreasing water content (Waring and Running, 1978), but this cannot be incorporated in this elementary model because the water content of the tissue changes with height within the stem of the tree. In the approach used here, stem sapwood is therefore assumed to have the same properties all over the bole. It is therefore not treated explicitly, but rather it is assumed that, with the water flux per unit ground surface the same at all height levels, a decreasing conductivity higher up the bole as a result of lower xylem water potential and lower relative water content, is compensated for by a larger sapwood area.

Using Ohm's law again, bulk xylem resistance can be expressed as being inversely proportional to sapwood basal area (G_{sw}), and directly proportional to the pathway length for transport or, in the case of trees, to the height of the stand (h): $r_x = r_{x,sp} \times h / G_{sw}$. Using the values given in the example above (h = 30 m, G_{sw} = 20 m^2 ha^{-1}, and r_x = 100 – 140 bar m^2 s g^{-1}), this gives for $r_{x,sp}$ a value of 70 – 90 x 10^{-4} bar m s g^{-1} (note the differences in dimension between $r_{r,sp}$ and $r_{x,sp}$ that arise because of the different definitions used for the resistances).

In the case of tall plants such as trees, an additional component of the water potential in the foliage is the gravitational potential $\rho \times g \times H$ (bar) where ρ is the density of water, g is the gravity constant, and H is the height of the tree in m. To predict ψ_f from ψ_s and r_p, the equation derived from Equation 4.13 now reads:

$$\psi_f = \psi_s - r_p \times E - \rho \times g \times H \qquad \text{(bar)} \qquad (4.15)$$
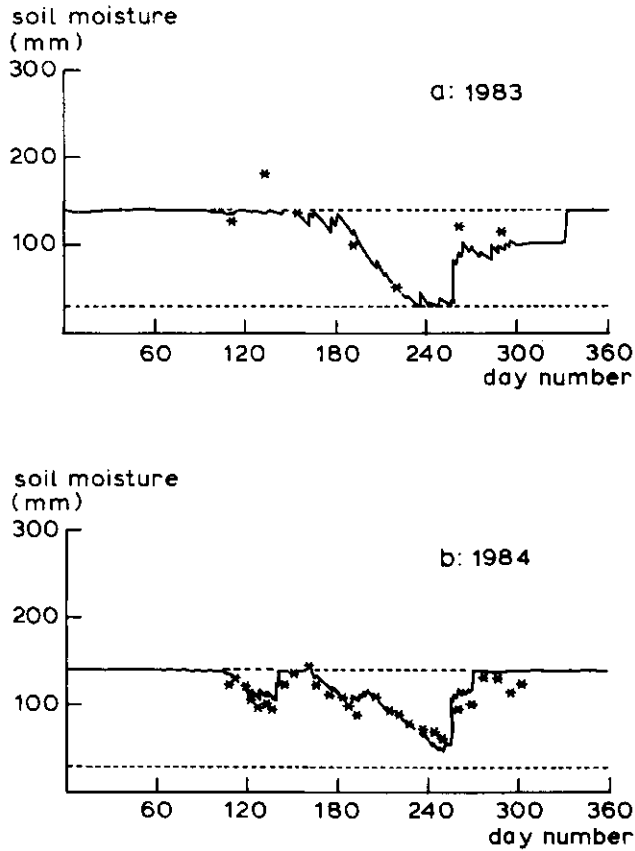
Figure 4.4
Soil moisture content of the root zone in the field plot WB, during
1983 (Figure 4.4a) and 1984 (Figure 4.4b). Drawn line: simulation
results. Asterisks: field measurements.

For the simulations represented in Figure 4.3 field capacity is chosen
between 2.0 and 2.3, the exact value used was for each plot chosen in accor-
dance with measured water content at the beginning of the growing season.

If lateral soil moisture movements can be ignored, then any decrease in
soil moisture will be caused by either soil evaporation, by root uptake, or

by percolation to the non-rooted underground. In absence of capillary rise from below the root zone, the stock of soil moisture is replenished by infiltration of the precipitation that reaches the forest floor. Soil evaporation under a closed canopy is of minor importance as compared to root uptake, and percolation to the underground occurs only when the soil is at field capacity. The change in water content of the vegetation can be ignored when considering periods longer than a few days, which implies that root uptake is about equal to transpiration. The result is that the actual moisture content of the soil, when the latter is below field capacity, is the result of precipitation, interception, and transpiration. Precipitation data are input to the model, but interception and transpiration are both unknown in the field. This complicates model evaluation to a considerable extent. Overestimation of interception may be compensated by underestimation of transpiration and root uptake, and this compensatory effect may not show up in the simulation results. This is even more complicated in case of incomplete canopy closure, where soil evaporation does play a significant role. This is the case in the field plots D12, D25 and SP4. Hence a good fit of the outcome of the simulation with the field data does not validate the interception and transpiration calculations.

When data on both transpiration and interception are lacking, there is no alternative than to compare simulation results with literature data from comparable situations. For temperate forests, total annual interception appears to be 30 % to 50 % of total precipitation (Gash et al., 1978; Calder and Newson, 1979; Mulder, 1983). Simulated values for annual interception for the 1983 simulations fall within this range, see Table 4.1.

Table 4.1
Annual values for precipitation, interception, transpiration, and percolation
for the field plots D12, D25, and SP4 in 1983. All values in mm.

Plot:	Precipitation	Interception	Evaporation	Transpiration	Percolation
D12	1040	330	105	150	448
D25	995	316	93	177	409
SP4	995	337	89	190	381

Consideration of the foregoing, together with the circumstance that the
interception model used has been evaluated elsewhere (Gash, 1979), does not
lead to serious doubts about the interception model used. With regards to
transpiration: the simulated values are consistent with the values given in a
review by Roberts (1983). Combining the arguments given above does not
validate the simulation of soil moisture, but does not lead to rejection of
the approach taken. Additional evidence for the correctness of the model is
given in Figure 4.4b, where an independent measurement set of the field plot
WB is compared with simulated soil moisture. The simulation results fit the
field measurements reasonably well.

4.6.2   The influence of water availability on growth

When the amount of available moisture in the rooted zone decreases because
of root uptake and transpiration, soil water potential decreases, foliage
water potential declines, and maximum stomatal conductance is lower. This in
turn, leads to decreased primary production and hence to less dry weight
increment. Water availability is determined mainly by precipitation and soil
moisture holding capacity of the rooted part of the soil profile. In addition
to the total amount of precipitation, its distribution over the year and its
size distribution, are important. As described in Section 2.2.1., size
distributions for monthly amounts of precipitation were generated using the
approach described by Geng et al. (1985). The effects of differences in total
rainfall, and of different distribution over the years are shown in Table

4.2. From this table it appears that on good sites (with large water holding capacity), an amount of precipitation of 600 mm annually, suffices to attain near optimal growth, provided the precipitation is homogeneously distributed over the year. Either less storage capacity, or less rainfall within the growing season, leads to considerable growth decline.

When annual precipitation is increased to some 960 mm, the importance of the distribution during the year again becomes visible: there is hardly an influence of moisture holding capacity on growth in case of homogeneously distributed rainfall, whereas there appears to be a considerable (30 %) growth decline even on the intermediate site when rainfall during the growing season (from April through September) is decreased by 50 %. This implies that also on favourable sites, with a fairly large moisture holding capacity, effects of drought on growth may occur, even in years with more than average (750 mm) rainfall.

Table 4.2
Effects of amount and seasonal distribution of precipitation on annual growth
per hectare of a reference stand on three sites whose soil moisture availability
differs. Age = 50 yrs, N_2 = 400 trees per hectare, LAI = 7, Height = 27.5 m,
dbh = 33 cm, BA_{sw} = 15 m^2. Tabulated criteria: the degree of water stress,
expressed as the ratio between actual yearly canopy assimilation and potential
canopy assimilation. Weather data used are 30 averages for Wageningen, the num-
ber of rain days each month is assumed to be 18 throughout the year. Available
moisture is 75 mm for Site I, 150 mm for Site II, and 225 mm for Site III. The
growing season is assumed to consist of April, May, June, July, August, and Sep-
tember.

Site conditions:	Canopy ass. (10^3 kg CH_2O)	Net prod. (10^3 kg DM)	Ann. incr. (m^3 stem volume)	Ann. transp. (mm)	Actual:Potential assimilation
Prec = 600 mm, 25 mm p.m. in growing season.					
Site I: 75 mm	23.6	7.0	7.5	108	0.45
Site II: 150 mm	28.3	9.6	10.5	136	0.55
Site III: 225 mm	33.4	12.6	13.9	174	0.71
Prec = 600 mm, 50 mm p.m. in growing season.					
Site I: 75 mm	34.7	13.4	14.7	172	0.72
Site II: 150 mm	38.8	15.7	17.5	202	0.81
Site III: 225 mm	43.9	18.7	21.1	238	0.95
Prec = 960 mm, 40 mm p.m. in growing season.					
Site I: 75 mm	28.9	10.1	11.0	137	0.56
Site II: 150 mm	33.8	12.8	14.2	170	0.69
Site III: 225 mm	40.1	16.5	18.4	213	0.85
Prec = 960 mm, 80 mm p.m. in growing season.					
Site I: 75 mm	43.9	18.7	21.1	238	0.95
Site II: 150 mm	44.1	18.8	21.2	240	0.96
Site III: 225 mm	44.1	18.8	21.2	240	0.96

5   NITROGEN AND PHOSPHORUS REQUIREMENTS AND SUPPLY

5.1   Introduction

In the previous chapters, primary production, dry weight increment, and
stem volume increment were calculated for production situations in which
growth was limited by three factors: climate, species parameters and water
availability. As well as hydrogen, oxygen and carbon, plant tissue contains
elements such as nitrogen (N), phosphorus (P) and sulphur (S) in proteins,
and potassium (K) accompanying organic anions. Many other elements play a
role or in enzymes as part of the cell material, but these will not be
considered here. To date, modelling of plant nutrition has mainly been
limited to nitrogen and phosphorus (with most emphasis on nitrogen; see
reviews by Penning de Vries, 1981, 1983). The model described in this thesis
is also limited to nitrogen and phosphorus, because in general these elements
are considered to be the main nutrients limiting forest growth on sandy soils
(Fiedler et al., 1973; Gussone, 1974; Miller, 1984).

For a given species, the nitrogen and phosphorus content of the structural
dry matter varies within certain limits: dry weight increment requires a
minimum amount of these elements, and can incorporate a certain maximum.
Beyond the minimum concentration there is no further growth and at the
maximum concentration there is no further uptake. Hence, for a known growth
rate (calculated from weather conditions, canopy closure, and water availa-
bility) the accompanying nutrient requirements can be calculated. These
nutrient requirements have to be met either by drawing from the stock of
available nutrients in the plant itself (through redistribution), or by root
uptake of nutrients available in the soil.

Nitrogen and phosphorus are both linked to metabolic activity, and carbon
dioxide assimilation decreases when nitrogen or phosphorus content of the
foliage is less than optimal. The decreased growth acts as a feedback mecha-
nism on nutrient requirements. This trade-off between uptake and supply can
be simulated with an elementary model in which supply and demand determine
the actual nutrient status and the accompanying growth reduction, if any.

phosphorus. Since foliage also exhibits the main metabolic activity, foliar analysis is most suitable for assessing tree and stand nutrient status, and for estimating the influence of nutrient status on growth. In the analysis, most emphasis was placed on the concentrations of nitrogen and phosphorus in the needles. It was assumed that branch, stem and root concentrations vary accordingly between their proper minimum and maximum concentrations.

The maximum and minimum values for nitrogen and phosphorus in situations without any mutual interference, as used in the model for all biomass components, are given in Table 5.1. Differences in concentrations in the tissue resulting from changes in age or development stage have not been taken into account, as the the model was applied only to closed stands beyond the juvenile stage.

Table 5.1
Minimum and maximum concentrations in needles, branches, stems and roots as used in the model. Data from Blok et al. (1975), Turner et al. (1979), Foerst (1980), Mead (1984), and van den Burg (1985).

	N_{min}	N_{max}	P_{min}	P_{max}
needles	0.80	2.00	0.08	0.30
branches	0.15	0.50	0.02	0.08
stemwood	0.02	0.10	0.005	0.02
roots	0.15	0.50	0.02	0.08

Applying the data from Table 5.1 to a theoretical stand with 10 000 kg needles, 20 000 kg branches, 200 000 kg stems, half of which is dead heartwood, and 25 000 kg roots, results in total amounts of nitrogen and phosphorus in the living biomass (excluding heartwood) of 525 N kg and 78 P kg, respectively, for a situation with maximum concentrations, and 208 N kg and 27 P kg for a situation with minimum concentrations of nitrogen and phosphorus in all biomass components.

5.2.2   Redistribution of nitrogen and phosphorus before litter loss

When modelling the amount of nutrients, that is available for incorpora-
tion into newly formed biomass, several possible sources of nutrients must be
considered, e.g. nutrients mineralizing from soil organic matter and litter,
nutrient input from the atmosphere, and retranslocation of nutrients within
the tree. These processes depend to different degrees on stand characteris-
tics and death rates of biomass components, and have to be considered sepa-
rately e.g. in terms of distinct nutrient cycles (see Miller, 1979). This was
not pursued here; instead, an overall distinction was made between retranslo-
cation of nutrients already in the biomass, the release of nutrients from the
amounts stored in the rooted soil compartment, and external inputs of
nutrients. Retranslocation of nutrients takes place prior to abscission of
dead needles and branches, and during the transformaticn from sapwood to
heartwood. Part of the nutrients contained in the old tissue can be mobilized
and withdrawn from the dying material. Thus, once taken up, nutrients may be
used efficiently within the tree. The magnitude of this internal re-use of
nutrients depends on the mobility of the nutrient itself, and on the demand
for nutrients in the rest of the tree. When nitrogen and phosphorus are in
ample supply in the soil, and there is no restriction on uptake by the trees,
then there is less need for internal re-use than in the situation where
nitrogen and phosphorus are scarce and only small amounts are available for
incorporation in new tissue (van den Driessche, 1984).

Both nitrogen and phosphorus can be re-used to a considerable extent, data
indicate that phosphorus is more mobile than nitrogen (Turner, 1975, 1981).
As the extent to which retranslocation of nutrients depends on environmental
conditions and nutrient availability in the soil is not clear enough to be
modelled in detail, nutrient withdrawal before litter loss was assumed to be
the same under all conditions. It was calculated as a fixed fraction of the
amount of nitrogen and phosphorus in the organic matter prior to abscission.

Dying biomass is not the only source of retranslocatable nutrients. If the
nutrient concentrations in older needles are higher than the initial nutrient
concentrations in the current needles, it is feasible that redistribution
will also occur from living needles to the newly formed foliage. In the model
it was assumed that all the tissue of a biomass component has the same
nutrient concentration, regardless of age class, or position in the tree. In

this way, continuous retranslocation was assumed. Additional retranslocation still occurs at the time of shedding or dying of part of the living biomass. In this way, internal redistribution prior to litter fall, as well as lower nutrient concentrations in the litter, are both accounted for. As branches and sapwood have a longer life-span than needles and fine roots, it was assumed that redistribution of nutrients from branches and stemwood was more efficient than in the case of needles and roots, where abscission is much more rapid, and that a greater portion of nitrogen and phosphorus contained in branch and sapwood are retained. When needle biomass decreases because of sudden crown damage, e.g. that is caused by gales, there can be no redistribution at all, and the dead material has a higher concentration of nitrogen and phosphorus than in the case of natural dying. This was not taken into account, as it was assumed that wind damage is only a minor cause of litter loss.

Investigations by Turner (1975) show redistribution of about 25 % for nitrogen and 35 % for phosphorus from the amounts contained in root and foliage biomass, and 50 % for both nitrogen and phosphorus in the dying of branches and in the transition from sapwood to heartwood (see also van den Driessche, 1984). These rates are used in the model, with the fractions redistributed from dying roots being the same as for foliage and branches.

5.2.3   Nitrogen and phosphorus requirements for growth

Using maximum and minimum concentrations, together with the percentages of redistribution mentioned above, minimum nitrogen and phosphorus requirements and maximum nitrogen and phosphorus uptake can be calculated in situations where the growth and death rates of the biomass components are known. The latter can be calculated according to the approach described in the previous chapters or if, for example, field trials are being evaluated, they can be based on field measurements of increment rates.

In a situation where there are no limits imposed on primary production other than temperature and radiation, optimal growth is attained by a completely closed canopy. Under Dutch conditions, the model gives potential growth rates of 20 000 to 22 000 kg DM ha^{-1}yr^{-1}. Using a growth rate of 20 000 kg dry matter, consisting of 4 000 kg of foliage, about 1 000 kg of branch biomass, 10 000 kg of stem biomass, and 5 000 kg root biomass, maximum

nitrogen and phosphorus needs amount to 120 and 18.8 kg ha^{-1}yr^{-1}, respectively. With a redistribution of 32.5 kg nitrogen and 6.5 kg phosphorus, the amounts remaining to be taken up from the soil equal 87.5 kg nitrogen ha^{-1}yr^{-1} and 12.3 kg phosphorus ha^{-1}yr^{-1}. When growth is less, e.g. as a result of water shortage or incomplete canopy closure, maximum nutrient uptake rates are decreased accordingly.

5.3   Nitrogen and phosphorus availability

Nutrient availability depends on the soil volume that is rooted by the trees, on the concentration of nutrients in the soil solution, and on the rates of release from the nutrient pools in the soil together with the input of nutrients to the rooted soil compartment.

Both nitrogen and phosphorus in the soil are not only taken up by the plants, but are subject to other processes as well, which in addition to the input processes mentioned previously, further complicate their chemistry in the soil. Deterministic simulation approaches are difficult under these circumstances, and so far only complex, comprehensive models have been developed (van Veen, 1977; Penning de Vries, 1981). These models can be used to study dynamics of the processes in detail, but lack of quantitative knowledge prevents them from being implemented in general primary production models. In the case of a perennial crop such as a forest, however, an average value for nutrient availability suffices.

The most simple model would be to estimate availability as a fixed fraction of the total amount of nutrients within the system. This might be useful in an equilibrium situation with a constant growth rate and constant nutrient input rates. However, growth as well as input rates change with stand age, and this influences nutrient availability, even in situations where the amounts of nutrients added to the system each year are small compared with the amounts already present in the soil. Therefore, a somewhat more complicated model which incorporates slow as well as fast changing processes has to be used. The approach used is essentially the same for phosphorus and nitrogen; the only differences are in the parameter values used in the transfer processes. As the exact nature and magnitude of the underlying processes are of no great explanatory value here, an elementary model such as the one

described by de Wit and Wolf (1984a,b), suffices to evaluate the effects of nitrogen and phosphorus on growth.

In the models developed by de Wit and Wolf, two nutrient pools in the soil are considered (for nitrogen and phosphorus independently): a stable slow-release pool, and an unstable fast-release pool, both of which relate to the amounts of nutrients in the rooted zone of the soil profile only. All input into the soil compartment, either through atmospheric input, litter decomposition, biological fixation or fertilization, are either taken up by the trees, lost through denitrification and leaching, or added to the stable or unstable pools. Figure 5.2 gives a relational diagram of the nutrient transfers in the soil.

From the diagram in Figure 5.2, it can be seen that even in this simple model some 20 transfer- and distribution-coefficients have to be estimated for each element. The estimation can however, be simplified by lumping of relatively unknown but comparable input processes. If detailed information is lacking, there is no point in treating industrial fertilizer input, input from decomposition, and atmospheric background input, separately. Instead, the same estimate for the transfer coefficients can be used; this simplifies the matrix of coefficients to a large extent. Also, in case of phosphorus, atmospheric deposition and biological fixation do not occur, and leaching of soluble phosphate out of the profile is negligible. Reducing the number of coefficients to be estimated in that way, the remainder has to be estimated from the behaviour of applied fertilizer in soils. It must be stressed that the preliminary parameter values that are used here are based on rough estimates for acid, sandy forest soils from general knowledge only, and have to be re-estimated when using the model in detailed studies. The parameter of prime importance is the recovery rate, which is applied to fertilizer input and to the fraction of each element that becomes available from the unstable pool. Table 5.2 gives the parameter estimates that have been used in the model.

Stable and unstable pools are in dynamic equilibrium, and transfer rates between the two can be represented by first-order equations, in which the stable pool (SP) acts as a slow-release pool with all nutrients that are released being added to the unstable pool (LP).

Figure 5.2
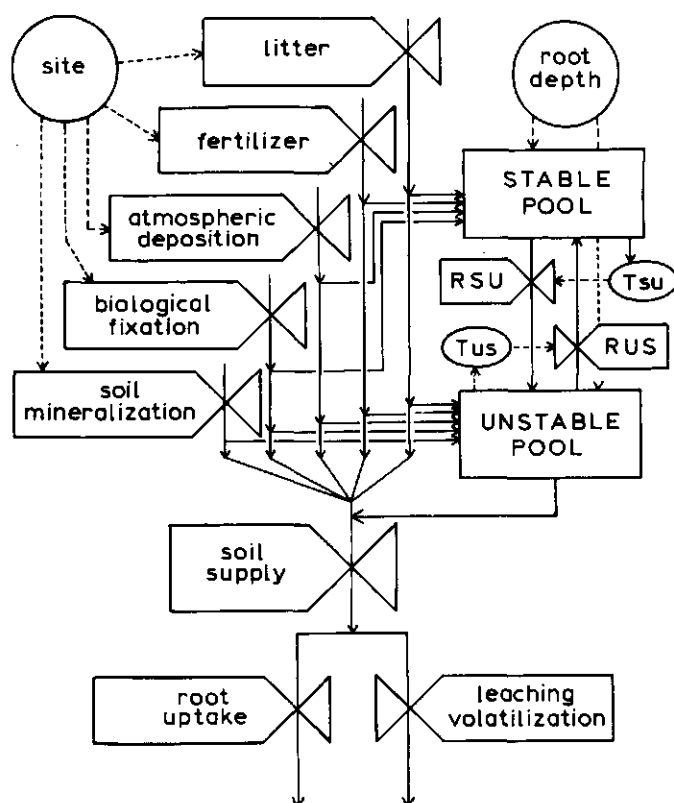Relational diagram of the nutritional part of the model. Solid
lines: material flows; dotted lines: relationships between rate
variables and state variables, and between driving, intermediate,
and rate variables. RSU and RUS represent the tranfers from the
stable to the unstable pool, and from the unstable to the stable
pool, respectively. The time-coefficients involved are represented
by TSU and TUS.

Table 5.2
Transfer coefficients used to calculate nutrient supply. All coefficients
are dimensionless fractions. Loss covers both leaching and denitrification.

From: to:	trees	loss	unstable	stable
nitrogen:				
litter:	0.4	0.2	0.3	0.1
fertilizer:	0.4	0.3	0.2	0.1
atm. input:	0.2	0.3	0.4	0.1
biol. fix.:	0.2	-	0.6	0.2
unstable pool $(R_{LP,t})$:	0.67	0.33	-	-
phosphorus:				
litter:	0.05	-	0.75	0.2
fertilizer:	0.05	-	0.85	0.1
atm. input:	-	-	-	-
biol. fix.:	-	-	-	-
unstable pool $(R_{LP,t})$:	1.0	-	-	-

The rate of change of the stable pool can be expressed as follows:

$$\frac{dSP}{dt} = \frac{LP_t}{TUS} - \frac{SP_t}{TSU} + I_{SP,t} \qquad (kg\ ha^{-1}yr^{-1}) \quad (5.1)$$

SP_t/TSU and LP_t/TUS represent the transfer rates from the stable pool to the
unstable pool, and vice versa (RSU and RUS in Figure 5.2). The transfer
coefficient describing the release to the unstable pool (TSU, in yr), is
approximately 150 years for nitrogen, and 60 years for phosphorus. The
coefficient used to describe the transfer from unstable to stable (TUS, in
yr) was assumed to be 8 for nitrogen and 5 for phosphorus; these coefficients
depend on the soil type involved. $I_{SP,t}$ represents the input to the stable
pool as a result of fertilizer use, atmospheric input, biological fixation,
and litter fall. $I_{SP,t}$ was

calculated from annual input rates, using the coefficients in Table 5.2. For the rate of change of the unstable pool, the equation reads:

$$\frac{dLP}{dt} = \frac{SP_t}{TSU} - \frac{LP_t}{TUS} + I_{LP,t} - R_{LP,t} \qquad (kg\ ha^{-1}yr^{-1}) \quad (5.2)$$

in which $R_{LP,t}$ is the net release from the unstable pool, and $I_{LP,t}$ the amount added as a result of fertilizer use etc. Both transfer rates were calculated at the end of the year, and using them, the values for the stable and unstable pools were updated. In the case of nitrogen, the amount released by the unstable pool is either taken up by the trees, or lost by processes such as denitrification and leaching. The distribution of $R_{LP,t}$ over tree uptake and loss will be comparable to the distribution of the amount of nitrogen in the litter over these two. The resulting coefficients are given in Table 5.2. The loss is, among others, due to part of the release taking place during the dormant season, when little or no uptake by the roots takes place. Phosphorus is much less mobile in the soil, and leaching losses are negligible. All phosphorus released from the unstable pool was therefore assumed to be available for uptake. In the case of availability exceeding nutrient demands it was assumed for nitrogen that the surplus was partly retained in the unstable pool, and partly leached out of the profile, corresponding to the distribution of nitrogen contained in the litter loss over these two sink-terms. For phosphorus, the remainder is completely restored in the unstable pool, when availability exceeds uptake.

Soil nutrient availability, or potential uptake (U_p), now equals the amount of nutrients that can be taken up immediately by the trees from the inputs by fertilizer use, atmospheric deposition, biological fixation, and litter fall, together with the maximum amount available from release by the unstable pool. The total amount released by the unstable pool can be estimated from the known recovery fraction of applied fertilizer, assuming that the availability of fertilizer is the same as the availability of the nutrients in the unstable pool. This is based on the observation that a few days after fertilizer application, phosphate fertilizer is already indistinguishable from unstable phosphate in the soil (Lehr et al., 1959; Henstra et al., 1981; Leenaars-Leijh, 1985). The model is essentially the same for nitrogen and phosphorus, the only differences being in the parameter values (Table 5.2). Recovery rates for phosphorus are, in general, low, because of the capacity

of the soil to immobilize the phosphate applied. In acid sandy forest soils, the recovery for phosphorus fertilizer in general, will vary between 0.03 and 0.10 (Driessen, 1986, Wolf et al., 1987). The recovery for applied nitrogen is, on a annual basis, usually higher: around 0.2-0.3.

In the case of phosphorus an additional, virtually inert pool may be distinguished apart from the stable and unstable pool described above. From this inert pool, nutrients are only very slowly released. In the model it was assumed that this pool contains half of the total amount of phosphorus in the rooted zone and that this amount mineralizes at a rate of 0.05 % per year. If there is 2 000 kg P per hectare in the rooted zone, this mineralization rate is 0.5 kg $ha^{-1}yr^{-1}$. The rest of the total amount of phosphorus was distributed over the stable and unstable pools.

The rates of fertilization, organic matter decomposition, atmospheric deposition and biological fixation are input data to the model, and must be specified by the user. Also to be specified, in addition to the input rates and transfer coefficients which are site specific, are the initial amounts of nutrients in the stable and unstable pools. A first estimate of the distribution of nutrients over stable and unstable can be derived from the transfer coefficients between stable and unstable pools, assuming that an equilibrium situation exists between the two $(LP_t/TUS = SP_t/TSU)$.

Fertilizers are rarely applied to Dutch forest stands, and therefore, atmospheric input is the only major flux of nutrients entering the system. Traditionally, atmospheric input is small in relation to the annual uptake of a stand, or compared with the nutrient reserves in the soil, but considering the rotation length and longevity of a forest stand, it can be of considerable importance. The atmospheric input of phosphorus other than from dust is negligible, and therefore the total input of phosphorus is negligible. It was set to zero in the model. Background atmospheric input of nitrogen, either as wet (ammonium or nitrate in rain) or dry (ammonia) deposition can vary considerably in time and with location of the site. Natural background input in western Europe is around 10 - 20 kg $ha^{-1}yr^{-1}$ (Minderman, 1967), but in the Netherlands has increased in recent years to values around 50 kg nitrogen $ha^{-1}yr^{-1}$, because of, among others, fertilization and the production and spreading of excess manure from intensive livestock farming (van Aalst, 1984; van Breemen et al., 1982, 1983).

5.4   Simulating the influence of nitrogen and phosphorus on growth

Using the elementary nitrogen and phosphorus models described in the
preceding section, demand and supply rates can be compared and balanced at
the end of each year, by decreasing or increasing the concentrations of
nitrogen and phosphorus in the newly formed biomass.
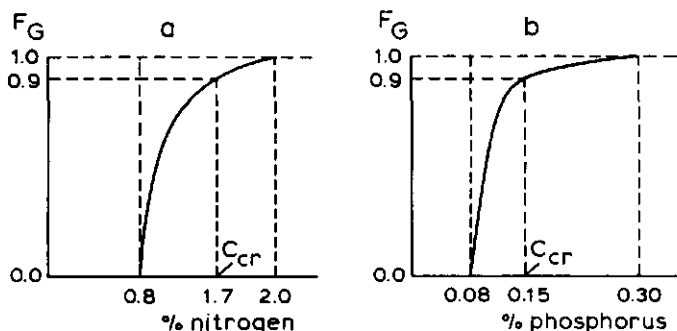
Figure 5.3
Relationship between growth reduction and element concentration in
the current needles for nitrogen (a) and phosphorus (b), as used in
the model. F_G denotes the reduction in growth deduced from the
element concentration. C_{CR} denotes the critical element concentra-
tion at which growth is reduced by 10 %, hence F_G equals 0.9.

The nitrogen and phosphorus content of the needles affects total stand
growth. A suggested relation between growth reduction (F_G) and the nitrogen
or phosphorus content of the needles is given in Figure 5.3. At the maximum
concentration the growth is determined by other factors such as canopy
closure or water availability. Between the minimum and the maximum concentra-
tion, growth is reduced and in addition to the growth factors described
previously, nitrogen or phosphorus determine productivity. At the minimum
concentration, the growth is zero. The shape of the curve in Figure 5.3 is
based on the observation that at a nitrogen content of about 1.7 %, or at a
phosphorus content of 0.15 %, growth is reduced by 10 % (Bengtson and
Holstener-Jørgensen, 1971; van den Burg, 1985).

Taking into account only the nitrogen content and the needle biomass, the calculation of growth and uptake proceeds as follows. Let the needle biomass in the year t be W_t and the amount of nitrogen in this biomass N_t. The nitrogen fraction in the needle biomass is then:

$$c_t = N_t / W_t \qquad\qquad \text{(kg kg}^{-1}) \qquad (5.3)$$

The weight of the needle biomass in the year t+1 (W_{t+1}) can now be estimated as

$$W_{t+1} = W_t + I_t - L_t \qquad\qquad \text{(kg ha}^{-1}) \qquad (5.4)$$

The annual needle increment (I_t) equals

$$I_t = F_G \times \text{(simulated increase)} \qquad\qquad \text{(kg ha}^{-1}\text{yr}^{-1}) \quad (5.5)$$

in which F_G is read from the graph in Figure 5.3, using c_t as the independent variable, and the simulated increase is the increment that would occur when nitrogen is in ample supply. Litter loss (L_t) is equal to annual litter loss as calculated in Chapter 3.

The amount of nitrogen in the needles in the year t+1 is equal to

$$N_{t+1} = N_t + U_t - LN_t \qquad\qquad \text{(kg ha}^{-1}) \qquad (5.6)$$

Using f_w for the fraction of the total amount of nitrogen that is withdrawn before abscission, the loss of nitrogen (LN_t) can be calculated as:

$$LN_t = (1 - f_w) \times c_t \times L_t \qquad\qquad \text{(kg ha}^{-1}\text{yr}^{-1}) \quad (5.7)$$

The uptake of nitrogen (U_t in Equation 5.6) is the minimum of the potential uptake (U_p) of the nitrogen in the soil and the maximum of the nitrogen that can be taken up by the needles:

$$U_t = \text{Min} (U_p, W_{t+1} \times c_{max} - (N_t - LN_t)) \qquad \text{(kg ha}^{-1}\text{yr}^{-1}) \quad (5.8)$$

The presence of branches, roots and stems were taken into account by assuming that their relative element contents are proportional to the contents of the needle biomass. Increment, litter loss and turnover were taken from the primary production model (Chapter 3).

Similar calculations as given above for nitrogen, can be performed for phosphorus. For both elements, the concentration in the needles are calculated, and using the corresponding reduction factors derived from Figure 5.3, the separate influences on growth of nitrogen and phosphorus are estimated. The strongest reduction on increment (smallest value for F_G) resulting from either nitrogen or phosphorus limitations is used in the model.

6   SIMULATION RESULTS AND EVALUATION OF THE MODEL

6.1   Introduction

The model was developed to simulate the growth of a stand over a period of
several decades. The main interest was in total growth (expressed as stem
volume per hectare) particularly the relationship between site conditions and
growth. Less attention was paid to the growth of individual trees. To evalu-
ate how the model behaves, the results it gives have to be compared with
measurements of growth and total stem volume production in permanent field
plots. Ideally, the simulated value for all biomass components (foliage,
branches, stems, and roots) should be compared with data from field plots,
but because it is difficult to estimate biomass weights other than stem
biomass non-destructively in forest stands, no time series of this type are
available. The model's performance for foliage, branches and roots was
evaluated by comparing the results of simulations with published data from
other sites.

Because the field plots D12, D25 and SP4 were used when developing the
model, the model's performance could not be compared against the field data
from these plots. Note that the assimilate distribution that is used has been
chosen to give a good fit with the stem volume measurements from the same
three field plots, within the limits of published values: see Section 3.5.3.
An additional, independent data set was therefore required to evaluate the
model's performance, and therefore another field plot was used. This control
plot, coded D2, was not simulated until the model had been developed and all
the model's parameters had been estimated.

The model relies on the assumption that any major change in tree growth
during stand development can be explained by changes in assimilate distribu-
tion, and by considering variations in climate, light interception and the
availability of water, nitrogen and phosphorus. The availability of water and
nutrients define the productivity of the site, given that the potential
growth level is determined by climate and species properties. Both water and
nutrients influence growth throughout the rotation in much the same way. The

influence of the availability of nitrogen and phosphorus is less variable
than the influence of water availability, because these elements do not
depend on an annually varying input such as precipitation. Light interception
is the factor that depends most on canopy structure and which changes during
stand development. Assimilate distribution is the main physiological variable
determining changes in growth during the ageing of the trees. There is no
ageing of photosynthetic performance or of root activity, because both
biomass components rejuvenate through growth in combination with litter loss
and turnover of older tissue.

6.2   Permanent field plots

The data used to evaluate the overall performance of the model were, as
mentioned briefly in Chapter 2, time series of stem volume measurements from
permanent plots. The permanent plot data used are part of the large data base
on which the yield tables currently used in the Netherlands are based. The
construction of yield tables and the descriptive modelling of forest growth
rely largely on statistical models that require a substantial data base for
parameter estimation (see Fries, 1974, and Fries, Burkhart and Max, 1978, for
examples of descriptive growth and yield models, and LaBastide and Faber,
1972, and Bergel, 1985, for examples of yield tables).

Permanent field plots for Douglas fir growth and yield research were
established in the Netherlands as early as 1923, and thus some 50 years of
data are now available. The three field plots used for this study consisted
of an old stand, planted in 1882 on a near-optimum site which shows no
indication of water, nitrogen or phosphorus shortage influencing yield, and
of two younger stands, planted in 1921 and 1928, which exhibited growth
reductions because of limitations of water and of nutrient availability. The
plots were made available by the Dorschkamp Research Institute for Forestry
and Landscape Planning in Wageningen (plots D12 and D25), and the Department
of Forest Management of the Wageningen Agricultural University (plot SP4).
Figure 1.1 shows the location of the plots.

The field plot data consist of recordings of individual tree diameter
(dbh, 1.3 m) and tree height. Using a volume equation together with the
number of trees per plot, tree and stand volumes were calculated. The inter-
val between two measurements varied from 2 to 6 years. The plots had been

laid out in young stands after the canopy had closed, and had been remeasured
for as long as possible. If a plot was to be thinned it was measured before
and after, and the trees removed by thinning were indicated in the plot
records. Summaries of the field plot data for the three main plots are given
in Tables 6.1.a, 6.1.b, and 6.1.c.

The soil types are deeply reworked brown podzolic forest soils in pregla-
cial fine to coarse sands, without any influence of a water table. The latter
is located at great depth (5-10 m) below the forest floor, hence capillary
rise could be ignored. The near-optimum site D12 (see Table 6.1.a) consists
of old arable land, rich in organic matter to a considerable depth (80-90
cm). This explains its large moisture-holding capacity and also the large
amounts of nitrogen and phosphorus in the rooted zone.

The data sets used here were part of the data base used in earlier re-
search carried out by de Vries (1961) on thinning regimes, by Veen (1951,
1958) on provenance selection for the Netherlands, and by LaBastide and Faber
(1972) on yield tables. The independent plot D2 was used by Faber (1983) in
research on stand structure and competition. The field plots are described in
detail in these author's publications.

All the field plots have been subjected to forest management practices
common in the Netherlands. In general, this implied moderate thinning from
below, in which a number of trees whose volume was less than average for the
plot, were removed. Thinning was done at 3- to 10-year intervals, during the
winter. In the model, thinning is done at the end of the year, in agreement
with the thinning management carried out in the field. Individual thinning
operations were characterized by the number of trees removed, and by the
fraction of the total stem volume that was removed by the thinning. Both
variables were taken from the field data sets and used as input to the
simulation model. In this way, comparison of simulation results and field
measurements of growth and total yield is not blurred by the effects of
thinning operations.

Table 6.1.a
Plot D12: data summary.

Year of emergence:	1882.		Plot area:		0.2507 ha.
Maximum rooting depth:	1.60 m.		Measurement period:		60 yrs.

Nutrients in the rooted soil profile: 5 400 kg P, 15 000 kg N.
Available soil moisture when at field capacity: 170 mm.

date	age yrs	h_{dom} m	N ha^{-1}	d_g cm	basal area $m^2 ha^{-1}$	volume $m^3 ha^{-1}$
11-'23	42.	25.8	227	50.0	44.7	444.9
11-'28	47.	29.3	227	52.8	49.7	552.4
11-'33	52.	31.9	227	54.9	53.8	643.1
			211	56.4	52.7	632.8
11-'38	57.	33.8	211	59.3	58.5	733.4
10-'43	62	35.2	211	61.3	62.3	810.4
			195	61.4	57.9	752.9
11-'48	67.	35.8	195	61.8	58.7	775.9
11-'51	70.	37.0	195	63.2	61.2	818.3
			187	63.4	59.1	799.4
12-'54	73.	38.0	187	63.7	59.8	826.3
1-'57	75.	38.6	187	64.1	60.5	843.2
			148	66.0	50.5	709.4
1-'60	78.	38.6	148	67.0	52.0	728.7
3-'65	83.	39.0	148	67.4	52.7	744.8
1-'70	88.	39.2	148	67.5	52.9	750.9
			144	68.0	52.0	738.5
5-'75	93.	39.9	144	69.0	53.7	774.1
10-'83	102.	40.4	144	71.7	58.2	806.2
			136	71.7	54.9	759.3

Table 6.1.b
Plot D25: data summary.
Year of emergence: 1920.   Plot area: 0.2000 ha.
Maximum rooting depth: 1.20 m.   Measurement period: 36 yrs.
Nutrients in the rooted soil profile: 2 000 kg P, 4 000 kg N.
Available soil moisture when at field capacity: 90 mm.

date	age yrs	h_{dom} m	N ha^{-1}	d_g cm	basal area $m^2 ha^{-1}$	volume $m^3 ha^{-1}$
7-'49	30.	16.4	1025	16.9	23.0	171.2
1-'52	32.	18.1	1025	18.3	27.0	215.8
			830	19.4	24.6	197.6
2-'57	37.	20.7	830	21.6	30.4	265.9
			715	22.6	28.7	252.7
9-'59	40.	22.7	715	23.6	31.4	296.6
			640	24.4	29.9	283.8
11-'62	43.	24.0	640	25.5	32.7	323.9
			550	26.2	29.7	295.6
1-'66	46.	25.1	550	27.3	32.2	328.0
			515	27.8	31.3	320.3
5-'70	50.	26.3	515	29.1	34.2	360.7
			440	30.0	31.0	328.9
11-'74	55.	28.7	440	32.4	36.4	419.9
			420	32.4	34.7	401.2
12-'77	58.	29.2	420	33.4	36.7	430.2
			360	34.1	32.3	379.6
10-'84	65.	30.1	360	36.9	38.6	441.5

Table 6.1.c
Plot SP4: data summary.

Year of emergence:	1927.		Plot area:		0.2400 ha.
Maximum rooting depth:	1.20 m.		Measurement period:		36 yrs.
Nutrients in the rooted soil profile:	1 600 kg P, 5 600 kg N.				
Available soil moisture when at field capacity: 140 mm.					

date	age yrs	h_{dom} m	N ha^{-1}	d_g cm	basal area $m^2 ha^{-1}$	volume $m^3 ha^{-1}$
1-'48	21.	14.7	1097	15.1	19.5	122.4
12-'49	23.	16.3	1097	16.7	23.9	164.8
			903	17.3	21.1	147.0
1-'52	25.	17.7	903	18.5	24.4	186.4
			739	19.3	21.6	167.7
9-'53	27.	19.0	739	21.1	25.9	212.6
			664	21.5	24.1	198.7
8-'56	30.	21.4	664	23.3	28.2	250.8
			522	24.3	24.1	216.4
7-'59	33.	22.3	522	26.5	28.9	274.4
			478	26.9	27.1	258.5
9-'63	37.	24.2	478	28.6	30.7	307.0
			420	29.1	28.0	280.5
6-'66	39.	25.3	420	30.2	30.0	311.2
			394	30.5	28.7	298.0
11-'70	44.	25.9	394	32.6	32.9	340.9
			363	33.3	31.6	328.0
5-'75	48.	28.3	363	35.1	35.1	391.9
			336	35.6	33.4	364.2
10-'80	54.	29.0	336	37.5	37.2	424.2
			279	37.8	31.2	356.1

Table 6.1.d
plot D2: data summary.

| Year of emergence: | 1904. | Plot area: | 0.2100 ha. |
| Maximum rooting depth: | 1.4 m. | Measurement period: | 50 yrs. |

Nutrients in the rooted soil profile: 4 500 kg P, 12 000 kg N.
Available soil moisture when at field capacity: 160 mm.

date	age yrs	h_{dom} m	N ha^{-1}	d_g cm	basal area $m^2 ha^{-1}$	volume $m^3 ha^{-1}$
6-'23	19.	10.2	4780	10.1	38.5	198.3
6-'28	24.	13.8	4780	11.4	49.0	320.9
			4000	11.6	42.5	279.6
6-'33	29.	17.3	4000	12.8	51.6	399.3
			2411	14.1	37.7	295.9
6-'38	34.	20.2	2411	15.8	47.5	412.3
			1376	19.0	39.1	343.0
6-'43	39.	22.9	1376	20.7	46.4	439.5
			1021	22.6	40.9	391.2
6-'48	44.	24.4	1021	24.4	47.8	488.0
			596	26.9	33.8	347.9
1-'51	47.	26.0	596	27.9	36.5	393.5
			538	28.0	32.7	352.5
10-'53	50.	27.7	538	29.0	35.5	394.4
			481	29.3	32.5	361.6
9-'55	52.	27.9	481	30.3	34.7	387.1
			433	30.9	32.5	363.8
4-'58	54.	29.3	433	31.6	33.9	391.2
			395	32.1	31.9	369.2
10-'59	56.	29.2	395	32.5	32.8	381.9
			329	33.1	28.2	328.7
5-'64	60.	29.6	329	34.7	30.3	355.5
			295	34.7	28.0	329.9
10-'66	63.	29.7	295	35.3	28.8	340.5
2-'72	68.	30.9	295	36.7	31.3	379.4
			290	36.6	30.5	370.0

Thinning also reduces biomass components other than stem biomass. In the
model, the amounts of foliage, branches and roots were decreased proportio-
nally to stem biomass when the stand was thinned. The amounts of nitrogen and
phosphorus removed by thinning or transferred from the trees to the soil
compartment, were calculated from the actual concentrations of these elements
in the tissue, as no retranslocation occurs prior to thinning. The nitrogen
and phosphorus in the stem biomass of the trees that were thinned, was
removed from the site. It was assumed that only stem biomass was harvested
during thinning, and the amounts of nitrogen and phosphorus contained in the
foliage, branches and roots were added to the soil compartment.

6.3   Simulating stem volume increment

The main test of the primary production model is to see how well it
simulates the accumulation of stand volume during stand development. Total
stem volume is closely related to stem dry weight, and therefore stem volume
is a primary trait of primary production. To avoid bias, simulated stem
volume for the whole stand was compared with the stem volume in the field
plots, which was calculated from diameter measured at breast height and tree
height. If simulated diameter were compared with measured diameter, stand
height would have to be simulated with considerable accuracy, because the
model results for diameter are sensitive to bias in calculations of height
growth. To avoid this, it is better to calculate stem volume in the field
plots from measured diameter and height, and subsequently compare it with
simulated stem volumes.

When simulating field plots, the simulation run was started with the field
data from the first time of measurement, as input to the model. Only data on
diameter, height, and number of trees were used, and initial values for the
biomass component weights other than stemwood were derived from published
data (e.g. Turner and Long, 1975; Kestemont, 1977; Keyes and Grier, 1981).
Using these as a starting value, the model was allowed to run for a few
years, so that the initial estimates of biomass could be evaluated. It was
assumed that foliage and fine root mass were fairly constant after canopy
closure. Branch and coarse root mass were allowed to increase slowly. From
the results of these simulations, the initial values used in the main simula-
tion runs were obtained.

In this way total stand volume was simulated for the field plots D12, D25, and SP4, and for the independent plot D2. The results for D12, D25 and SP4 are shown in Figures 6.1, 6.2 and 6.3. The graphs contains simulated and measured stem volumes, as well as simulated and measured periodic annual increments of stem volume. Periodic annual increments were calculated as the average rate of increment (in m^3 $ha^{-1}yr^{-1}$) between two measurements, over periods of 2 to 5 years. This estimation procedure makes the values for periodic annual increment prone to measurement errors, e.g. because of change of field crew or equipment between individual measurements over the years.

It appeared that the model reasonably simulates the pattern and total amount of growth in the three field plots. As mentioned previously, the assimilate distribution used in the model was partly derived from the three field plots simulated, and therefore agreement between model outcome and field measurement in this case does not validate the underlying assumptions, but only indicates the consistency of the model. The versatility of the model is indicated by the observation that the model yields satisfactory results in very different stands, such as D12 and D25. For a more stringent evaluation, the model was run against the independent dataset of plot D2. The simulation results of this test are given in Figure 6.4, which again indicates that the outcome agrees with field measurements. The data used for the simulation of plot D2 are given in Table 6.1.d, together with the field data on total stand volume. From this independent trial it was concluded that the model can be used to calculate total stand growth of Douglas fir under the growing conditions prevailing in the Netherlands.
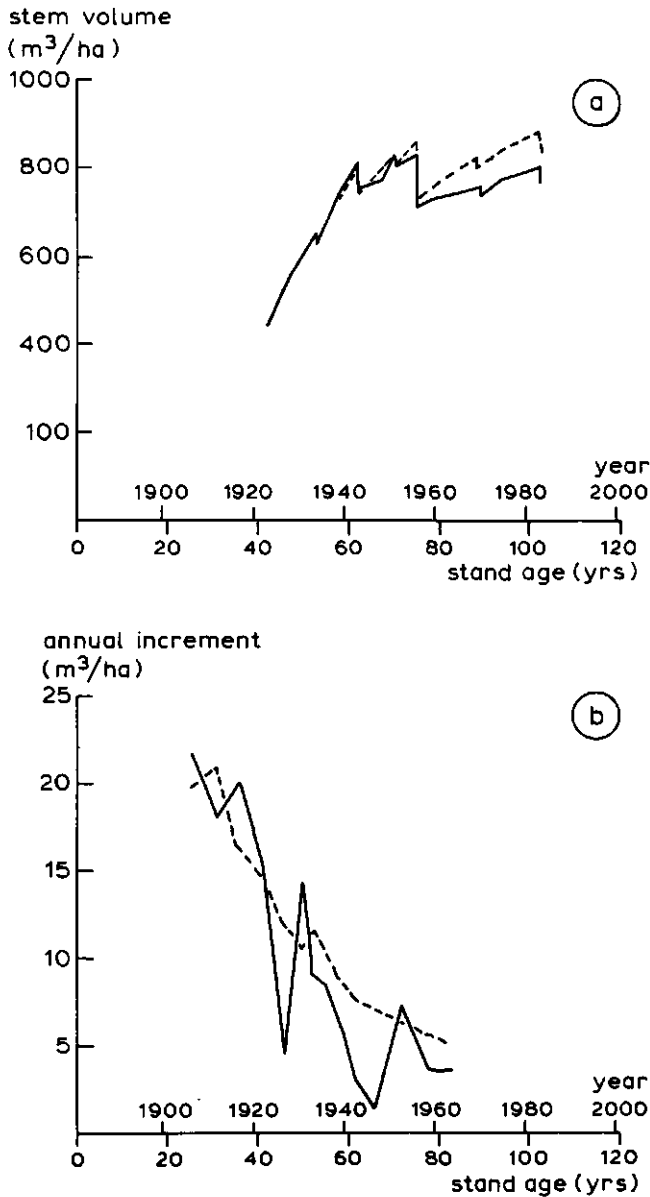
Figure 6.1
Simulated stem volume together with measurements from field plot
D12. a: Total stem volume in $m^3 ha^{-1}$; b: rates of annual stem volume
increment, in $m^3 ha^{-1} yr^{-1}$. Solid lines: field measurements. Dotted
lines: model results. For detailed plot measurements, see Table
6.1.a.

stem volume
(m³/ha)
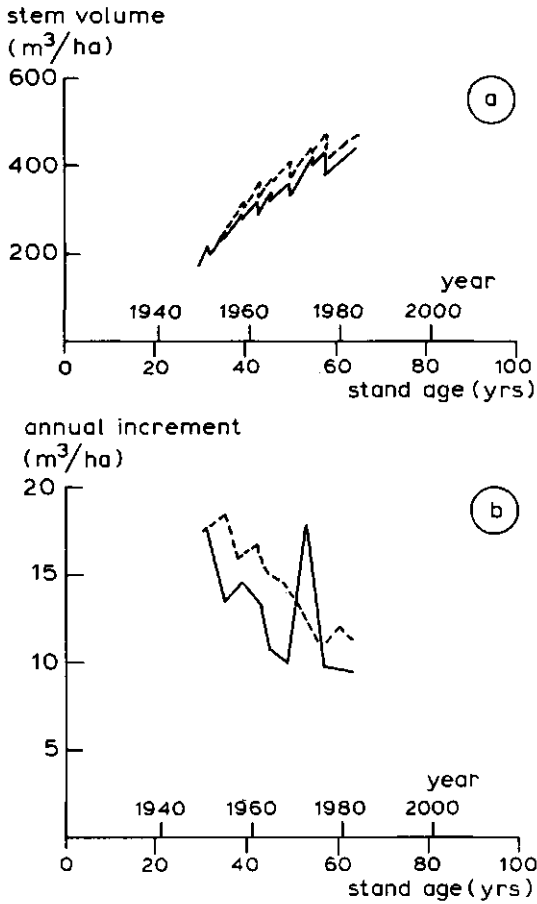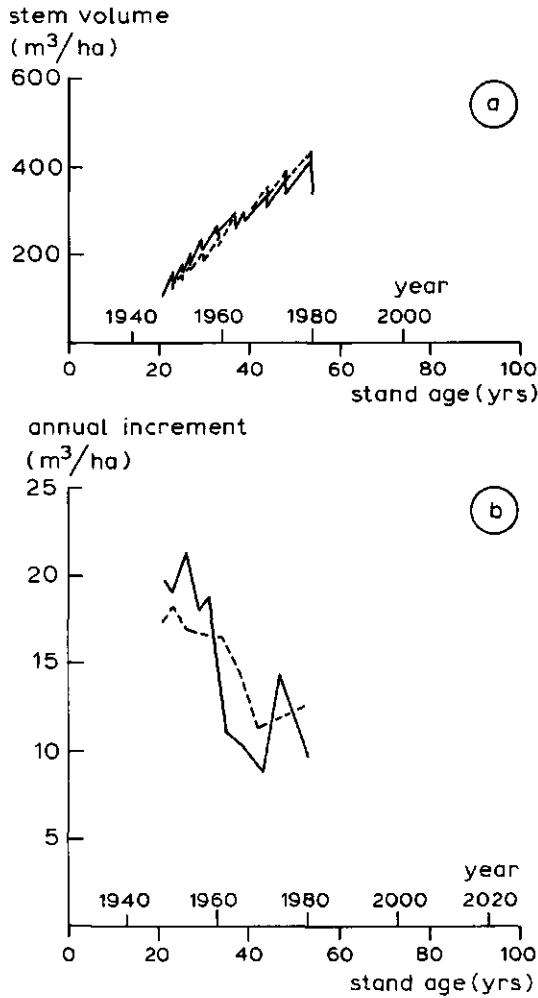

annual increment
(m³/ha)

Figure 6.2

Simulated stem volume together with measurements from field plot
D25. a: Total stem volume in m³ ha⁻¹ ; b: rates of annual stem volume
increment, in m³ ha⁻¹ yr⁻¹ . Solid lines: field measurements. Dotted
lines: model results. For detailed plot measurements, see Table
6.1.b.

Figure 6.3
Simulated stem volume together with measurements from field plot
SP4. a: Total stem volume in $m^3 ha^{-1}$; b: rates of annual stem volume
increment, in $m^3 ha^{-1} yr^{-1}$. Solid lines: field measurements. Dotted
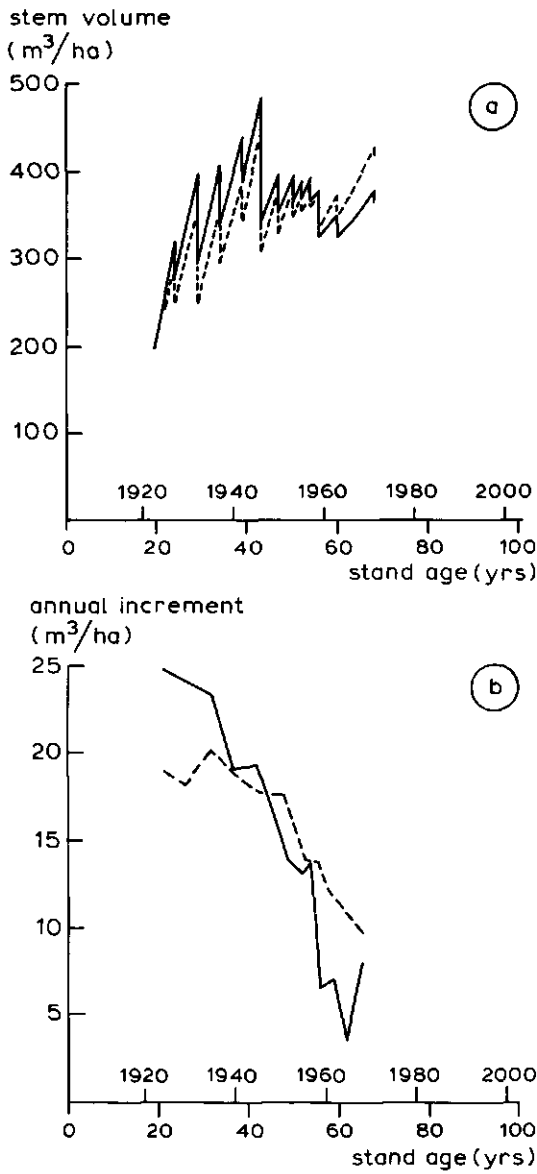lines: model results. For detailed plot measurements, see Table
6.1.c.

Figure 6.4
Simulated stem volume together with measurements from the independent plot D2. a: Total stem volume in $m^3 ha^{-1}$; b: rates of annual stem volume increment, in $m^3 ha^{-1} yr^{-1}$. Solid lines: field measurements. Dotted lines: model results. For detailed plot measurements, see Table 6.1.d.

As well as the overall fit of the model with the field data on total stem
volume per hectare, simulated and measured increment rates were also studied,
to ascertain the influence of the individual growth-limiting factors.
Simulated and measured increment rates can be compared in three respects: the
maximum rate of increment in stem volume, the trend of the stem volume
increment, and the annual fluctuations in the increment rate. Growth rates
are controlled by external as well as internal variables, and the influence
of these may vary between sites, between years, and during stand development.
This variation may be largely unpredictable, as in the case of weather
conditions, or it may depend on site or canopy variables. Some variation
during stand development may result from cone production. This was not taken
into account in the model as, in general, cone production comprises only a
small portion of primary production (Matthews, 1963; Eis et al., 1965).

By considering the aspects of increment mentioned above, together with the
activity of the individual growth-limiting factors that depend on plant and
site conditions, the model's performance with respect to these growth-limi-
ting factors can be evaluated. Optimal growing conditions for a site imply
ample water and nutrient supply. When the canopy is completely closed under
these conditions, stem volume increment is determined by total canopy assimi-
lation, respiration, and the fractions of assimilates allocated to the stems.
Complete canopy closure means that there are no gaps between the crowns, no
decreased interception of light (such as may result from clustering of needle
biomass), and a sufficiently high value of LAI to intercept all incoming
photosynthetically active radiation. During stand development, a sufficiently
high LAI occurs after canopy closure in a young stand, when the foliage
biomass has reached its maximum level. The moment of canopy closure depends
on plant density and the rate of crown expansion in the horizontal plane. If
the stocking density is 4 500 trees per hectare, this generally occurs some
10 - 15 years after stand establishment.

Assimilate distribution and maintenance requirements change during stand
development: maintenance requirements increase during early stages of stand
development, when the living biomass is accumulating; the change in alloca-
tion of assimilates to the separate biomass components of a tree varies as
described in Section 3.5.3. Stem growth slows down beyond a stand age of 50
years. The large proportion of total canopy assimilation allocated to stem
growth between age 20 and age 50, coincides in part with the period of rapid

However, from Figures 6.1, 6.2, 6.3 and 6.4, especially the graphs for plots D12 and D2, it can be seen that the decrease in increment exceeds a change from 50 % to 30 %. Of the remaining possible causal factors, water availability as such does not change with stand development; however, pathway resistance through the trees, and thus the average water status of the needles, is influenced by tree height and the amount of sapwood present as conducting tissue. Both enhance the effect of limited water availability in tall trees.

A decrease in canopy closure resulting in less light interception immediately reduces growth. Both horizontal and vertical canopy closure are important in this respect, and both may decrease as a stand ages. Incomplete canopy closure may also be caused by a non-optimal distribution of the trees in the field at high stand ages. When a stand of full-grown or almost full-grown trees is thinned, the remaining stand may no longer be able to exploit the space that becomes available. As a result, canopy closure is decreased more than estimated by the model, which assumes an optimal distribution of the trees in the field.

A detailed comparison reveals that additional growth reductions that are not simulated by the model occur incidentally in the field plots. There are several possible explanations for this. One is that the plots may have suffered from hardwood competition e.g. as can be caused by abundant undergrowth of Prunus serotina. Such undergrowth adds to the total evapotranspiration of the plot, and may cause additional shortage of water and nutrients. This was the case in plot D25 (Figure 6.2), in which considerable growth of oak occurred during the first 10 years of the measurement series.

In the model, annual variations in increment rate can only be caused by variations in weather variables such as radiation, temperature, and precipitation. Their influence is mediated either through photosynthesis rates, or through water availability and transpiration. Increased evapotranspiration during part of the year may lead to water shortage on sites with low moisture- holding capacity, because the stock of soil moisture is depleted. In general, precipitation varies most between consecutive years. Its effects on total stand growth depend on the site's susceptibility to drought.

Figure 6.5 gives simulated and measured dominant height for the three
field plots. As with simulation of stem volume, initial height at the begin-
ning of the simulation is taken from the first field measurement. Figure 6.5
indicates that if this is done and annual height growth is corrected using
the ratio between actual and potential canopy assimilation, then the model
fits the field data reasonably. Some discrepancy remains, however. Appar-
ently, height growth is determined by more factors than those contained in
the model. For the simulation experiments here, where a run is initiated with
dominant height measured from the field plots, the deviations of the model
from the observed values are not excessive. When the simulation results of a
trait that may be expected to be sensitive to the simulation of dominant
height, are compared with field data, it is better to use measurements of
dominant height as a forcing function in the model.

Figure 6.6 gives simulated annual diameter increment in cm for field plots
D12 and D2. Figure 6.7 contains simulation results for annual diameter
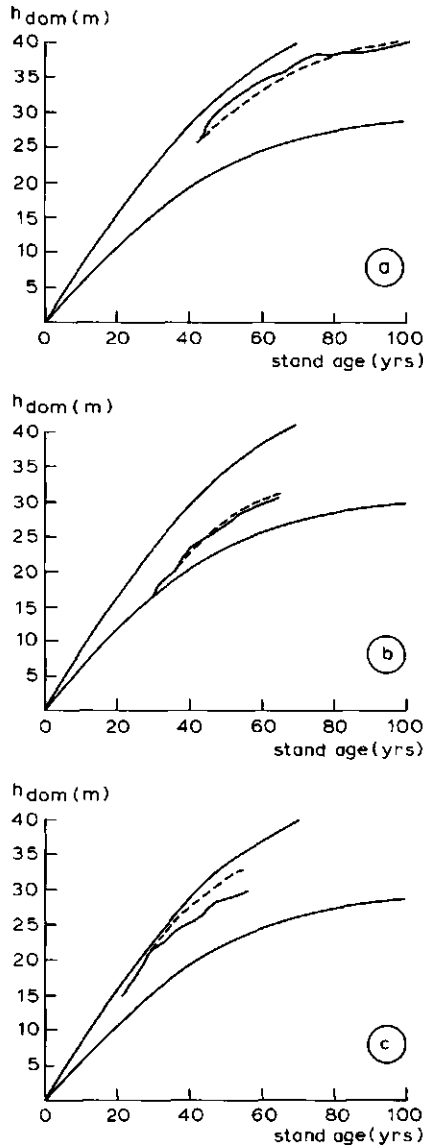increment in plots D25 and SP4.

Figure 6.5

Simulated and measured dominant height in m, for the field plots D12
(a), D25 (b), and SP4 (c). Dotted line: model results. Solid lines:
measured dominant height of the field plots. The upper and lower
lines in the graphs represent height curves for site indices 30 and
45, calculated using Equation 2.1.

Diameter increment
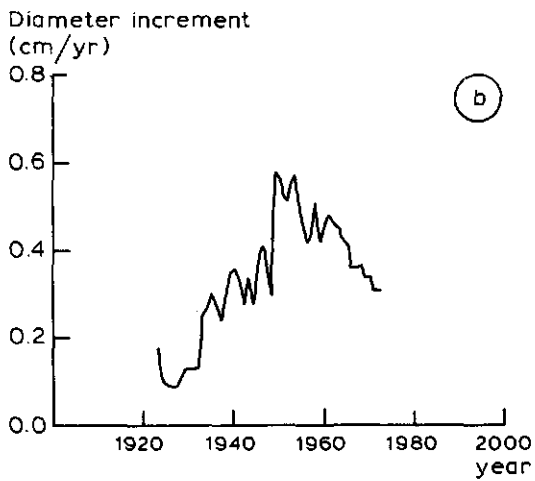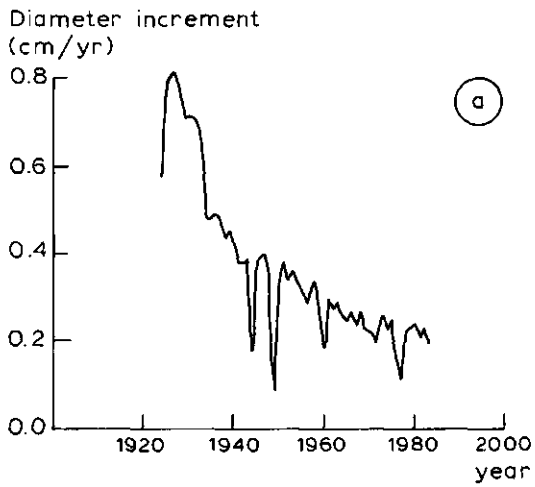(cm/yr)

Diameter increment
(cm/yr)

Figure 6.6
Annual diameter growth of the field plots D12 (a) and D2 (b),
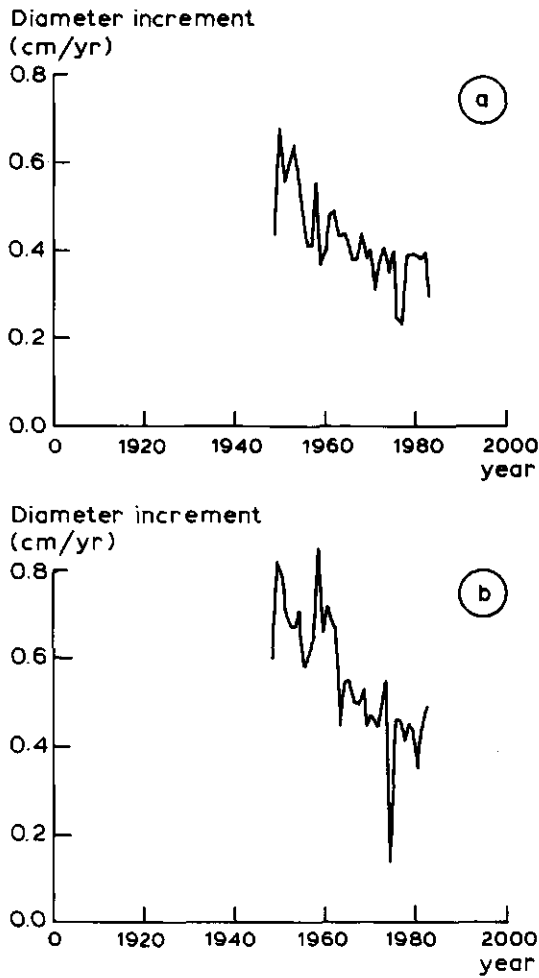corresponding to the simulated increment in the Figures 6.1 and 6.4.

Figure 6.7
Annual diameter growth of the field plots D25 (a) and SP4 (b),
corresponding to the simulated increment in the Figures 6.2 and 6.3.

6.4   The influence of the availability of water, nitrogen and phosphorus

Potential rates of increment when the canopy is closed are determined by total canopy assimilation and stand respiration, and by the amount of assimilates allocated to stem biomass. The model may over- or underestimate both assimilation and respiration simultaneously, and this effect cannot be distinguished other than by measuring assimilation and respiration independently, which is difficult in a forest. However, the photosynthesis rates on which the canopy assimilation model relies, seem realistic, and as the assimilation model itself is derived from well-tested existing models (de Wit et al., 1978; Spitters, 1986), with the respiration rates within the range of rates reported in the literature, there is no reason to suppose that photosynthesis and respiration were both overestimated or were both underestimated.

Differences in maximum increment rates between the plots result from differences in the availability of water or nutrients. Of these two, the influence of nutrient availability for uptake by the trees (here only nitrogen and phosphorus) as simulated by the model, changes only gradually over the years. Nitrogen and phosphorus availability was estimated from total annual litter fall, atmospheric input, and from annual release from pools within the rooted soil: thus, except for litter fall in a year with thinning, these rates do not exhibit sudden changes between consecutive years. Water availability, however, depends on the water-holding capacity of the rooted soil, on transpiration rates and on the rate that soil moisture is replenished by precipitation and infiltration. Precipitation may vary considerably from year to year, and between different locations. This means that the effect of water shortage can be expected to be an important cause for differences in increment rates between consecutive years, and between sites. In the field plots used, D25 is much more prone to effects of limited moisture supply than D12, which has a larger soil storage capacity. This results in greater annual variation in increment in D25.

Typical values as calculated with the model for annual transpiration rates in closed stands under conditions in the Netherlands are 250-300 mm yr^{-1}; most transpiration takes place during the active growing period in summer, starting with budflush around the end of April, and proceeding well into October. Average rainfall in this period is about 350 mm, of which 150-200 mm

is intercepted and lost. This means that about 100-150 mm of water should be available for uptake from the stock of soil moisture at the beginning of the growing season. This amount of water drawn from soil moisture is replenished again during winter and spring. Taking into account interception losses of 100-150 mm during the winter period as well, it follows that 100-200 mm water draines to the deep underground.

Considering the soil moisture availability required to meet transpiration demands for maximum growth as indicated above, it is concluded that water availability may very often limit growth during the period following canopy closure. Moreover, the height of the trees in combination with a decreasing sapwood cross-sectional area at high stand ages also promotes midday decreases in the water potential of needles, thus inducing drought and stomatal closure.

The four field plots available do not allow the influence of the availability of nitrogen and phosphorus on yield to be evaluated thoroughly. As described in Chapter 5, the model essentially consists of a demand component, determined mainly by growth rate and nutrient concentrations within the tissues formed, and an estimate of nutrient availability in the soil, based on total amounts of nitrogen and phosphorus in the rooted zone. The latter component in the model is somewhat speculative, as already discussed in Section 5.3. The evaluation was therefore limited to calculating maximum and minimum demands for the three main field plots, and to comparing of calculated nitrogen and phosphorus content with data on levels of nitrogen and phosphorus in the needles, ascertained from samples taken from the field plots in 1983.

The maximum nitrogen and phosphorus requirements for potential growth were estimated in Chapter 5; they were some 120 kg N and 20 kg P $ha^{-1}yr^{-1}$. Assuming that 25 % of the nitrogen and of 35 % of the phosphorus present in dying biomass is re-used through redistribution, the demands for root uptake are about 90 kg nitrogen and 13 kg phosphorus per hectare per year. Using the maximum and minimum nitrogen and phosphorus concentrations from Table 3.6, the amounts of nitrogen and phosphorus that can be incorporated in the new tissue can be calculated, if dry weight increment is known for all biomass components. In this way, the amounts of nitrogen and phosphorus that have to be available through uptake from the soil and from redistribution within the

plant can be estimated. The maximum and minimum demands calculated this way
are given in Figure 6.8 for the three field plots. In Figure 6.8, the nitro-
gen and phosphorus supplies estimated with the model are also given. Supply
here incorporates nutrient withdrawal before loss to the litter, together
with estimated availability of nutrients in the soil. The graphs show that in
field plot D12, rates of nitrogen and phosphorus supply considerably exceed
the minimum requirements. This means that availability generally satisfies
demand, and that the influence of nitrogen or phosphorus availability on
growth and yield is small. It is clear that D12 is indeed located on an
optimal or near optimal site, as was expected from the amounts of nitrogen
and phosphorus that were estimated to be contained in the rooted zone, and
from measured stem volume increments. The calculations of demand and supply
for the field plots indicate that maximum uptake under optimal growing
conditions would require total amounts of nitrogen and phosphorus in the
rooted profile to be in the order of 8000 kg nitrogen and 5000 kg phosphorus
(assuming a background input for N of 30 kg $ha^{-1}yr^{-1}$, and no fertilization of
either nitrogen or phosphorus, and including the inert phosphorus).

In the graphs for the plots D25 and SP4, it can be seen that both nitrogen
and phosphorus are in short supply at the beginning of the measurement
series. From the graphs it cannot be deduced whether nitrogen or phosphorus
shortage has the more pronounced effect. Assuming that the atmospheric input
of nitrogen increased from about 15 kg ha^{-1} yr^{-1} at the beginning of the
measurement series in the 1920s, to around 50 kg ha^{-1} yr^{-1} (as found recent-
ly: van Aalst, 1984; van Breemen et al., 1982, 1983), the initial nitrogen
deficiencies in stands D25 and SP4 are completely removed. The result of the
increased nitrogen input from the atmosphere is that nitrogen content in the
needles is approaching its maximum, and no more effects of nitrogen addition
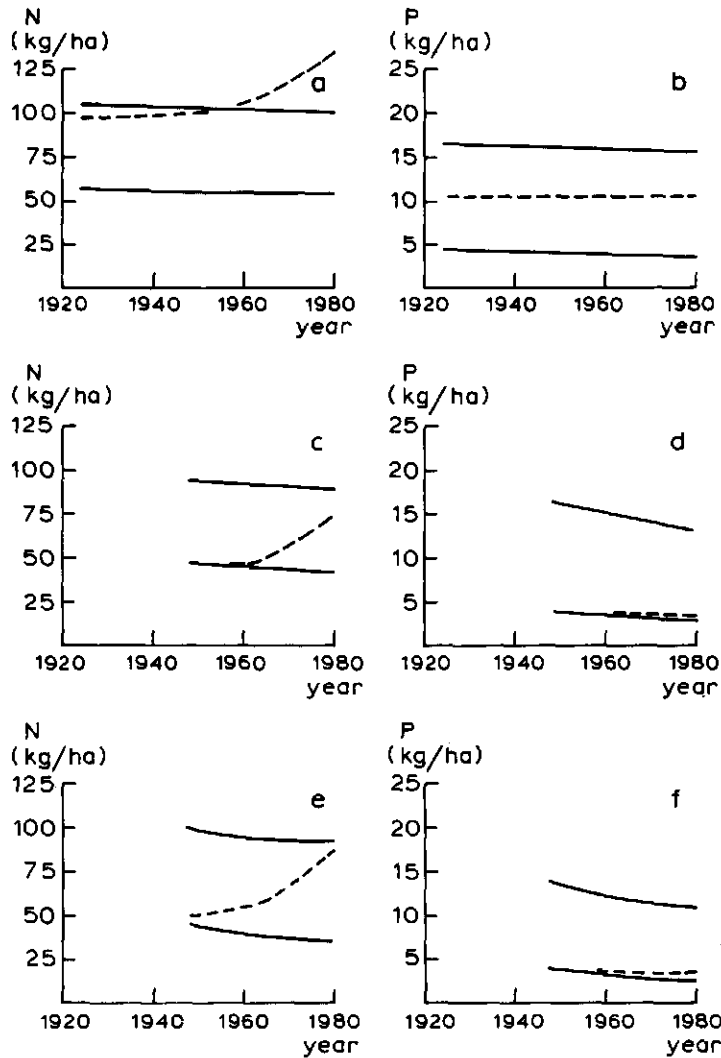will occur.

Figure 6.8

Calculated maximum and minimum demands for nitrogen and phosphorus
(drawn lines) together with the estimated supply (dotted lines) for
the field plots D12 (a), D25 (b), and SP4 (c). Maximum and minimum
demands do not incorporate any effects of redistribution of
nutrients from dying biomass. When redistribution is 25 % for
nitrogen, and 35 % for phosphorus, and when litter loss is about
equal to increment, demands for uptake will be reduced also by 25 %
and 35 %, respectively. The estimated supply denotes the supply of
nutrients within the soil, thus incorporates nutrients from litter
fall, but takes no account of nutrient supply through redistribution
within the living biomass.

Given the coupling between nitrogen and phosphorus in the plant (Bengtson & Holstener-Jørgensen, 1971), and taking into account the low availability of phosphorus in stands D25 and SP4, this increased nitrogen content has resulted in the phosphorus becoming limiting. For both plots, the rates of phosphorus supply (U_p) calculated with the model are around 4 kg ha^{-1}yr^{-1}. They remain virtually constant during the period simulated, whereas for nitrogen the supply increases substantially. The graphs show that at the beginning of the measurement series of both D25 and SP4, minimum requirements for nitrogen and phosphorus were approximately met by reserves in the soil. This remains the case at the end of the period for phosphorus, but nitrogen availability at the end of the period is approximately equal to, or exceeds maximum requirements. This implies that the availability of both nitrogen and phosphorus is limited at the beginning of the simulation period, and that growth is limited by phosphorus at the end of this period. The nitrogen content of needles sampled in February 1984 revealed values of around 2.0 % of needle dry weight, with phosphorus concentrations of about 0.10 % (Table 6.3). Old fertilization experiments done during the 1950s and 1960s (Blok et al., 1975) suggest that under comparable growing conditions, nitrogen and phosphorus concentrations of around 1.5 % and 0.12-0.20 % respectively would be expected. Table 6.3 also gives the simulated nitrogen and phosphorus concentrations for 1960 and 1980. These results reveal a change in the nutrient status of the foliage, when the situation in 1960 is compared with that in 1980. In that period, nitrogen content in the needles increased considerably, whereas phosphorus content remained constant or even decreased.

Phenomena identical to those revealed in the simulation were also found when data from an old fertilizer experiment (Blok et al., 1975) were compared with data obtained in 1984 from the same plot. Table 6.4 gives some of the results taken from Mohren et al. (1986). The data from 1957 and 1958 show a response to both nitrogen and phosphorus fertilization. In 1984, all treatments appeared to be saturated with nitrogen, and exhibited minimum concentrations of phosphorus. This was reflected very clearly in the nitrogen to phosphorus ratios of the needles. This change in nutrient status resulting from an increase in nitrogen input, was considered to be typical of most Douglas fir stands on sandy soils in the Netherlands.

Table 6.3
Nitrogen and phosphorus concentrations of current-year needles taken from the
field plots D12, D25 and SP4 in February 1984, together with the concentrations
as simulated by the model.

	D12		D25		SP4	
	meas. 1984	sim. 1960 1980	meas. 1984	sim. 1960 1980	meas. 1984	sim. 1960 1980
Nitrogen	1.85	1.85 1.96	2.02	1.31 1.95	1.97	1.47 2.00
Phosphorus	0.17	0.28 0.29	0.10	0.13 0.10	0.09	0.09 0.09

Table 6.4
Nitrogen and phosphorus concentrations of current-year needles in the Kootwijk
fertilization experiment, 1, 2, and 28 years after fertilizer application. The
soil contained 18 mg P/100 g soil, and 0.1 % of soil dry weight nitrogen, in
the top soil layer (0-25 cm). Fertilizer treatments consisted of 35 kg ha$_{-1}$
phosphorus, applied as basic slag at the beginning of 1956, and 100 kg ha^{-1} of
nitrogen in the form of calcium ammonium nitrate at the beginning of 1957. For
further details, see Mohren et al. (1986).

	Nitrogen			Phosphorus			N/P ratio		
	'57	'58	'84	'57	'58	'84	'57	'58	'84
Treatment*:									
0	1.04	0.91	2.01	0.12	0.11	0.09	9	8	22
N	1.46	1.02	1.96	0.10	0.10	0.11	15	10	18
K	1.31	1.15	1.91	0.15	0.14	0.09	9	8	21
NK	1.71	1.20	1.76	0.10	0.13	0.10	17	9	18
P	1.01	0.98	1.76	0.19	0.17	0.10	5	6	18
PN	1.54	1.03	1.87	0.13	0.14	0.10	12	7	19
PK	1.41	1.53	1.88	0.22	0.23	0.10	6	7	19
PNK	1.68	1.41	2.16	0.15	0.17	0.09	11	8	24

* Phosphorus fertilization consisted of 35 kg ha^{-1} phosphorus, applied as basic
slag at the beginning of 1956. Nitrogen and Potassium fertilization was car-
ried out in the beginning of 1957, using 100 kg nitrogen in the form of cal-
cium ammonium nitrate in the first treatment (N), 66 kg potassium as muriate
of potash in the second treatment (K), and 100 kg nitrogen combined with 66
kg potassium in the third treatment (NK, all quantities per hectare).

6.5   Relative importance of the main growth-limiting factors

The main growth-limiting factors considered were: i) canopy assimilation,
respiration and assimilate distribution; ii) canopy structure and light
interception; iii) water availability; iv) nitrogen and phosphorus availa-
bility. These will be discussed briefly with regard to their consequences on
growth and yield under the conditions prevailing in the field plots used.

It has already been pointed out in the discussion of the results in
Section 6.4, and in the description of this part of the model in Chapter 3,
that the parameters determining canopy assimilation and assimilate distribu-
tion greatly influence the behaviour of the model. The main differences in
primary production between species can be viewed against the background of
these parameters that define the basic processes involved in primary produc-
tion. Table 6.5 indicates the model's sensitivity to small changes in the
main parameters involved: maximum assimilation rate (A_m), photosynthetic
light efficiency (ε), and assimilate distribution. The influences of the
changes were compared with the standard situation for annual primary produc-
tion, annual transpiration, and stem increment. As expected, the model is
sensitive to maximum assimilation rate, and assimilate distribution. The
importance of these parameters holds for all conditions, and does not depend
on site or stand.

When all other factors are optimal, canopy structure and light intercep-
tion determine whether the potential growth rate can be attained. The impli-
cation of this for any silvicultural system aiming at high production rates
is that management should be directed to achieving complete canopy closure as
soon as possible after planting, and at maintaining canopy closure as long as
possible as a stand ages. The latter aspect, canopy closure at high ages, is
more important than canopy closure at the beginning of stand development,
because incomplete canopy closure during early stages of stand development is
usually temporary, because the remaining tree crowns have the ability to
expand and fill the gaps. At high ages, the trees crowns have reached maximum
spatial extent, and cannot regain canopy closure after it has been reduced
e.g. by thinning. Table 6.5 gives the results of a sensitivity analysis of
the influence of horizontal canopy closure, and the degree of clustering of
the needle area on primary production.

Table 6.5
Sensitivity analysis of some of the main physiological parameters involved in
the models of primary production, some of the input weather variables, and some
of the parameters characterizing stand structure. The calculations were done for
a reference stand, as used in Chapter 4, Table 4.2. The sensitivity of the
results from the model, for a change in a particular parameter is expressed as
percentage of the outcome of the standard situation, given at the top of the
Table. Calculated changes were all taken as minus and plus 20 % of the original
parameter values. The model results are expressed as percentage of the results
using the original parameter value. The simulated results for different values
for CCH have been added, for comparison. In the standard run CCH was set to
equal 0.95.

Variable:	Gross primary production	Annual Transpiration	Annual increment
	47 200 kg	270 mm	20.7 m^3
A_m (15 kg ha^{-1}hr^{-1})	94 - 102	94 - 101	91 - 102
ε_o (0.5 kg ha^{-1}h^{-1}J^{-1}m^{2}s)	88 - 105	88 - 102	83 - 106
Root:Shoot ratio (0.2)	100 - 100	100 - 100	95 - 103
Stem distr. coeff (0.5)	100 - 99	100 - 98	78 - 120
Global radiation:	96 - 99	92 - 102	95 - 98
Temperature	91 - 81	90 - 107	95 - 65
Vapour pressure	85 - 100	106 - 74	77 - 100
Wind speed	99 - 100	103 - 97	99 - 100
SLA (0.55 m^2 kg^{-1})	97 - 97	93 - 98	96 - 95
LAIC (1.5 m^2 m^{-2})	99 - 101	102 - 98	98 - 101
Crown shape (0.225)	102 - 104	101 - 98	102 - 97
CCH = 0.7	91	91	87
CCH = 0.4	70	67	58

The influence of water availability in the three main field plots - other conditions again being optimal - can be evaluated by removing its effect on growth. This can be done e.g. by increasing soil water availability such that the soil is at field capacity and soil water potential equals -0.1 bar. The simulation results are shown in Table 6.6 for the four field plots. As it appears from the Table, increasing water supply alone hardly increases growth in the field plots. In combination with ample nutrient supply, however, there is a substantial increase in total stem volume increment in plot D25. This plot has the smallest amount of available soil moisture: 90 mm, as compared with 140 mm, 160 mm, and 170 mm for SP4, D12, and D2, respectively. Given that D25 should be considered as being a favourable site for Douglas fir growth in the Netherlands, it can be concluded that soil moisture shortage is an important actual or potential growth-limiting factor in Douglas fir forestry in the Netherlands.

Table 6.6
Stand growth for field plots D12, D25, SP4 and D2, as predicted by the model, assuming ample availability of water and nutrients, and for a needle-age distribution derived from Silver (1962). For the results in the Table, total stem volume at the end of the simulation period was compared with total stem volume as simulated with the complete model (including the influence of the availability of water, nitrogen and phosphorus. The results are expressed as percentages, of the results presented in Figures 6.1 through 6.4.

	D12	D25	SP4	D2
Reference value $(m^3\ ha^{-1})$:	827	469	398	429
Needle-age distribution derived from (Silver, 1962):	101	102	104	101
Ample water supply:	101	102	100	101
Ample nutrient supply:	101	113	126	101
Ample supply of both water and nutrients:	102	122	129	102

The influence of nitrogen and phosphorus availability can be investigated by running a simulation without the reduction in increment that would be calculated by the model. Table 6.6 also gives the results of these calculations. As expected from the simulation runs for nitrogen and phosphorus demand and supply in the actual situation, D12 shows hardly any effect of nitrogen or phosphorus on yield. Field plots D25 and SP4, however, exhibit a clear reduction in yield, mainly because of phosphorus deficiency. The less than optimal response to increased nutrient supply in D25 is probably the result of a shortage of water.

In addition to the growth-limiting factors incorporated in the model and discussed above, a range of other factors can reduce stand growth, such as the occurrence of pests, diseases, competition from other species (weeds), pollution, and damage from wind and frost. Together with the main growth determining and growth limiting factors, these influence the actual yield achieved at a given site. The group of growth-reducing factors may act to decrease canopy closure (as in the case of insect attack reducing foliage area), influence basic growth and ageing processes (such as maximum photosynthesis rates and needle longevity in the case of pollution with sulphur and nitrogen oxides), or disturb the production system altogether (as with catastrophic wind damage). They were not included in the present model of primary production, and their influence was assumed to be restricted in the field plots used. No detailed information on the occurrence of important growth disturbances was available in the records of the permanent plots. In the case of major disturbance, such as wind throw, the field plot was excluded from further measurements if badly damaged. This was the case in plot D2, which was not measured any further after the catastrophic gales of November 1972. Growth-disturbing factors such as mentioned above did probably have small influences. Some of these were taken into account implicitly, in the choice for the assimilate distribution. This, however, only holds for those growth disturbances that acted similarly on all field plots used.

Air pollution may be an important factor influencing the growth of forest stands in industrialized regions, and it may be necessary to incorporate this into a physiologically based growth model. It was not explicitly taken into account here, because modelling of the effects of air pollutants has only recently started, and summary models suitable for incorporation in a general model are not yet available. The effects of air pollution may have been

incorporated implicitly by using the needle-age distribution as determined
from the 1984 samples, and in the maximum photosynthesis rates that have been
used in the model, which were measured on excised branches. There are indica-
tions that gaseous pollutants will decrease needle longevity, thereby decrea-
sing LAI and also total canopy assimilation, and that they may alter photo-
synthesis rates. The model's sensitivity to changes in the maximum photosyn-
thesis rate are given in Table 6.5. When the needle-age distribution publi-
shed by Silver (1962) is used to calculate the needle loss coefficient, total
needle biomass increases, because needles live longer, and there is a greater
portion of older needles in the total foliage. In the model, this may result
in a decrease in average photosynthesis rate, because the latter decreases
with age of the foliage. In this way, increased light interception resulting
from more foliage, may be compensated for by lower assimilation rates. The
results for field plots D12, SP4 and D25 are shown in Table 6.6, and it
appears that the model is insensitive to the change in needle distribution
carried out.

Using a physiological model as a starting point, the effects of the
disruptive agents on total biomass at the stand level as mentioned above, can
be evaluated if their effects on individual state variables or on individual
processes can be quantified (Rabbinge et al., 1987). For forest stands it may
be necessary to incorporate competition for water and nutrients from unwanted
species such as vigorously growing shrubs or other tree species. Such under-
growth adds to the total evaporation from the site, and may cause additional
water shortage (Spittlehouse and Black, 1982).

6.6   Concluding remarks

The main aim of constructing and evaluating a simulation model of primary production in forests was to quantify and integrate the different aspects of growth in order to study and explain tree and stand growth. Compared with the descriptive models hitherto used in studies of forest growth and yield, the research reported here has shown that relatively simple models based on plant physiology, give a much better insight in the growth processes under field conditions.

The evaluation of the model revealed the model's weaknesses. These can be rectified by doing additional experiments or obtaining more field measurements. Aspects of growth that have hitherto been neglected but which gain importance when they are viewed in relation to the influence of the other limiting factors, can thus be identified. Examples of this are light interception in old stands, and the supply and uptake of phosphorus under conditions of ample nitrogen supply. In this way, the model can guide the experimental work, and serve its purpose as a tool for directing further research.

The advantages of this modelling approach to study primary production and growth apply to all kinds of crops, forests as well as arable crops or grasslands. The benefits of using dynamic simulation in forestry are especially great, because stand development and rotation length are very long and the expenses involved in establishing and maintaining permanent field plots may therefore be prohibitive if research aims cannot be defined precisely. The usefulness of a modelling approach in forest research has also been demonstrated by others (Ågren and Axelsson, 1980; Linder, 1985; Sievänen, 1983). This approach can also be used in research on structure and function of uneven-aged forests (Shugart, 1984).

In addition to this, a hierarchical simulation model in which process descriptions on a lower level are integrated into an explanatory model of stand growth, can be used .to evaluate the influence of changes or disturbances at the process level on total stand growth, without, as in descriptive research, actually measuring changes in total stand growth. In this way, a model can be used to simulate experiments with the real-world system from which it is derived. This allows, for example, disturbances to canopy assimilation caused by air pollution to be evaluated, when changes in total

stand growth cannot yet be measured with sufficient accuracy for final
conclusions to be drawn. Examples of the use of modelling in this respect are
West et al. (1980) and Kercher and Axelrod (1984).

When using the model to study the effects of different management regimes,
it may be necessary to simulate thinning in more detail, by considering
individual tree size distribution together with the influence of thinning on
this (see e.g. Alder, 1979). This requires tree size distribution to be
simulated by incorporating an individual-tree component in the model. It has
been shown (van Gerwen et al., 1987) that this can be done by simulating
competition between the trees in a stand, by distributing dry weight incre-
ment over the individual trees in the stand. The distribution should be done
according to the fraction of total canopy assimilation that is accounted for
by the individual trees. By breaking down stand growth into individual tree
growth in this way, a whole-stand model as described in this thesis, can be
expanded to include an individual-tree model. This opens the possibility for
simulating uneven-aged stands and, by incorporating germination and morta-
lity, will allow primary production to be studied in relation to the popula-
tion dynamics of trees in a forest.

LITERATURE REFERENCES

Aalst, R., 1984. Acidification by atmospheric deposition - Atmospheric processes and deposition
(in Dutch). Publicatiereeks Milieubeheer, MvL/MvVROM, pp. 76.

Ägren, G.I. and Axelsson, B., 1980. PT - A tree growth model. In: T. Persson, (Ed.): Structure
and Function of Northern Coniferous Forests - An Ecosystem Study. Ecological Bulletin
(Stockholm), 32: 525-536.

Ägren, G.I., Axelsson, B., Flower-Ellis, J.G.K., Linder, S., Persson, H., Staaf, H. and Troeng
E., 1980. Annual carbon budget for a young Scots pine. In: T. Persson (Ed.): Structure and
function of Northern Coniferous Forests - An Ecosystem study. Ecological Bulletin
(Stockholm), 32: 307-313.

Albrektson, A., 1984. Sapwood basal area and needle mass of Scots pine (Pinus sylvestris L.)
trees in Central Sweden. Forestry, 57: 35-43.

Alder, D., 1979. A distance - independent tree model for exotic conifer plantations in East
Africa. Forest Science, 25: 59-71.

Amthor, J.S., 1984. The role of maintenance respiration in plant growth. Plant, Cell and
Environment, 7: 561-569.

Avery, T.E. and Burkhart, H.E., 1983. Forest Measurements. 3rd revised edition, McGraw Hill, New
York, 331 pp.

Bengtson, G.W. and Holstener-Jørgensen, H., 1971. Interactions of nitrogen and phosphorus: Their
effects on forest tree response to N - P fertilization and on the diagnostic value of foliar
analysis. In: Proceedings section 21 - Research on site factors. XV IUFRO Congress,
Gainesville, Florida, U.S.A., 1971. Wageningen, The Netherlands, 1976, p. 65-86.

Bergel, D., 1985. Douglasien-Ertragstafel für Nordwest-Deutschland. Niedersächsischen
Forstlichen Versuchsanstalt, Abteilung Waldwachstum; Fachhochschule Hildesheim/Holzminden,
Fachbereich Forstwirtschaft, Göttingen, 72 pp.

Björkman, O., 1981. Responses to different quantum flux densities. In: O.L. Lange, P.S. Nobel,
C.B. Osmond and H. Ziegler (Eds.): Physiological plant ecology I. Responses to the physical
environment. Springer Verlag, Berlin, p. 57-107.

Blok, H., Burg, J. van den, Goor, C.P. van, Jager, K. and Oldenkamp, L., 1975. Bemesting en
minerale voeding van Douglas-cultures. Rijksinstituut voor onderzoek in de Bos- en
Landschapsbouw 'De Dorschkamp', Wageningen, Intern Rapport Nr. 69, 147 + 186 pp.

Bosshard, H., 1974. Holzkunde. Band 2: Zur Biologie, Physik, und Chemie des Holzes. Birkhäuser
Verlag, Basel, 312 pp.

Boysen Jensen, P., 1932. Die Stoffproduktion der Pflanzen. Gustav Fischer Verlag, Jena, 108 pp.

Breemen, N. van, Burrough, P.A., Velthorst, E.J., Dobben, H.F. van, Wit, T. de, Ridder, T.B. and
Reijnders, H.F.R., 1982. Soil acidification from atmospheric ammonium sulphate in forest
canopy throughfall. Nature, 299: 548-550.

Breemen, N. van, Grinsven, J.J.M. van, and Jordens, E.R., 1983a. H^+-budgets and nitrogen trans-
formation in woodland soils in the Netherlands influenced by high input of atmospheric
ammonium sulphate. Verein Deutscher Ingenieure, VDI-Berichte, 500: 345-348.

Brouwer, R. and de Wit, C.T., 1968. A simulation model of plant growth with special attention to
root growth and its consequences. Proceedings of the 15 th. Easter School of Agricultural
Science, University of Nottingham, pp. 224-242.

Brunt, D., 1932. Notes on radiation in the atmosphere. Quarterly Journal of the Royal Meteorolo-
gical Society, 58: 389-420.

Burg, J. van den, 1976. De invloed van het stikstofgehalte van de organische stof in kalkloze
zandgronden op de groei van naaldhoutsoorten, in afhankelijkheid van de fosfaat- en de vocht-
voorziening. Rijksinstituut voor onderzoek in de bos- en landschapsbouw 'De Dorschkamp',
Wageningen, Intern Rapport nr. 87.

Burg, J. van den, 1985. Foliar analysis for determination of tree nutrient status - A compila-
tion of literature data. Rijksinstituut voor onderzoek in de Bos- en Landschapsbouw 'De
Dorschkamp', Rapport nr. 414, 615 pp.

Burger, H., 1935. Holz, Blattmenge und Zuwachs. II Die Douglasie. Mitteilungen der
Schweizerische Anstalt für das forstliche Versuchswesen, 19: 21-72.

Calder, I.R., 1976. The measurement of water losses from a forested area using a 'natural' lysimeter. Journal of Hydrology, 30: 311-325.

Calder, I.R. and Newson, M.D., 1979. Land-use and upland water -resources in Britain - a strategic look. Water Resources Bulletin, 15: 1628-1639.

Campbell, R.K. and Sugano, A.I., 1975. Phenology of bud burst in Douglas-fir related to provenance, photoperiod, chilling and flushing temperature. Botanical Gazettte, 136 (3): 290-298.

Cannell, M.G.R., 1982. World forest biomass and primary production data. Academic Press, London, pp. 391.

Chen, J., 1984. Mathematical analysis and simulation of crop micrometeorology. Ph.D Dissertation, Agricultural University, Wageningen, 115 pp.

Dik, E.J., 1984. Estimating the wood volumes of standing trees in forestry practice. Wageningen, 'De Dorschkamp' Research Institute for Forestry and Landscape Planning. Extensive Report, Volume 19, nr. 1, 114 pp.

Doorenbos, J. and Kassam, A.H., 1979. Yield response to water. FAO Irrigation and drainage paper 33, FAO, Rome, 193 pp.

Driessche, R. van den, 1984. Nutrient storage, retranslocation and relationship of stress to nutrition. In: G.D. Bowen and E.K.S. Nambiar, (Eds.): Nutrition of Forest Trees in Plantations. Academic Press, London. p. 181-209.

Driessen, P.M., 1986a. Nutrient demand and fertilizer requirements. In: H. van Keulen and J. Wolf, (Eds.): Modelling Agricultural Production: weather, soils and crops. Simulation Monograph. Pudoc, Wageningen, p. 182-200.

Driessen, P.M., 1986b. The water balance of the soil. In: H. van Keulen and J. Wolf, (Eds.): Modelling Agricultural Production: weather, soils and crops. Simulation Monograph. Pudoc, Wageningen, p. 76-116.

Ducrey, M., 1981. Action des basses températures hivernales sur la photosynthèse du cèdre et du Douglas. Annales des Sciences Forestières, 38: 317-329.

Duvigneaud, P. (Ed.), 1971. Productivity of forest ecosystems. Proceedings of the UNESCO-IBP Brussels Symposium, 27-31 october 1969, 707 pp.

Edelin, C., 1977. Images de l'architecture des conifères. Dissertation, Université de Montpellier, 254 pp.

Edelin, C., 1981. Quelques aspects de l'architecture végétative des Conifères. Bulletin Societé botanique Francaise, Lettres botanique, 128: 177-188.

Edmonds, R.L. (Ed.), 1982. Analysis of coniferous forest ecosystems in the Western United States. Stroudsburg, Pa., Hutchinson and Ross Publishing House.

Ehleringer, J. and Björkman, O., 1977. Quantum yields for CO_2 uptake in C_3 and C_4 plants. Plant Physiology, 59: 86-90.

Eis, S., 1974. Root system morphology of Western Hemlock, Western red Cedar, and Douglas-fir. Canadian Journal of Forest Research, 4: 28-38.

Eis, S., Garmau, E.H. and Ebell, L.F., 1965. Relation between cone production and diameter increment of Douglas-fir (Pseudotsuga menziesii (mirb.) Franco), Grand fir (Abies grandis (Dougl.) Lindl.), and Western white pine (Pinus monticola Dougl.). Canadian Journal of Botany, 43: 1553-1559.

Emmingham, W.H. and Waring, R.H., 1977. An index of photosynthesis for comparing forest sites in western Oregon. Canadian Journal of Forest Research, 7: 165-174.

Evers, P.W., 1981a. Growth and morphogenesis of shoot initials of Douglas fir, Pseudotsuga menziesii (Mirb.) Franco, in vitro. I Plant, nutritional and physical factors. Dorschkamp Research Institute for Forestry and Landscape Planning, Uitvoerig Verslag, Band 16, nr. 1.

Evers, P.W., 1981b. Growth and morphogenesis of shoot initials of Douglas fir, Pseudotsuga menziesii (Mirb.) Franco, in vitro. II Growth factors, topophysis and seasonal changes. Dorschkamp Research Institute for Forestry and Landscape Planning, Uitvoerig Verslag, Band 16, nr. 2.

Faber, P.J., 1983: Concurrentie en groei van bomen binnen een bosopstand. Rijksinstituut voor onderzoek in de Bos- en Landschapsbouw 'De Dorschkamp', Wageningen, Uitvoerig Verslag, Band. 18, nr. 1.

Farquhar, G.D., Schulze, E.-D. and Kuppers, M., 1980. Responses to humidity by stomata of Nicotiana glauca L. and Coryllus avellana L. are consistent with the optimization of carbon

dioxide uptake with respect to water loss. Australian Journal of Plant Physiology, 7: 315-327.

Fengel, D. and Wegener, G., 1983. Wood: Chemistry, Ultrastructure, reactions. Berlin, de Gruyter Verlag, 613 pp.

Fiedler, H.J., Nebe, W. and Hoffmann, F., 1973. Forstliche Pflanzenernährung und Düngung. Gustav Fisher Verlag, Jena, 481 pp.

Foerst, K., 1980. Standort, Wuchsleistung und Ernährungszustand älterer bayerischer Bestände der Grünen Douglasie (Pseudotsuga menziesii (Mirb.) Franco var. menziesii). München, Mitteilungen aus der Staatsforstverwaltung Bayerns, Heft 41, 256 pp. + Anlagen.

Fogel, R. and Hunt, G., 1979. Fungal and arboreal biomass in a western Oregon Douglas-fir ecosystem: Distribution patterns and turnover. Canadian Journal of Forest Research, 9: 245-256.

Ford, E.D., 1985. Branching, crown structure and the control of timber production. In: M.G.R. Cannell and J.E. Jackson (Eds.): Attributes of trees as crop plants. Institute of Terrestrial Ecology, Monks Wood Experimental Station, Abbots Ripton, Huntingdon, England. p. 228-252.

Forstliche Bundesversuchsanstalt Wien (Hrsg.), 1983. Forest growth modelling and simulation. Papers presented at the meeting of IUFRO Subject Group S4.01-00, 4-8 October 1982, Vienna, Austria. Mitteilungen der Forstliche Bundesversuchsanstalt Wien, Heft 147, 278 pp.

Fowells, H.A. (ed.), 1965. Silvics of forest trees of the United States. USDA Forest Service, Agricultural Handbook no. 271, 762 pp.

Fries, J., (Ed.), 1974. Growth models for tree and stand simulation. Proceedings of a meeting of IUFRO working party S4.01-04 in 1973. Royal college of Forestry, Stockholm, Research Note 30, 379 pp.

Fries, J., Burkhart, H.E. and Max, T.A. (Eds.), 1978. Growth models for long term forecasting of timber yields. Virginia Polytechnic Institute and State University, Division of Forestry and Wildlife Resources, FWS-1-78, 249 pp.

Gash, J.H.C., 1979. An analytical model of rainfall interception by forests. Quarterly Journal of the Royal Meteorological Society, 105: 43-55.

Gash, J.H.C., Oliver, H.R., Shuttleworth, W.J. and Stewart, J.B., 1978. Evaporation from forests. Journal of the institution of water engineers and scientists, 32: 104-110.

Geng, S., Penning de Vries, F.W.T. and Supit, I., 1986. A simple method for generating daily rainfall data. Agricultural and Forest Meteorology, 36: 363-376.

Gerwen, C.P. van, Spitters, C.J.T. and Mohren, G.M.J., 1987. Simulation of competition for light in even-aged stands of Douglas-fir. Forest Ecology and Mangement, in press.

Gholz, H.L., Fitz, F. and Waring, R.H., 1976. Leaf area differences associated with old-growth forest communities in the western Oregon Cascades. Canadian Journal of Forest Research, 6: 49-57.

Goudriaan, J., 1977. Crop micrometeorology: a simulation study. Simulation Monographs. Pudoc, Wageningen, 249 pp.

Goudriaan, J., 1979. MICROWEATHER. Simulation model applied to a forest. In: S. Halldin (Ed.): Comparison of forest water and energy exchange models. International Society for Ecological Modelling (ISEM), Copenhagen, p. 47-57.

Goudriaan, J., 1982. Potential production processes. In: F.W.T. Penning de Vries and H.H. van Laar, (Eds.): Simulation of plant growth and crop production. Simulation Monograph. Pudoc, Wageningen, p. 98-113.

Goudriaan, J., 1986. A simple and fast numerical method for the computation of daily total s of crop photosynthesis. Agricultural and Forest Meteorology, 38: 249-254.

Goudriaan, J. and van Roermund, H, 1987. Modelling of ageing, development, delays and dispersion. In: R. Rabbinge, S.A. Ward, and H.H. van Laar, Simulation and systems management in crop protection. Simulation Monographs. Pudoc, Wageningen, in preparation.

Goudriaan, J. and van Laar, H.H., 1978. Relation between leaf resistance, CO_2 concentration and CO_2 assimilation in Maize, Beans, Lalang grass and Sunflower. Photosynthetica, 12: 241-249.

Grier, C.C. and Waring, R.H., 1974. Conifer foliage mass related to sapwood area. Forest Science, 20(3): 205-206.

Guehl, J.-M., 1982. Potentiel du photosynthèse hivernale du Douglas (Pseudotsuga menziesii Mirb.) en relation avec la regime thermique. Annales des Sciences Forestieres, 39: 239-258.

Guehl, J.-M., de Vitry, C. and Aussenac, G., 1985. Photosynthèse hivernale du douglas vert (Pseudotsuga mensiesii (Mirb.) Franco) et du cèdre (Cedrus atlantica Manetti et Cedrus libani Loud.). Essai de modélisation à l'échelle du rameau. Acta Oecologia, Oecologia Plantarum, 6: 125-146.

Gussone, H.A., 1974. Uber forstliche Düngungsversuche mit spezieller Zielsetzung für den Waldbau des nordwestdeutschen Flachlandes. Schriftenreihe der Forstliche Fakultät der Universität Göttingen und Mitteilungen der Niedersächsischen Forstliche Versuchsanstalt, Band 46: 1-127.

Halldin, S., 1985. Leaf and bark area distribution in a pine forest. In: Hutchison, B.A. and Hicks, B.B. (Eds.): The Forest-Atmosphere interaction. D. Reidel Publishing Company, Boston USA, p. 39-58.

Hallé, F. and Oldeman, R.A.A., 1970. Essai sur l'architecture et la dynamique de croissance des arbres tropicaux. Masson, Paris, 178 pp.

Hallé, F., Oldeman, R.A.A. and Tomlinson, P.B., 1978. Tropical trees and forests: an architectural analysis. Springer, Heidelberg, 441 pp.

Hapla, F. and Knigge, W., 1985. Untersuchungen über die Auswirkungen von Durchforstungsmassnahmen auf Die Holzeigenschaften der Douglasie. Schriften aus der Forstlichen Fakultät Göttingen und der Niedersächsischen Forstlichen Versuchsanstalt, Band 81: 1-142.

Hari, P., Kaipiainen, L., Korpilahti, E., Mäkelä, A., Nilson, T., Oker-Blom, P., Ross, J. and R. Salminen, 1985. Structure, radiation and photosynthetic production in coniferous stands. University of Helsinki, Department of Silviculture, Research Notes No: 54, 233 pp.

Hari, P. and Kellomäki, S., 1981. Modelling of the functioning of a tree in a stand. In: S. Linder (Ed.): Understanding and predicting tree growth. Studia Forestalia Suecica, nr. 160, p. 39-42.

Heemst, H.D.J. van, Keulen, H. van, and Stolwijk, H., 1978. Potentiële produktie, bruto- en nettoproduktie van de Nederlandse landbouw. Verslagen van Landbouwkundige onderzoekingen 879, 25 pp.

Hellkvist, J., Richards, G.P. and Jarvis, P.G., 1974. Vertical gradients of water potential in Sitka spruce trees measured with the pressure chamber. Journal of Applied Ecology, 11: 637-667.

Henstra, S., van der Eijk, D., Boekestein, A., Thiel, F. and van der Plas, L., 1981. Compositional changes in triplesuperphosphate granules. Scanning Electron Microscopy: 439-446.

Hinckley, T.M., Lassoie, J.P. and Running, S.W., 1978. Temporal and spatial variations in the water status of forest trees. Forest Science Monograph 20, 72 pp.

IBM, 1975. Continuous System Modelling Program III (CSMP III), Program Reference Manual. IBM SH19-7001-3. Technical Publications Department, White Plains, U.S.A., 206 pp.

Jarvis, P.G., James, G.B. and Landsberg, J.J., 1976. Coniferous forest. In: J.L. Monteith (Ed.): Vegetation and Atmosphere. Vol. 2: Case studies. Academic Press, London, p. 171-239.

Johnson, L.W. and Riess, R.D., 1977. Numerical analysis. Addison - Wesley Publishing Company, Reading, Massachusetts, USA. 370 pp.

Kay, M., 1978. Foliage biomass of Douglas fir in a 53-year-old plantation. New Zealand Journal of Forest Science, 8: 315-326.

Keller, Th., 1965. Uber den winterlichen Gaswechsel der Koniferen im Schweizerischen Mittelland. Schweizerische Zeitschrift für das Forstwezen, 116: 719-729.

Kellomäki, S., 1982. Growth dynamics of young Scots pine crowns (Pinus sylvestris). Metsäntutkimuslaitoksen Julkaisuja, 98.4, 50 pp.

Kercher, J., and Axelrod, M.C., 1984. Analysis of SILVA: A model for forecasting the effects of SO_2 pollution on growth and succession on Western coniferous forests. Ecological Modelling, 23: 165-184.

Kestemont, P., 1977. Biomasse et productivité primaire de la Douglasière à Mirwart Plantation de Pseudotsuga menziesii. In: P. Duvigneaud and P. Kestemont, (Eds.): Productivité biologique en Belgique, p. 177-189.

Keulen, H. van, 1975. Simulation of water use and herbage growth in arid regions. Simulation Monographs. Pudoc, Wageningen, 184 pp.

Keulen, H. van, and van Heemst, H.D.J., 1986. Meteorological data. In: Keulen, H. van and J. Wolf, (Eds.), 1986. Modelling of Agricultural Production: weather, soils and crops. Simulation Monographs. Pudoc, Wageningen, p. 208-211.

Keulen, H. van, Penning de Vries, F.W.T. and Drees, E.M., 1982. A summary model for crop growth. In: Penning de Vries, F.W.T. and van Laar, H.H. (eds): Simulation of plant growth and crop production. Simulation Monograph, Pudoc, Wageningen, pp. 87-97.

Keulen, H. van and J. Wolf, (Eds.), 1986. Modelling of Agricultural Production: weather, soils and crops. Simulation Monographs. Pudoc, Wageningen, 479 pp.

Keyes, M.R. and Grier, C.C., 1981. Above- and below-ground net production in 40-year-old Douglas-fir stands on low and high productivity sites. Canadian Journal of Forest Research, 11: 599-605.

Kinerson, R.S. and Fritschen, L.J., 1971. Modelling a coniferous forest canopy. Agricultural Meteorology, 8: 439-445.

Kira, T. and Shidei, T., 1967. Primary production and turnover of organic matter in different forest ecosystems of the Western Pacific. Japanese Journal of Ecology, 17: 70-87.

Knigge, W., 1958. Untersuchungen über die Beziehungen zwischen Holzeigenschaften und Wuchs der Gastbaumart Douglasie. Schriftenreihe der Forstliche Fakultät der Universität Göttingen und Mitteilungen der Niedersächsischen Forstlichen Versuchsanstalt, Band 20, 101 pp.

KNMI, 1935-1984. Maandelijkse overzichten van de weersgesteldheid in Nederland. Koninklijk Nederlands Meteorologisch Instituut, De Bilt.

Kofman, D., 1983. De oogst van biomassa in dunningen en de gevolgen voor de bodemvruchtbaarheid. Rijksinstituut voor onderzoek in de bos- en landschapsbouw 'De Dorschkamp', Wageningen, Rapport nr. 335.

Kraalingen, D. van, Spitters, C.J.T. and van Keulen, H., 1987. Coupling of models, the crop. In: R. Rabbinge, S.A. Ward and H.H. van Laar (Eds.): Simulation and systems management in crop protection. Simulation Monograph, Pudoc, Wageningen, in preparation.

Krabbenborg, A.J., Poelman, J.N.B. and van Zuilen, E.J., 1983. Standaard - vochtkarakteristieken van zandgronden en veenkoloniale gronden. STIBOKA, Wageningen, Rapport nr. 1680.

Kramer, P.J. and Kozlowski, T.T., 1979. Physiology of woody plants. New York, Academic Press, 811 pp.

Krahmer, R.L. and Côté, W.A., 1963. Changes in coniferous wood cells associated with heartwood formation. TAPPI, 46: 42-49.

Kriek, W., 1974. Douglas fir IUFRO provenances in the Netherlands. 1966/67 series. Nederlands Bosbouw Tijdschrift, 46 (1): 1-14.

Kriek, W., 1975. Douglas fir IUFRO provenances in the Netherlands. 1968-69 series. Nursery results. Nederlands Bosbouw Tijdschrift, 47 (3): 100-116.

Kriek, W., 1983. Results in Dutch field trials with Douglas fir IUFRO provenances and progenies of the 1968/1969 series. Rijksinstituut voor onderzoek in de Bos- en Landschapsbouw 'De Dorschkamp', Wageningen, Rapport nr. 343, 39 pp.

Krueger, K.W. and Ferrell, W.K., 1965. Comparative photosynthetic and respiratory responses to temperature and light by Pseudotsuga menziesii var. menziesii and var. glauca seedlings. Ecology, 46: 794-801.

Krueger, K.W. and Ruth, R.H., 1969. Comparative photosynthesis of red alder, Douglas-fir, Sitka spruce and western Hemlock seedlings. Canadian Journal of Botany, 47: 519-527.

Kuiper, P.J.C., 1964. Water uptake of higher plants as affected by root temperature. Mededelingen Landbouwhogeschool Wageningen, 64-4.

Künstle, E., 1971. Der Jahresgang des CO_2-Gaswechsels von ein jährigen Douglasien trieben in einem 20 jährigem Bestand. Allgemeine Forst- und Jagdzeitung, 142: 105-108.

Künstle, E., 1972. CO_2-Gaswechsel und Transpiration von verschieden alten Douglasientrieben in einem Stangenholz während der Vegetationszeit. Angewandte Botanik, 46: 49-58.

Künstle, E., and Mitcherlich, G., 1975. Photosynthese, Transpiration und Atmung in einem Mischbestand im Schwarzwald. I Teil: Photosynthese. Allgemeine Forst- und Jagdzeitung, 146: 45-63.

LaBastide, J.G.A. and Faber, P.J., 1972. Revised yield tables for six tree species in the Netherlands. Wageningen, Forestry Research Institute 'De Dorschkamp', Uitvoerig verslag band, 11, nr. 1.

Larcher, W., 1963. Die Eignung abgeschnittener Zweige und Blätter zur Bestimmung des Assimilationsvermögens. Planta, 60: 1-18.

Larcher, W., 1980. Physiological plant ecology (second revised edition), Berlin, Springer Verlag, Heidelberg, New York. 303 pp.

Larson, P.R., 1960. A physiological consideration of the springwood summerwood transition in red pine. Forest Science, 6: 110-122.

Larson, P.R., 1963. Stem form development in forest trees. Forest Science Monograph 5, 42 pp.

Larson, P.R., 1969. Wood formation and the concept of wood quality. Yale School of Forestry, Bulletin Nr. 74.

Leenaars-Leijh, M.J.S., 1985. Electronenmicroscopisch onderzoek naar de chemische omzetting van meststoffosfaat in de grond. Verslagen en Mededelingen 1985-1, Department of Soil Science and Plant Nutrition, Agricultural University, Wageningen, The Netherlands.

Lehr, J.R., Brown, W.E. and Brown, E.H., 1959. Chemical behaviour of monocalcium phosphate monohydrate in soils. Soil Science Society of America, Proceedings, 23: 3-7.

Leverenz, J.W., 1981a. Photosynthesis and transpiration in large forest-grown Douglas-fir: diurnal variation. Canadian Journal of Botany, 59: 349-356.

Leverenz, J.W., 1981b. Photosynthesis and transpiration in large forest-grown Douglas-fir: interactions with apical control. Canadian Journal of Botany, 59: 2568-2576.

Levert, C., 1954. Regens, een statistische studie. KNMI Mededelingen en Verhandelingen 62, Staatsdrukkerij- en uitgeversbedrijf, 's-Gravenhage, 246 pp.

Lieth, H. (Ed.), 1973. Primary production in temperate forests. Ecological Studies, Berlin, Springer Verlag.

Linder, S., 1979. Photosynthesis and respiration in conifers. A classified reference list, 1891-1977. Studia Forestalia Suecica 149, 71 pp.

Linder, S., 1981. Photosynthesis and respiration in conifers. A classified reference list, Supplement 1. Studia Forestalia Suecica 161, 32 pp.

Linder, S. (ed.), 1981. Understanding and predicting tree growth. Studia Forestalia Suecica, Nr. 160, 87 pp.

Linder, S. and Rook, D.A., 1984. Effects of mineral nutrition on carbon dioxide exchange and partitioning of carbon in trees. In: G.D. Bowen and E.K.S. Nambiar, (Eds.): Nutrition of Plantation Forests. Academic Press, London, pp. 211-236.

Lohammar, T., Larson, S., Linder, S. and Falk, S.O., 1980. FAST - simulation models of gaseous exchange in Scots pine. In: T. Persson (Ed.): Structure and function of Northern coniferous forests - An ecosystem study. Ecological Bulletin (Stockholm), 32: 505-523.

Long, J.N. and Turner, J., 1975. Above-ground biomass of understorey and overstorey in an age sequence of four Douglas fir stands. Journal of Applied Ecology, 12: 178-188.

Lopushinski, W. and Kaufmann, M.R., 1984. Effects of cold soil on water relations and spring growth of Douglas fir seedlings. Forest Science, 3: 628-634.

Louwerse, W. and van Oorschot, J.L.P., 1969. An assembly for routine measurements of photosynthesis, respiration and transpiration of intact plants under controlled conditions. Photosynthetica, 3: 305-315.

Makkink, G.F. and Heemst, H.D.J. van, 1975. Simulation of the water balance of arable land and pastures. Simulation Monograph, Pudoc, Wageningen, 79.

Massman, W.J., 1982. Foliage distribution in old growth conifer tree canopies. Canadian Journal of Forest Research, 12: 10-17.

Matthews, J.D., 1963. Factors affecting the production of seed by forest trees. Forestry Abstracts, 24: 1-13.

Mayhead, G.J., 1973. Some drag coefficients for British forest trees derived from wind tunnel experiments. Agricultural Meteorology, 12: 123-130.

McMinn, R.G., 1963. Characteristics of Douglas-fir root systems. Canadian Journal of Botany, 41: 105-122.

Mead, D.J., 1984. Diagnosis of nutrient deficiencies in plantations. In: G.D. Bowen and E.K.S. Nambiar, (Eds.): Nutrition of Plantation Forests. Academic Press, London, p. 254-291.

Meinzer, F., 1982a. The effect of vapor pressure on stomatal control of gas exchange in Douglas fir (Pseudotsuga menziesii) saplings. Oecologia (Berlin), 54: 236-242.

Meinzer, F., 1982b. The effect of light on stomatal control of gas exchange in Douglas fir saplings. Oecologia (Berlin), 54: 270-274.

Meinzer, F., 1982c. Models of steady-state and dynamic gas exchange responses to vapor pressure and light in Douglas fir (Pseudotsuga menziesii) saplings. Oecologia (Berlin), 55: 403-408.

Miller, H.G., 1979. The nutrient budgets of even-aged forests. In: E.D. Ford, D.C. Malcolm and J. Atterson (Eds.): The ecology of even-aged forest plantations. Institute of Terrestrial Ecology, Cambridge, p. 221-255.

Miller, H.G., 1984. Dynamics of nutrient cycling in plantations ecosystems. In: G.D. Bowen and E.K.S. Nambiar, (Eds.): Nutrition of Forest Trees in Plantations. Academic Press, London, p. 53-78.

Minderman, G., 1967. The production of organic matter and the utilization of solar energy by a forest plantation of Pinus nigra var. austriaca. Pedobiologia, 7: 11-22.

Mitchell, K.J., 1975. Dynamics and simulated yield of Douglas fir. Forest Science Monograph, No. 17, 39 pp.

Mitscherlich, G., 1970. Wald, Wachstum und Umwelt. Band I: Form und Wachstum von Baum und Bestand. J.D. Sauerländers Verlag, Frankfurt am Main, 2nd rev. edition, 1978, 144 pp.

Mitscherlich, G., 1975. Wald, Wachstum und Umwelt. Band 3: Boden, Luft und Produktion. J.D. Sauerländers Verlag, Frankfurt am Main, 352 pp.

Mohren, G.M.J., van den Burg, J. and Burger, F.W., 1986. Phosphorus deficiency induced by nitrogen input in Douglas fir forests in the Netherlands. Plant and Soil, 95: 191-200.

Mohren, G.M.J., van Gerwen, C.P. and Spitters, C.J.T., 1984. Simulation of primary production in even-aged stands of Douglas-fir. Forest Ecology and Management, 9: 27-49.

Møller, C.M., 1945. Untersuchungen über Laubmenge, Stoffverlust und Stoffproduktion des Waldes. Det forstlige Forsøgsvaesen i Danmark, 17: 1.287.

Møller, C.M., Müller, D. and Nielsen, J., 1954a. Graphic presentation of dry matter production of European beech. Det forstlige Forsøgsvaesen i Danmark, 21: 327-335.

Møller, C.M., Müller, D. and Nielsen, J., 1954b. Respiration in stems and branches of beech. Det forstlige Forsøgsvaesen i Danmark, 21: 273-301.

Monteith, J.L., 1965. Evaporation and Environment. Symposium of the Society for Experimental Biology, 19: 205-234.

Monteith, J.L., 1973. Principles of environmental physics. Edward Arnold, London, 241 pp.

Mulder, J.P.M., 1983. A simulation model of rainfall interception in a pine forest. Dissertation, University of Groningen, Groningen, 109 pp.

Müller, D. and Nielsen, J., 1965. Production brute, pertes par respiration et production nette dans la fôret ombrophile tropicale. Det forstlige Forsøgsvaesen i Danmark, 29: 69-160.

Newbould, P.J., 1967. Methods for estimating the primary production of forests. IBP Handbook No. 2, Blackwell Scientific Publications, Oxford, ix + 62 pp.

Nnyamah, J.U., Black, T.A. and Tan, C.S., 1978. Resistance to water uptake in a Douglas-fir forest. Soil Science, 126: 63-76.

Patterson, S.S., 1956. The forest area of the world and its potential productivity. Dissertation, Göteborg, Sweden, 216 pp.

Pearce, A.J., Gash, J.H.C. and Stewart, J.B., 1980. Rainfall interception in a forest stand estimated from grassland meteorological data. Journal of Hydrology, 46: 147-163.

Penman, H.L., 1948. Natural evaporation from water, bare soil and grass. Proceedings of the Royal Society, Series A, 193: 120-146.

Penning de Vries, F.W.T., 1974. Substrate utilization and respiration in relation to growth and maintenance in higher plants. Netherlands Journal Agricultural Science, 22: 40-44.

Penning de Vries, F.W.T., 1975. The cost of maintenance processes in plant cells. Annals of Botany, 39: 77-92.

Penning de Vries, F.W.T., 1981. Simulation models of growth of crops, particularly under nutrient stress. In: A. von Peter and H. Künzli (Eds.): Physiological aspects of crop productivity. Proceedings 15 th. Colloqium International Potash Institute, Bern (1980): 213-226.

Penning de Vries, F.W.T., 1983. Modelling of growth and production. In: O.L. Lange, P.S. Nobel, C.B. Osmond and H. Ziegler (eds.): Physiological Plant Ecology IV. Berlin, Springer Verlag, Encyclopedia of Plant Physiology, New Series, Vol. 12D: 118-120.

Penning de Vries, F.W.T., Brunsting, A. and van Laar, H.H., 1974. Products, requirements and efficiency of biosynthesis; a quantitative approach. Journal Theoretical Biology, 45: 339-377.

Penning de Vries, F.W.T. and van Laar, H.H., 1982. Simulation of growth processes and the model BACROS. In: F.W.T. Penning de Vries and H.H. van Laar, (Eds.): Simulation of plant growth and crop production. Simulation Monograph. Pudoc, Wageningen, p. 114-135.

Penning de Vries, F.W.T. and van Laar, H.H. (Eds.), 1982. Simulation of plant growth and crop production. Simulation Monographs. Pudoc, Wageningen, 308 pp.

Persson, T. (Ed.), 1980. Structure and function of northern coniferous forests. Ecological Bulletin (Stockholm), 32: 1-609.

Pienaar, L.V. and Turnbull, K.J., 1973. The Chapman-Richards generalization of von Bertalanffy's growth model for basal area growth and yield in even-aged stands. Forest Science, 19: 2-22.

Polge, H., 1982. Influence de la competition et de la disponibilité en eau sur l'importance de l'aubier du douglas. Annales des Sciences forestieres, 39: 379-398.

Polster, H., 1950. Die physiologischen Grundlagen der Stofferzeugung im Walde. Bayerischer Landwirtschaftsverlag, München, 96 pp.

Polster, H., 1961. Neue Ergebnisse auf dem Gebiet der Standortsökologischen assimilations und transpirations Forschung an Forstgewechse. Landwirtschaftwissenschaften, 10, Deutsche Akademie Berlin: Sitzungsberichte.

Prins, J.A. and Reesinck, J.J.M., 1946. Meteorologische waarnemingen te Wageningen tot 1 januari 1946 en helderheidsmetingen aan de hemel te Arnhem. Mededelingen Landbouwhogeschool 48, Verhandeling 3: 60-84.

Rabbinge, R., Ward, S.A. and van Laar, H.H., (Eds.), 1987. Simulation and systems management in crop protection. Simulation Monographs. Pudoc, Wageningen, in preparation.

Raschke, K., 1975. Stomatal action. Annual Review of Plant Physiology, 26: 309-340.

Reed, K.L., 1980. An ecological approach to modelling growth of forest trees. Forest Science, 26(1): 33-50.

Reesinck, J.J.M. and Vries, D.A. de, 1942. De jaarlijkse en dagelijkse gang van het daglicht in Nederland. Mededelingen Landbouwhogeschool 46, Verhandeling 1: 1-24.

Reichle, D.E. (Ed.), 1981. Dynamic properties of forest ecosystems. IBP 23, Cambridge University Press, Cambridge, 683 pp.

Richards, F.J., 1959. A flexible growth model for empirical use. Journal of Experimental Botany, 10: 290-300.

Richer, H., 1972. Wie entstehen Saugspannungsgradienten in Bäumen? Berichte Deutsche botanische Gesellschaft, 85: 341-351.

Roberts, J., 1983. Forest transpiration: a conservative hydrological process? Journal of Hydrology, 66: 133-141.

Rook, D.A., Grace, J., Beets, P.N., Whitehead, D., Santantonio, D. and Madgwick, H.A.I, 1985. Forest canopy design: biological models and management implications. In: M.G.R. Cannell and J.E. Jackson, (Eds.): Attributes of trees as crop plants. Institute of Terrestrial Ecology, Monks Wood Experimental Station, Abbots Ripton, Huntingdon, England, p. 507-524.

Running, S.W., 1976. Environmental control of leaf water conductance in conifers. Canadian Journal of Forest Research, 6: 104-112.

Running, S.W., 1984. Microclimate control of forest productivity: analysis by computer simulation of annual photosynthesis/transpiration balance in different environments. Agricultural and Forest Meteorology, 32: 267-288.

Rutter, A.J., 1968. Water consumption by forests. In : T.T. Kozlowksi (ed.): Water deficit and plant growth, vol.II New York, Academic Press, p. 23-84.

Rutter, A.J., 1975. The hydrological cycle in vegetation. In : J.L. Monteith (ed.): Vegetation and the Atmosphere, London, Academic Press, p. 111-154.

Rutter, A.J., Morton, A.J. and Robins, P.C., 1975. A predictive model of rainfall interception in forests. II: Generalization of the model and comparison with observations in some coniferous and hardwood stands. Journal of Applied Ecology, 12: 367-380.

Rydholm, S.A. 1965. Pulping processes. Wiley, New York, 1269 pp.

Salo, D.J., 1974. Factors affecting photosynthesis in Douglas-fir. PH.D. Dissertation, University of Washington, Seattle, 150 pp.

Santantonio, D. and Hermann, R.K., 1985. Standing crop, production, and turnover of fine roots on dry, moderate, and wet sites of mature Douglas-fir in western Oregon, Annales des Sciences Forestieres, 42: 113-142.

Sarkanen, K.C. and Ludwig, C.H., 1971. Lignins. Wiley, New York, 916 pp.

Satoo, T. and Madgwick, H.A.I, 1982. Forest Biomass. Nijhoff/Junk Publishers, The Hague. 152 pp.

Schaedle, M., 1975. Tree photosynthesis. Annual review of plant physiology, 26: 101-115.

Schelling, J., 1961. The high forest soils of the central Netherlands (in Dutch, with an English Summary). Detailed reports of the Forest Research Station 'De Dorschkamp', Wageningen, Band 5, Nr. 1, 67 pp.

Schelling, J. and van Goor, C.P., 1958. Soil evaluation and soil fertility (in Dutch). Nederlands Bosbouw Tijdschrift, 30: 47-51.

Schumacher, F.X. and Hall, F.D.S., 1933. Logarithmic expression of timbertree volume. Journal Agricultural Research, 47: 719-734.

Setlik, I. (ed.), 1970. Prediction and measurement of photosynthetic productivity. Proceedings of the IBP/PP Technical Meeting, Trebon, 14-21 september 1969. Pudoc, Wageningen, 632 pp.

Shinozaki, K., Yoda, K., Hozumi, K. and Kira, T., 1964. A quantitative analysis of plant form - the pipe model theory. I. Basic Analysis. Japanese Journal of Ecology, 14: 97-103.

Shinozaki, K., Yoda, K., Hozumi, K. and Kira, T., 1964. A quantitative analysis of plant form - the pipe model theory. I. Further evidence of the theory and its application in forest ecology. Japanese Journal of Ecology, 14: 133-139.

Shugart, H.H., 1984. A theory of forest dynamics. The ecological implications of forest succession models. Springer Verlag, Berlin, 278 pp.

Shugart, H.H., Goldstein, R.A., O'Neill, R.V. and Mankin, J.B., 1974. TEEM: A terrestrial ecosystem energy model for forests - Oecologia Plantarum, 9: 231-264.

Sievänen, R., 1983. Growth model for mini-rotation plantations. Communicationes Instituti Forestalis Fenniae, nr. 117, 41 pp.

Silver, G.T., 1962. The distribution of Douglas-fir foliage by age. Forestry Chronicle, 38: 433-438.

Smith, D.M., 1955. Relationship between specific gravity and percentage of summerwood in wide-ringed, second-growth Douglas-fir. USDA Forest Products Laboratory, Madison, Report no. 2045.

Snell, J.A.K. and Brown, J.K., 1978. Comparison of tree biomass estimators - DBH and sapwood. Forest Science, 24: 455-457.

Sorensen, F.C. and Campbell, R.K., 1978. Comparative roles of soil and air temperature in the timing of spring budflush in seedling Douglas-fir. Canadian Journal of Botany, 56: 2307-2308.

Spitters, C.J.T., 1986. Separating diffuse and direct component of global radiation and its implications for modelling canopy photosynthesis. II Canopy photosynthesis. Agricultural and Forest Meteorology, 38: 239-250.

Spitters, C.J.T., Toussaint, E. and Goudriaan, J., 1986. Separating diffuse and direct component of global radiation and its implications for modelling canopy photosynthesis. I: Components of incoming radiation. Agricultural and Forest Meteorology, 38: 225-237.

Spittlehouse, D.L., 1981. Measuring and modelling evapotranspiration from Douglas-fir stands. Ph.D. Thesis, University of British Columbia, Vancouver, Canada, 276 pp.

Spittlehouse, D.L. and Black, T.A., 1982. A growing season water balance model used to partition water use between trees and understorey. Proceedings of the Canadian Hydrology Symposium. Associate Committee on Hydrology, Ottawa, National Research Council of Canada, p. 195-214.

Stroosnijder, L., 1982. Simulation of the soil water balance. In: F.W.T. Penning de Vries and H.H. van Laar, (Eds.): Simulation of plant growth and crop production. Simulation Monograph. Pudoc, Wageningen, p. 175-193.

Szaniawski, R.K., 1981. Growth and maintenance respiration of shoot and roots in Scots pine seedlings. Zeitschrift für Pflanzenphysiologie, 101: 391-398.

Szaniawski, R.K., Wierzbicki, B., 1978. Net photosynthetic rate of some coniferous species at diffuse high irradiance. Photosynthetica, 12: 412-417.

Szeicz, G., 1974. Solar radiation for plant growth. Journal of Applied Ecology, 11: 617-636.

Thomson, A. and Moncrieff, S.M., 1982. Prediction of bud-burst in Douglas-fir by degree-day accumulation. Canadian Journal of Forest Research, 12: 448-452.

Turner, J., 1975. Nutrient cycling in a Douglas-fir ecosystem with respect to age and nutrient status. Seattle, University of Washington, Ph.D. Dissertation, 191 pp.

Turner, J., Dice, S.F., Cole, D.W. and Gessel, S.P. 1978. Variation of nutrients in forest tree foliage - a review. College of Forest Resources, University of Washington, Institute of Forest Products, Contribution 35, 31 pp.

Turner, J., 1981. Nutrient cycling in and age sequence of western Washington Douglas fir stands. Annals of Botany, 48: 159-169.

Turner, J. and Long, J.N., 1975. Accumulation of organic matter in a series of Douglas fir stands. Canadian Journal of Forest Research, 5: 681-690.

Veen, B., 1951. Herkomstenonderzoek van de Douglas in Nederland. Dissertation, Wageningen, 130 pp.

Veen, B., 1958. Het herkomstenvraagstuk van de groene Douglas. Nederlands Bosbouw Tijdschrift, 30: 44-46.

Veen, J.A. van, 1977. The behaviour of nitrogen in soil. A computer simulation model. Ph.D. thesis, Free University, Amsterdam, 164 pp.

Vries, D.A. de, 1955. Solar radiation at Wageningen. Mededelingen Landbouwhogeschool, 55(6): 277-304.

Vries, P.G. de, 1961. Een onderzoek naar de productiviteit van verschillende Douglas-herkomsten in Nederland. Mededelingen van de Landbouwhogeschool Wageningen, 61(13): 1-40.

Waring, R.H., 1983. Estimating forest growth and efficiency in relation to canopy leaf area. Advances in Ecological Research, 13: 327-354.

Waring, R.H. and Running, S.W., 1976. Water uptake, storage and transpiration by conifers: a physiological model. In: O.L. Lange, L. Kappen and E.-D. Schulze, (Eds.): Water and plant life. Ecological Studies no. 19, Springer Verlag, Berlin, p. 189-202.

Waring, R.H. and Schlesinger, W.H., 1985. Forest ecosystems. Concepts and management. Academic Press, New York, 340 pp.

Webb, W.L., 1975. Dynamics of photoassimilated carbon in Douglas-fir seedlings. Plant Physiology, 56: 455-459.

Webb, W.L., 1977. Seasonal allocation of photoassimilated carbon in Douglas-fir seedlings. Plant Physiology, 60: 320-322.

West, D.C., McLaughlin, S.B. and Shugart, H.H., 1980. Simulated forest response to chronic air pollution stress. Journal of Environmental Quality, 9: 43-49.

Whitehead, D., 1978. The estimation of foliage area from sapwood basal area in Scots pine. Forestry, 51: 137-149.

Whitehead, D., and Jarvis, P.G., 1981. Coniferous forests and plantations. In: Kozlowski, T.T. (ed.): Water deficits and Plant growth. Vol. 6, Academic Press, New York, p. 50-152.

Whitehead, D., Edwards, W.R.N. and Jarvis, P.G., 1984. Conducting sapwood area, foliage area, and permeability in mature trees of Picea sitchensis and Pinus contorta. Canadian Journal of Forest Research, 14: 940-947.

Whiteley, G.M., Utomo, W.H. and Dexter, A.R., 1981. A comparison of penetrometer pressures and the pressure exerted by roots. Plant and Soil, 61: 351-364.

Wieringa, J. and Rijkoort, P.J., 1983. Windklimaat van Nederland. Klimaat van Nederland 2, KNMI, De Bilt, Staatsuitgeverij, Den Haag.

Wiersma, J.H., 1963. A new method of dealing with results of provenance tests. Silvae Genetica, 12: 200-205.

Wit, C.T. de, 1965. Photosynthesis of leaf canopies. Agr. Res. Rep. 663, Pudoc, Wageningen, 57 pp.

Wit, C.T. de, 1968. Plant Production. Miscellaneous Papers, Landbouwhogeschool Wageningen, No. 3: 25-50.

Wit, C.T. de, van Laar, H.H. and van Keulen, H., 1979. Physiological potential of crop production. In: J. Sneep and A.J.T. Hendriksen (eds.): Plant breeding perspectives. Pudoc, Wageningen, p. 47-82.

Wit, C.T. de, and F.W.T. Penning de Vries, 1982. La synthese et la simulation des systemes de production primaire. In: F.W.T. Penning de Vries, & M.A. Djiteye (eds.): La productivité des Paturages Sahéliens. Agricultural Research Report Nr. 918, Pudoc, Wageningen, p. 23-27.

Wit, C.T. and Wolf, N.J., 1984a. The modelling of the response to nitrogen. Staff working paper, SOW-84-13, 21 pp.

Wit, C.T. and Wolf, N.J., 1984b. The modelling of the response to phosphate. Staff working paper, SOW-84-14, 13 pp.

Wit, C.T. de, et al., 1978. Simulation of assimilation, respiration and transpiration of crops. Simulation monographs, Pudoc, Wageningen, 140 pp.

Wolf, J., de Wit, C.T., Janssen, B.H. and Lathwell, D.J., 1987. Modelling the long-term response crop response to fertilizer phosphorus. I: The model. Agronomy Journal, in prep.

Wong, S.C., Cowan, I.R. and Farquhar, G.D., 1985. Leaf conductance in relation to rate of CO_2 assimilation. Plant Physiology, 78: 821-825, 826-829, 830-839.

Zabuga, V.F., Zabuga, G.A. and Zinoveva, V.P., 1983. Ecological characteristics of respiratory CO_2 exchange in the growing trunk of Scots pine. Translated from Fiziologiya Rastenii, 29: 1212-1218.

Ziegler, H., 1967. Biologische Aspekte der Kernholzbildung. In: Proceedings of the 14 th. IUFRO Congress, München, Volume 9: 93-116.

Zimmerman, M.H., 1983. Xylem structure and the ascent of sap. Springer Verlag, Berlin, 143 pp.

Zimmerman, M.H. and Brown, C.L., 1971. Trees, structure and function. Springer Verlag, New York, 4th. printing, 1980, 336 pp.

SUMMARY

Forest growth in relation to weather and soils is studied using a
physiological simulation model. Growth potential depends on physiological
characteristics of the plant species in combination with ambient weather
conditions (mainly temperature and incoming radiation). For a given site,
growth may be lower because of incomplete canopy closure, shortage of water
and nutrients, and the occurrence of growth-disturbing factors such as pests,
diseases, and damage to the plants, e.g. by windthrow or frost. Attention is
focused on the main growth-limiting factors, i.e. canopy closure, and the
availability of water, nitrogen and phosphorus, so that differences in growth
between different sites can be explained as a function of the properties of
plant and soil, and of the ambient weather at a particular site. The model is
applied to even-aged Douglas fir stands in the Netherlands because of the
availability of field data for testing and evaluating it.

The life cycle of trees and forests encompasses many years, and in order
to be able to study overall stand dynamics, the model aims at simulating
growth over periods of several decades. This allows the results of the model
to be evaluated against data from permanent field plots, that are also being
used in conventional, descriptive research on growth and yield. Furthermore,
simulating forest growth over such long periods makes the results from the
model comparable with the results of practical forest management. Variations
in growth during the year are caused by changes in incoming radiation,
temperature and water availability in the soil. To simulate this, time
intervals of one day are used for the main part of the simulation model.

The particular value of simulation models in forestry lies in the
possibility they offer of combining different aspects of growth in an overall
approach, and of studying stand dynamics over a long period of time without
having to rely entirely on expensive and time-consuming field trials.
Moreover, in a situation where the environment for forest growth may change
e.g. as the result of industrial pollution, or as a consequence of gradual
climatic changes, modelling is one of the important means by which to assess
these changes and potential damage.

The subject of the study, an even-aged coniferous forest stand, is described in terms of the biomass components foliage, branches, stems and roots. These four components are the main state variables in the model. To enable comparisons to be made between the results from the model and the data from permanent field plots, only stem biomass and stem volume are considered, together with the number of trees. This reflects a top-down approach to growth, which is calculated as total stand growth per unit of soil surface area, before it is distributed over individual trees. In addition to state variables that denote biomass amounts, stand structure is also characterized by stand height, average dimensions of the tree crowns, and total depth of the rooted soil profile. All other state and intermediate variables of the trees (such as the Leaf Area Index of the stand), are derived from simulated biomass components and stand structure. In the model, ambient weather is characterized using meteorological data from a local weather station: total daily global radiation, daily minimum and maximum temperatures, daily vapour pressure of the air, average wind speed at 10 m above short vegetation, and precipitation. The latter is characterized by daily rainfall and the average number of rainfall events per day. Only the rooted soil profile is used to describe the soil compartment. Soil moisture retention properties are the main variables for the hydrological submodel. The simulation of nutrient dynamics is based on the total amount of nutrients retained in the rooted soil profile and incorporated in the stand biomass. Nutrient inputs to the system are described by forcing functions, and used as input to the model.

Chapter 3 shows how primary production is calculated for the whole stand. Canopy assimilation is calculated from the distribution of photosynthetically active radiation over the foliage, together with the photosynthesis/light response curve at ambient temperature for the surface of an individual leaf. The assimilation submodel uses a three-point Gaussian integration, as described recently by Goudriaan (1986), and Spitters (1986). The distribution of photosynthetically active radiation over the foliage accounts for gaps in the canopy, and allows for clustering of the foliage, as in the case of grouping of needles around branches in old stands. Typical aspects of canopy assimilation in Douglas fir stands, are the evergreen habitus of the stand, and the generally low maximum photosynthesis rates, (around 15 kg CH_2O $ha^{-1}h^{-1}$). These low rates of photosynthesis are coupled with high stomatal resistances for the diffusion of both carbon dioxide and water vapour.

After canopy assimilation has been estimated, net growth is calculated by accounting for maintenance respiration, and by allocating the assimilates available for growth to the biomass components. Growth respiration is taken into account when converting assimilate products to structural dry matter. To calculate maintenance respiration, sapwood is distinguished from heartwood. It is found that the hypothesis (Boysen Jensen, 1928; Kira and Shidei, 1967) that tree growth declines with age of the trees because maintenance requirements increase with accumulation of stem biomass does not hold when maintenance requirements are related to sapwood only. Sapwood (like foliage, branches and roots) has a limited life-span, and the maximum value it attains during stand development depends on site productivity. This maximum value is reached within 15 years of the time of maximum annual increment. Growth respiration is calculated by taking the chemical composition of the biomass formed into account. The allocation of assimilates to the biomass components is based on a distribution key derived from published data. The distribution of growth over the biomass components changes during stand development, and also depends on the productivity of the site. Stem dry weight increment is converted to volume increment by dividing the estimated dry weight increment by the basic density of the stem wood formed, i.e. the oven-dry weight per unit of fresh volume. Individual tree increment is calculated by dividing total stem volume increment by the number of trees in the stand, and only an average value for diameter at breast height is calculated from tree volume and height, using an empirical regression equation.

Chapter 4 describes the hydrological part of the model. The three main aspects considered in the model are: a) interception of precipitation by the canopy and the resulting net infiltration to the soil compartment; b) the soil moisture balance; c) and uptake and transpiration of soil moisture by the trees. Coniferous forests in western Europe are often located on sandy soils with a limited soil moisture holding capacity and restricted capillary rise. This means that in periods of drought, availability of soil moisture becomes limiting for growth. In the model, therefore, it suffices to simulate water availability with an elementary summary model that keeps track of soil moisture. Soil moisture content and the rate of infiltration are simulated by assuming that the soil horizons are filled to field capacity by a sharp wetting front proceeding from the top of the soil profile downwards. Root uptake is assumed to proceed until soil moisture is depleted to the wilting

point. Field capacity and wilting point are derived from soil suction curves, and depend on physical soil characteristics.

Tall forest stands have considerable aerodynamic roughness, and this means that the aerodynamic resistance to the transport of water vapour from the surface of the foliage to the overlying atmosphere is small (around 10 s m^{-1}). Besides, the large stomatal resistance of Douglas fir needles results in a minimum canopy resistance for the transpiration flux of 100 to 200 s m^{-1}; therefore, precipitation intercepted by the vegetation will evaporate at rates several times the transpiration rate under the same atmospheric conditions. Therefore, interception represents a real loss that has to be accounted for. To estimate interception, the amount of intercepted precipitation is subtracted from daily precipitation.

Daily transpiration is estimated with the Penman–Monteith combination equation, with total canopy resistance as one of the input variables. This resistance depends on: a) the vapour pressure deficit of the air (here assumed to pose a lower limit on stomatal resistance), b) the water status of the foliage, expressed in terms of needle water potential, and c) the stomatal opening resulting from photosynthesis. All three effects on stomatal resistance are calculated independently, and the largest resistance is used in the model to estimate total canopy resistance. The influence of vapour pressure and plant water status (through needle water potential), is assumed to be the same for all foliage in the canopy. The stomatal resistance estimated from net photosynthesis rates varies with varying photosynthesis rates inside the canopy. As in the calculation of canopy assimilation, a Gaussian integration procedure is used to estimate the weighted average foliage resistance. The resulting transpiration rates are found to be unexpectedly low during the growing season. Total annual transpiration, however, is in accordance with published data, and the simulated change in soil moisture during 1983 compares well with measurements from the field plots. It is concluded that on dry soils like those frequently occupied by coniferous stands in the Netherlands, water shortage may have considerable influence on growth, even though transpiration rates are low. In its present state the model can be used to calculate the reduction in growth caused by water shortage, for different sites, and for stands of different structure.

In chapter 5 the simulation of nutrient dynamics and the influence of ni-
trogen and phosphorus on growth are described. As it has been shown many
times that nitrogen and phosphorus may limit growth of coniferous stands on
sandy soils, only these two elements are incorporated in the model. No
attempt is made to model the dynamics of nitrogen and phosphorus in detail;
instead, an elementary model with time steps of one year is used in
combination with the simulations of daily canopy assimilation and hydrology.
Soil supply of nitrogen and phosphorus is estimated from total soil content,
by taking into account an unstable and a stable pool of nutrients in the
soil, each with different turnover rates. The demand for nitrogen and
phosphorus by the growing vegetation depends on the concentrations of these
elements in the tissue, and on the amounts redistributed before dead biomass
is shed, in combination with an estimated rate of biomass increment. By
adjusting the concentration in the tissue for the next period of growth,
demand and supply are balanced, and the influence of nutrient availability on
growth during the following year is estimated using an empirical relationship
between foliage nutrient concentration and growth. This approach assumes the
existence of maximum and minimum concentrations of both nutrients in the
tissue. Above the maximum concentration there is no further uptake; below the
minimum, growth ceases.

The final results from the model, together with the measurement series
from permanent field plots are given in chapter 6. The field plots used to
calibrate the model are discussed first; after this the model is tested
against an independent set of data. Overall model behaviour seems to follow
field measurements reasonably, both in the field plots used for calibration
and in the independent (control) plot. Maximum increment rates as measured in
the field are well reflected in the simulations, as is the decline in stem
increment in older trees. Most of the discrepancies between predicted and
real values are found to occur at higher ages of the stand. It is concluded
that this is probably because the model overestimates light interception,
because it takes no account of effects of uneven distributions of the trees
in the field. This becomes more important when stands are thinned at high
ages, when the crowns have only a limited ability to occupy the available
growing space.

Together with the evaluation of model behaviour, the value of the use of
modelling in forestry in general, and of the use of a physiologically-based

model like the one used here, is discussed. These models are needed for analysing growth and yield, and for contributing to the understanding of forest primary production. Moreover, they can be used to bridge the gap between widely different aspects of forest growth such as forest hydrology and forest nutrition. By integrating the main aspects of forest growth, these models also allow the main factors that determine total stand growth to be ascertained. As a result, possibilities for yield improvement, and the areas where research is mostly needed, can be identified. In the present case study, it appears that canopy growth often declines in the course of years because of decreased light interception. Current forestry practice in the Netherlands often includes an intensive thinning programme aimed at creating space for the individual crop trees. But this decreases stand growth. In general, this is not the intention, and therefore the efficacy thinning operations at higher stand ages that open up the stand to a degree that can no longer be utilized by the remaining trees, has to be reassessed.

Not only does availability of soil moisture limit growth; nitrogen and phosphorus availability may also play an important role in determining the production level of a stand. The elementary model used indicates the extent to which both nitrogen and phosphorus may influence stand growth, and the results are evaluated against the results of fertilizer experiments carried out in Douglas fir on a range of sites during the 1950s and the 1960s (Blok et al., 1975). The increase in atmospheric input of nitrogen, resulting from, among others, intensive livestock farming and manure-spreading on agricultural lands, has greatly increased nitrogen supply. As a result, widespread phosphorus deficiency has become apparent. In the Netherlands, all but the best sites currently available suffer from severe phosphorus deficiency. This situation, where widespread nitrogen deficiency has changed into a deficiency of phosphorus, demands attention from researchers and forest managers. Increasing phosphorus availability through additional fertilization can be expected to boost primary production and thus increase yield.

One of the possible applications of the model is to calculate the growth potential of a wide range of available soil types and growing conditions, thereby allowing potential forest growth to be assessed. It can also be used to evaluate management interventions. If employed in a target-oriented mode the model could be used to evaluate the efficacy of applying fertilizer. Some

of the growth- or stand-disturbing factors will have to be incorporated in the model before it can be used to calculate economic yield or optimal felling regimes.

The simulation programme is available upon request.

SAMENVATTING

Met behulp van een fysiologisch simulatiemodel van de groei van een bos is
de relatie tussen klimaat, bodem en produktie bestudeerd. Potentiële groei
van een aaneengesloten bos hangt af van fysiologische eigenschappen van de
betreffende boomsoort en van het weer op de groeiplaats. Voor de potentiële
groei zijn vooral straling en temperatuur van belang. Afwijkingen van de
potentiële groei kunnen worden veroorzaakt door onvolledige sluiting van het
kronendak, door gebrek aan water en voedingsstoffen, en door het optreden van
groeiverstorende en groeireducerende faktoren zoals ziekten en plagen,
onkruidconcurrentie, luchtverontreiniging en beschadigingen door wind en
vorst. Het onderzoek is vooral gericht op de belangrijkste groeibeperkende
faktoren zoals de mate van kroonsluiting, en de beschikbaarheid van water,
stikstof en fosfor. Stikstof en fosfor zijn de enige voedingselementen
waarvan de invloed op de primaire produktie in het model is opgenomen. De
beschikbaarheid van water, stikstof en fosfor wordt gebruikt om verschillende
groeisnelheden op verschillende groeiplaatsen te verklaren met behulp van
bodem- en planteigenschappen. Het model is ontwikkeld en toegepast in
gelijkjarige Douglas bossen in Nederland. Douglas is als proefboom gekozen
vanwege de beschikbaarheid van meetgegevens om het model te toetsen.

De levenscyclus van bomen en bossen omvat vele tientallen jaren. Om groei
en dynamiek van hele opstanden te kunnen bestuderen, berekent het ontwikkelde
model de groei over een periode van 40 tot 100 jaar. Simulatie van de
opstandsontwikkeling over een dergelijk lange periode maakt het mogelijk de
modelberekeningen te toetsen aan gegevens van permanente proefperken,
voorheen gebruikt in beschrijvend groei- en opbrengstonderzoek. Tevens zijn
de resultaten van het model op deze manier direkt overdraagbaar naar de
bosbouwpraktijk. Om de veranderingen in groeisnelheid gedurende het jaar te
kunnen simuleren, rekent het model met tijdstappen van één dag.

Het belang van simulatiemodellen voor de praktijk en het onderzoek in de
bosbouw ligt onder andere in de mogelijkheid om met een model verschillende
facetten van de groei van een bos met elkaar in verband te brengen in een
integrale benadering. Dit vergroot het inzicht in de werking van de

afzonderlijke groeifaktoren, en het leidt tot het vaststellen van die
gebieden waar onderzoek gewenst is. Daarnaast kan een dergelijk fysiologisch
model gebruikt worden om experimenten met de werkelijkheid te simuleren.
Bosbouwkundige veldproeven zijn veelal duur en tijdrovend, en het is van
groot belang al in een vroeg stadium te trachten om resultaten te
voorspellen. In situaties waar de omstandigheden voor groei voortdurend
veranderen, bijvoorbeeld door klimaatsveranderingen, zijn gecontroleerde
experimenten vaak niet mogelijk, en vormen simulatiemodellen een belangrijk
middel om toekomstige veranderingen in de primaire produktie van bossen te
bestuderen.

Het onderwerp van studie, gelijkjarig Douglasbos, wordt beschreven in
termen van totale hoeveelheden naalden, takken, stammen en wortels. Deze
biomassa componenten vormen de belangrijkste toestandsvariabelen in het
model. Om de model uitkomsten te vergelijken met meetgegevens van permanente
proefperken, wordt de hoeveelheid stambiomassa omgerekend naar stamvolume.
Naast de totale biomassa wordt het aantal bomen, hun hoogte, en de gemiddelde
kroonvorm gesimuleerd. Groei wordt op deze manier van bovenaf benaderd, door
eerst de opstandsgroei uit te rekenen om deze vervolgens toe te delen aan de
afzonderlijke bomen. Een aantal andere toestandsvariabelen (zoals de
bladoppervlakte-index) zijn afgeleid van de gesimuleerde biomassahoeveelheden
en van de struktuur van het kronendak. De klimatologische
groeiplaatsomstandigheden zijn weergegeven door het dagtotaal van de globale
straling, de dagelijkse minimum en maximum temperatuur, de waterdampdruk, en
de windsnelheid op 10 meter boven korte vegetatie. Neerslag in het model is
gekarakteriseerd met het dagtotaal aan neerslag, en het aantal buien per dag.
De bodemparameters in het model zijn beperkt tot de doorwortelde bodemlaag en
omvatten het waterbergend vermogen en de totale hoeveelheid stikstof en
fosfor in de doorwortelde laag. Toevoer van stikstof en fosfor van buitenaf,
bijvoorbeeld in de vorm van atmosferische depositie of door bemesting, is als
sturende variabele in het model opgenomen.

Hoofdstuk 3 laat zien hoe de primaire produktie van de gehele opstand
wordt berekend. De totale koolzuurassimilatie is berekend uit de verdeling
van het fotosynthetische aktieve deel van de straling over de naalden, op
basis van de fotosynthese-lichtresponse curve voor een afzonderlijk
naaldoppervlak. De gewasfotosynthese wordt berekend met behulp van de 3-punts
Gaussische integratie zoals beschreven in Goudriaan (1986) en Spitters

(1986). Bij de verdeling van de fotosynthetisch aktieve straling over de naalden wordt rekening gehouden met onvolledige kronensluiting en met eventuele clustering van naalden rondom de takken in de kroon. Kenmerkende aspekten van de fotosynthese in een Douglasbos zijn de lage maximale fotosynthesesnelheden (ongeveer 15 kg CO_2 ha^{-1} h^{-1} onder gunstige omstandigheden), en het feit dat de naalden gedurende het hele jaar aanwezig zijn, en ook aktief koolzuur kunnen assimileren. De lage fotosynthesesnelheden gaan gepaard met hoge stomataire weerstanden voor diffusie van zowel koolzuur als waterdamp. Dit leidt tot een hoge gewasweerstand en tot lage verdampingssnelheden.

Nadat de koolzuurassimilatie van de gehele opstand op deze manier is berekend, wordt de netto droge stof toename daaruit berekend met behulp van schattingen voor de onderhoudsademhaling, en door de overblijvende assimilaten te verdelen over de biomassa componenten. Groei-ademhaling vormt een verliespost in de omzetting van suikers, geproduceerd by de koolzuurassimilatie, in structurele droge stof. Voor de schatting van de onderhoudsademhaling wordt er onderscheid gemaakt tussen spint- en kernhout. Kernhout heeft alleen een mechanische funktie, en vereist geen onderhoud in de vorm van assimilatieprodukten. Indien de onderhoudsademhaling alleen wordt betrokken op het spinthout, de naalden, de takken en de wortelmassa, en daarmee alleen op de levende biomassa, leidt dit tot verwerping van de veronderstelling van Kira en Shidei (1967) dat de groei van een opstand afneemt naarmate de leeftijd en de totale biomassa toeneemt als gevolg van de toenemende onderhoudsademhaling. Spinthout, net als naalden, takken en wortels, heeft een beperkte levensduur, en de accumulatie die plaats vindt bestaat vooral uit dood kernhout, hetgeen niet leidt tot een toenemende onderhoudsademhaling met toenemende totale biomassa. De levende biomassa bereikt een maximale waarde in een vroeg stadium van de opstandsontwikkeling, enkele jaren nadat de opstand in sluiting is gekomen.

De verdeling van de assimilaten over de biomassa componenten in het model is gebaseerd op literatuur gegevens van droge stof verdelingen van vergelijkbare opstanden. Deze droge stof verdeling veranderd tijdens de opstandsontwikkeling, en hangt tevens af van de groeiplaatskwaliteit. De volume aanwas van de stammen wordt berekend uit de droge stof aanwas door deze te delen door de volumieke massa van het hout, het oven-droog gewicht

per eenheid van vers stamvolume. De volume aanwas per boom is berekend door
de totale volume aanwas te delen door het aantal bomen in de opstand. De

gemiddelde diameter is berekend als funktie van de boomhoogte en het
stamvolume.

Hoofdstuk 4 beschrijft het hydrologische deel van het simulatiemodel. De
belangrijkste aspekten van de waterhuishouding in het model zijn: a) de
interceptie van de neerslag door het kronendak, en de gereduceerde
infiltratie die dit tot gevolg heeft; b) het bodemvochtgehalte in het
doorwortelde gedeelte van het profiel, en daarvan afgeleid de beschikbare
hoeveelheid water in het profiel; en c) de opname van het bodemvocht door de
bomen, en de verdamping daarvan via de naalden. Naaldbossen in West Europa
staan vaak op zandgronden met een gering vochthoudend vermogen. Dit betekent
dat gedurende periodes van droogte, door lage luchtvochtigheid of door weinig
neerslag, de beschikbaarheid van bodemvocht op veel plaatsen de groei
beperkt. In het model wordt de hoeveelheid beschikbaar bodemvocht gesimuleerd
met behulp van een eenvoudig model. De beschikbare hoeveelheid bodemvocht
wordt bepaald door het vochtgehalte bij veldcapaciteit en het vochtgehalte
bij het verwelkingspunt. De doorwortelde zône wordt gekarakteriseerd door een
aantal bodemhorizonten, die tot aan veldcapaciteit gevuld worden, waarna het
overtollige water doorstroomt naar de onderliggende laag. De horizonten
worden allen op deze manier van bovenaf bevochtigd. De opname van water door
de wortels vindt plaats totdat de bodem zover is uitgedroogd dat het vocht-
gehalte gelijk is aan het verwelkingspunt. Het vochtgehalte bij
veldcapaciteit en bij het verwelkingspunt wordt per bodemhorizont bepaald met
behulp van standaard-vochtkrommen.

Bosopstanden hebben een grote aerodynamische ruwheid, en dit betekent dat
de weerstand voor het transport van waterdamp van het vegetatie-oppervlak
naar de atmosfeer klein is (ongeveer 10 s m^{-1}). De relatief grote stomataire
weerstand van Douglas bij maximale opening van de huidmondjes, leidt
daarentegen tot een totale gewasweerstand voor de transpiratie die groot is
ten opzichte van landbouwgewassen. Deze combinatie van een lage
aerodynamische transportweerstand met een hoge gewasweerstand, leidt ertoe
dat de verdamping van interceptie-water veel sneller verloopt dan de
transpiratie onder vergelijkbare omstandigheden. Dit betekent dat de
interceptie een netto verlies betekent voor de waterhuishouding. De

dagelijkse hoeveelheid interceptie is berekend met een eenvoudig model, door de hoeveelheid water die door het kronendak wordt onderschept in mindering te brengen op de hoeveelheid neerslag die de bodem bereikt.

De verdamping van de opstand is berekend met de Penman-Monteith vergelij-king, met de totale gewasweerstand als één van de invoervariabelen. Deze gewasweerstand wordt bepaald door a) het dampdrukdeficit van de lucht (in het model wordt aangenomen dat het dampdrukdeficit de ondergrens voor de stoma-taire weerstand bepaalt); b) de water status van de naalden, uitgedrukt als bulk water potentiaal voor de naalden; en tenslotte c) de openingstoestand van de huidmondjes zoals bepaald door de fotosynthese-snelheid. De invloed van deze faktoren op de huidmondjesweerstand wordt afzonderlijk berekend, waarna de grootste weerstand wordt gebruikt voor het berekenen van de totale gewasweerstand. De invloed van het dampdrukdeficit, en van de bulk water potentiaal is verondersteld gelijk te zijn voor alle naalden in het kronendak.

De huidmondjesweerstand die bepaald wordt uit de fotosynthese-snelheid varieert met de variatie van die fotosynthese-snelheid in het kronendak. Evenals bij de berekening van de gewasfotosynthese is ook voor de berekening van de gewasweerstand gebruik gemaakt van de Gaussische integratie. De berekende verdampingssnelheden blijken onverwacht laag te zijn gedurende het aktieve groeiseizoen, in de zomermaanden. De totale jaarlijkse verdamping echter, komt goed overeen met gepubliceerde meetgegevens, en de simulatie-resultaten voor het bodemvocht gedurende 1983, komen eveneens goed overeen met het gemeten verloop van het bodemvochtgehalte in de proefperken. De conclusie is dat ondanks lage verdampingssnelheden, de groei van naaldbossen op zandgronden in Nederland sterk beperkt kan zijn door bodemvochttekort. Hiertoe draagt vooral het interceptieverlies bij. Het hier ontwikkelde simulatiemodel kan gebruikt worden om de groeiredukties als gevolg van watertekort te berekenen, voor verschillende groeiplaatsen en voor opstanden van verschillende struktuur.

In hoofdstuk 5 wordt de simulatie van de stikstof- en fosforhuishouding beschreven, en de invloed van tekorten aan stikstof en fosfor op de groei. Aangezien herhaaldelijk is aangetoond dat zowel stikstof als fosfor groei-beperkend kunnen zijn voor de groei van naaldbossen op zandgronden, zijn beide voedingselementen in het model opgenomen. De stikstof- en

fosforhuishouding zijn niet tot in detail gemodelleerd, in plaats daarvan
wordt met behulp van een eenvoudig model, uitgaande van tijdstappen van een
jaar, vraag en aanbod van stikstof en fosfor berekend en op elkaar afgestemd.
Dit eenvoudige model is gebruikt in kombinatie met de modellen voor
assimilatie en waterhuishouding. Het aanbod van stikstof en fosfor in de
bodem wordt geschat uit de totale hoeveelheden die in het doorwortelde
profiel aanwezig zijn. Hierbij is aangenomen dat aanwezige hoeveelheden
stikstof en fosfor beide in een labiele, en in een stabiele vorm in de bodem
voorkomen. Ongeveer de helft van de totale hoeveelheid fosfor komt voor in
vrijwel inerte vorm, die slechts langzaam mineralizeert. Tussen labiele en
stabiele vormen bestaat een dynamisch evenwicht. De vraag naar stikstof en
fosfor door de groeiende vegetatie wordt bepaald door de groeisnelheid, door
de concentratie van beide elementen in het plant weefsel, en door de
hoeveelheden stikstof en fosfor die herverdeeld worden binnen de plant bij
het afsterven van levende biomassa. In het model, worden vraag en aanbod aan
het eind van elk jaar met elkaar vergeleken, waarna de concentratie in het
weefsel zodanig wordt aangepast dat vraag en aanbod met elkaar in
overeenstemming zijn. Nadat op deze manier een nieuwe concentratie is
berekend, wordt de invloed van de voedingsstoffen concentratie op de groei
van het komende jaar afgeleid aan de hand van een empirische relatie tussen
voedingsstoffen concentratie en groeireduktie. Deze benadering gaat uit van
absolute waarden voor minimum en maximum concentraties van de betrokken
elementen in het plantmateriaal: Boven het maximum vindt er geen opname meer
plaats, tussen maximum en minimum is de groei gereduceerd, en bij het minimum
vindt er geen groei meer plaats.

De uiteindelijke resultaten van het model, samen met de meetgegevens van
de permanente proefperken, worden besproken in hoofdstuk 6. De gebruikte
proefperken worden eerst besproken. Vervolgens wordt het model geëvalueerd
aan de hand van de simulatieresultaten van een onafhankelijk proefperk. In
zijn algemeenheid komen de modelresultaten goed overeen met de meetgegevens
van de proefperken. Dit geldt ook voor het onafhankelijke toetsplot. De
maximale volume aanwas zoals die is gemeten in de proefperken wordt ook
berekend door het model. De afname in bijgroei naarmate de opstanden ouder
worden wordt door het model eveneens goed gesimuleerd. De meeste afwijking
van de modelresultaten met de meetgegevens treden op bij hoge opstandleef-
tijd. Dit is waarschijnlijk een gevolg van een overschatting van de licht-
onderschepping door het model. Een van de redenen daarvoor is dat het model

geen rekening houdt met een eventuele ongelijke verdeling van de bomen in de opstand. Dit wordt des te belangrijker wanneer de opstand op hoge leeftijd nog gedund wordt, waarbij dan de kronen slechts weinig of geen gelegenheid meer hebben om te reageren op de beschikbaar gekomen groeiruimte.

Tegelijk met de evaluatie van het modelgedrag in de proefperken, wordt de waarde van simulatie en modellenbouw, vooral in het bosbouwkundige onderzoek, besproken. Modellen gebaseerd op de fysiologie van de boomsoort, en op de reaktie op klimaat en bodem, zijn vereist voor de analyse van groei en opbrengst. De ontwikkeling en het gebruik van deze modellen dragen bij tot het verkrijgen van inzicht in de primaire produktie processen in bossen. Het gebruik van fysiologisch gebaseerde simulatiemodellen in het onderzoek naar funktie en struktuur van vegetaties maakt het mogelijk verschillende aspekten van de primaire produktie met elkaar in verband te brengen, en de afstanden tussen verschillende onderzoeksdisciplines te overbruggen. Door integratie van de belangrijkste aspekten die de groei bepalen wordt het mogelijk de faktoren vast te stellen die de groei het sterkst beperken. Als gevolg hiervan kunnen de mogelijkheden voor verhoging van de groei en opbrengst worden onderzocht, en kan tevens worden vastgesteld op welke terreinen onderzoek het meest gewenst is.
Voor Douglasbossen in Nederland leidt dit tot de conclusie dat de afname van de aanwas tijdens het ouder worden van de opstand onder andere een gevolg is van de afnemende lichtonderschepping. In de huidige bosbouwpraktijk worden dunningsmaatregelen vooral gericht op het scheppen van groeiruimte voor de beste bomen in de opstand. Indien hierbij de kronensluiting afneemt, neemt tevens de aanwas per hectare af. Dit kan vooral een rol spelen indien de dunningen uitgevoerd worden in oudere opstanden, daar in dat geval de overblijvende bomen vaak niet meer ten volle gebruik kunnen maken van de hernieuwd beschikbaar gekomen groeiruimte.

Niet alleen de beschikbaarheid van bodemvocht beperkt de groei op de zand- gronden. Naast droogte spelen tekorten aan stikstof en fosfor soms een belangrijke rol in het bepalen van de maximale groeisnelheid. Het eenvoudige model dat hier is gebruikt, geeft aan welke hoeveelheden stikstof en fosfor benodigd zijn voor een ongeremde groei, en duidt op groeibeperkingen in Nederland door zowel stikstof en fosfor. Dit komt overeen met de konklusies van Blok et al. (1975), bij evaluatie van de resultaten van bemestings- experimenten uitgevoerd in Douglascultures gedurende de vijftiger en zestiger

jaren. De toegenomen atmosferische depositie van stikstof, samenhangend met de toegenomen aktiviteiten van de intensieve veehouderij, heeft geleid tot een grote toename van de stikstofbeschikbaarheid. Een van de gevolgen daarvan is het ontstaan van een wijdverspreid fosforgebrek in Douglas. Deze situatie, waarbij een wijdverspreid stikstofgebrek is omgezet in ernstig fosforgebrek, vraagt om aandacht vanuit het onderzoek, beleid en beheer. Indien de fosforbeschikbaarheid kan worden vergroot, bijvoorbeeld door aanvullende bemesting, mag verwacht worden dat de primaire produktie, en de aanwas toenemen. Hierdoor zal de opbrengst worden verhoogd.

Een van mogelijke toepassingen van het besproken model ligt in het berekenen van de groeimogelijkheden voor een breed scala aan bodem- en klimaatsomstandigheden, waardoor het mogelijk wordt de potentiële groei en opbrengst voor een gebied of regio te berekenen. Een dergelijk model kan daarnaast gebruikt worden om de gevolgen van beheersingrepen te evalueren. Tevens kunnen dit soort modellen gebruikt worden om de efficiëntie van bijvoorbeeld meststoffengebruik vast te stellen. Voordat het model gebruikt kan worden voor schattingen van economische opbrengst, of voor berekening van optimale dunnings- en oogstregimes, dienen er een aantal groei- of opstandsverstorende faktoren, zoals windworp, in het model opgenomen te worden.

Het simulatie programma is op aanvraag beschikbaar.

CURRICULUM VITAE

Frits Mohren werd geboren op 27 juli 1957, als zoon van Leen
Mohren-Bremmers en Jac Mohren, mijn- en rondhouthandelaar te Echt.
Van 1969 tot 1975 volgde hij de Atheneum-B opleiding aan het
Bisschoppelijk College te Echt. In 1975 begon hij zijn studie aan
de Landbouwhogeschool te Wageningen (studierichting Bosbouw), waar
hem in 1982 het ingenieursdiploma met lof werd uitgereikt. Tijdens
de studie bracht hij zijn praktijktijd door in Zwitserland, de
Verenigde Staten en Suriname. Van 1982 tot 1986 was hij aangesteld
als wetenschappelijk assistent bij de vakgroepen Theoretische
Teeltkunde en Bosteelt van de Landbouwhogeschool. Daarnaast was
hij in 1986 enkele maanden werkzaam bij het Centrum voor Agro-
biologisch Onderzoek te Wageningen, in het kader van het Informa-
tica Stimuleringsplan voor het Landbouwkundig Onderzoek. Ter ver-
dieping van zijn onderzoek werd hem door de Niels Stensen Stich-
ting te Amsterdam een stipendium toegekend voor een studieverlof,
in 1987 door te brengen in Zweden en in de Verenigde Staten.